論文 / 著書情報
Article / Book Information

題目(和文)	
Title(English)	Robust Unit Commitment under Uncertainties of Variable Renewable Energy Generation and Demand Response
著者(和文)	チョヨンチェ
Author(English)	Youngchae Cho
出典(和文)	学位:博士（工学）, 学位授与機関:東京工業大学, 報告番号:甲第12078号, 授与年月日:2021年9月24日, 学位の種別:課程博士, 審査員:井村 順一,石﨑 孝幸,三平 満司,中尾 裕也,早川 朋久
Citation(English)	Degree:Doctor (Engineering), Conferring organization: Tokyo Institute of Technology, Report number:甲第12078号, Conferred date:2021/9/24, Degree Type:Course doctor, Examiner:,,,,
学位種別(和文)	博士論文
Type(English)	Doctoral Thesis

Robust Unit Commitment under Uncertainties of Variable Renewable Energy Generation and Demand Response

by

Youngchae Cho

A dissertation submitted to the Department of Systems and Control Engineering
in partial fulfillment of the requirements for the degree of Doctor of Engineering

Tokyo Institute of Technology

2021

Abstract

The increasing use of variable renewable energy sources and demand response programs has posed challenges in solving many power system planning problems due to their inherent uncertainties. Among such is the unit commitment problem to determine the operating status of dispatchable power sources including conventional fossil-fuel generators on the following day. As its main contributions, this dissertation proposes three unit commitment models based on robust optimization for power systems under the uncertainty of variable renewable energy generation or that of demand response. The significance of the proposed models is that they optimize worst-case performances of such power systems in less conservative and more generalized ways than existing models. Simulation results verify the effectiveness of the proposed models.

Acknowledgements

I have received a great deal of assistance from many people throughout the writing of this dissertation, to whom I would like to express my sincere gratitude here.

First of all, I am deeply indebted to Professor Jun-ichi Imura, who has guided me through my PhD program. He has provided me with not only discipline-specific academic advice but also various opportunities to engage with academic communities. The completion of my dissertation would not have been possible without his support and nurturing.

I would like to extend my gratitude to Associate Professor Takayuki Ishizaki, whose valuable comments have greatly polished my research skills. He has also taught me the importance of appropriately delivering one's research to those in and out of the field.

Many thanks should also go to Professor Nacim Ramdani at the University of Orléans, who welcomed me so warmly during my visit to his laboratory. The intensive discussions with him were highly inspiring, which allowed me to learn the joy of collaboration.

I gratefully acknowledge the constructive suggestions from past and current members of Imura, Hayakawa, and Nakadai Laboratories at the inter-laboratory seminars.

Especially helpful to me were Mrs. Noriko Sugimoto, the secretary of Imura Laboratory, and Mrs. Akiho Setoguchi, a former technical staff member of Imura Laboratory.

Finally, I wish to thank my parents for their unconditional love and encouragement.

Contents

List of Publications

This dissertation is based on the following published articles:

- **Journal Papers**
  - Y. Cho, T. Ishizaki, N. Ramdani, and J. Imura, "Box-based temporal decomposition of multi-period economic dispatch for two-stage robust unit commitment," *IEEE Transactions on Power Systems*, vol. 34, no. 4, pp. 3109–3118, 2019, doi: 10.1109/TPWRS.2019.2896349.
  - Y. Cho, T. Ishizaki, and J. Imura, "Three-stage robust unit commitment considering decreasing uncertainty in wind power forecasting," to appear in *IEEE Transactions on Industrial Informatics*, doi: 10.1109/TII.2021.3079364.
- **Refereed International Conference Papers**
  - Y. Cho, T. Ishizaki, and J. Imura, "Hybrid method of two-stage stochastic and robust unit commitment," *2019 18th European Control Conference (ECC)*, 2019, pp. 922–927, doi: 10.23919/ECC.2019.8796153.
  - Y. Cho, T. Ishizaki, N. Ramdani, and J. Imura, "Economic dispatch cost reduction in box-based robust unit commitment," *IFAC-PapersOnLine*, vol. 53, no. 2, pp. 13248–13253, 2020, doi: 10.1016/j.ifacol.2020.12.153.
  - Y. Cho, T. Ishizaki, and J. Imura, "Two-stage robust unit commitment with uncertain demand response," *2021 European Control Conference (ECC)*, 2021, pp. 2104–2109.

Nomenclature

Sets and Parameters

$\hat{w}^{*}_{it}$	Upper limit of $(\overline{w}_{it} - \underline{w}_{it})$ at the day-ahead stage
$\mathbb{R}$	Set of real numbers
$\mathcal{I}$	Index set of buses
$\mathcal{J}$	Index set of preselected VRE generation scenarios
$\mathcal{L}$	Index set of transmission lines
$\mathcal{S}$	Set of possible VRE generation scenarios
$\mathcal{T}$	Index set of time periods
$\mathcal{W}$	Vaguity set
$\overline{\theta}^{\mathrm{r}}_{it}$	Upper limit of $\left(\theta_{it} - \theta_{i(t-1)}\right)$
$\overline{\theta}^{\mathrm{s}}_{i}$	Lower limit of $\sum_{t\in\mathcal{T}} \theta_{it}$
$\overline{\theta}_{it}$	Upper limit of θ_{it}
$\overline{s}_{it}$	Upper limit of s_{it}
$\overline{w}^{\mathrm{d}}_{it}$	Upper limit of $\overline{w}_{it}$ at the day-ahead stage
$\overline{w}_{it}$	Upper limit of w_{it} at the intra-day stage
$\overline{X}_{i}$	Maximum possible power output of generator i
$\overline{Y}^{\mathrm{s}}_{i}$	Upper limit of $\sum_{t\in\mathcal{T}} y_{it}$
$\overline{Y}_{it}$	Upper limit of y_{it}
Θ	Set of possible bid price profiles
θ_{it}	Bid price for flexible demand of customer i at time period t
$\underline{\theta}^{\mathrm{r}}_{it}$	Lower limit of $\left(\theta_{it} - \theta_{i(t-1)}\right)$
$\underline{\theta}^{\mathrm{s}}_{i}$	Lower limit of $\sum_{t\in\mathcal{T}} \theta_{it}$
$\underline{\theta}_{it}$	Upper limit of θ_{it}

$\underline{s}_{it}$	Lower limit of s_{it}
$\underline{w}^{\mathrm{d}}_{it}$	Lower limit of $\underline{w}_{it}$ at the day-ahead stage
$\underline{w}_{it}$	Lower limit of w_{it} at the intra-day stage
$\underline{X}_i$	Minimum possible power output of generator i
$\underline{Y}^{\mathrm{s}}_i$	Lower limit of $\sum_{t\in\mathcal{T}} y_{it}$
$\underline{Y}_{it}$	Lower limit of y_{it}
d_{it}	Power demand at bus i and at time period t
F_{il}	Power transfer distribution factor of bus i and transmission line l
F_l	Power flow capacity of transmission line l
I	Number of buses
L	Number of transmission lines
s_{it}	VRE generation at bus i and at time period t
T	Number of time periods
T^{d}_i	Minimum down time of generator i
T^{u}_i	Minimum up time of generator i
W_j	Probability associated with scenario j of VRE generation
w_{it}	Wind power at bus i and time period t
E^{i}_i	Charging efficiency of BESS i
E^{o}_i	Discharging efficiency of BESS i
R^{d}_i	Ramp-down rate of generator i
R^{sd}_i	Shut-down-ramp rate of generator i
R^{su}_i	Start-up-ramp rate of generator i
R^{u}_i	Ramp-up rate of generator i
S_{i0}	Initially stored energy in BESS i
S_i	Storage capacity of BESS i
X^{i}_i	Maximum possible power input of BESS i
X^{o}_i	Maximum possible power output of BESS i
X^{r}_i	Maximum possible spinning reserve of generator i

Decision Variables

$\overline{x}_{it}^{\mathrm{g}}$ Maximum allowable power output of generator i at time period t

$\overline{x}_{it}^{\mathrm{i}}$ Maximum allowable power input of BESS i at time period t

$\overline{x}_{it}^{\mathrm{o}}$ Maximum allowable power output of BESS i at time period t

$\underline{x}_{it}^{\mathrm{g}}$ Minimum allowable power output of generator i at time period t

$\underline{x}_{it}^{\mathrm{i}}$ Minimum allowable power input of BESS i at time period t

$\underline{x}_{it}^{\mathrm{o}}$ Minimum allowable power output of BESS i at time period t

u_{it}^{d} Shut-down status of generator i at time period t

u_{it}^{n} On/off status of generator i at time period t

u_{it}^{o} Charging/discharging status of BESS i at time period t

u_{it}^{u} Start-up status of generator i at time period t

x_{it}^{g} Power output of generator i at time period t

x_{it}^{i} Power input of BESS i at time period t

x_{it}^{o} Power output of BESS i at time period t

y_{it} Power consumption by customer i at time period t

z_i Winning status of customer i

Chapter 1

Introduction

This dissertation is concerned with the unit commitment (UC) problem for an electric power system under the prediction uncertainty of variable renewable energy (VRE) generation or that of demand response. In this chapter, the dissertation is overviewed. This chapter is organized as follows: Section 1.1 explains a brief background of the UC problem. Section 1.2 gives a literature review. Section 1.3 describes the main contributions of the dissertation and outlines the remaining chapters.

1.1 Background

To ensure that power supply and demand are finely balanced at the lowest operating cost, various power system planning problems are addressed on different time scales [1]. One of the most studied among them is the UC problem, the optimization problem of the commitment (on/off) status of generators. The UC problem is solved in advance, usually for an hourly demand forecast of the following day, as some generators may require a certain amount of time to start up or shut down. Nested in the UC problem, the optimization problem of the power outputs of generators in operation is called the economic dispatch (ED) problem. With the commitment status of generators represented by binary variables, the UC problem is formulated as a mixed-integer programming (MIP) problem whose objective function and constraints vary depending on specific context [2]–[4]. It is vitally important, and difficult at the same time, to formulate and solve the UC problem properly, because unexpected events, e.g., deviation of demand from the forecast and component failure, may happen while the commitment status of some generators cannot be changed quickly in real time. To hedge against such uncertainties, reserve requirements are imposed in traditional UC models according to deterministic criteria, e.g., the largest generator in terms of installed capacity and some percentage of the peak demand [5].

Meanwhile, the past few decades have witnessed an increasing penetration of VRE generation systems, e.g., wind turbines and solar photovoltaic systems, owing to their environmental and economic benefits [6]. Specifically, the global wind and solar power capacities have expanded from 16.93 GW in 2000 to 733.28 GW in 2020 and 1.23 GW in 2000 to 713.97 GW in 2020, respectively; for reference, Fig. 1.1 shows the yearly global growth of the installed capacity of wind and solar power from 2000 to 2020 [7]. Based on energy plans and policies from around the world as of 2019, the wind and solar

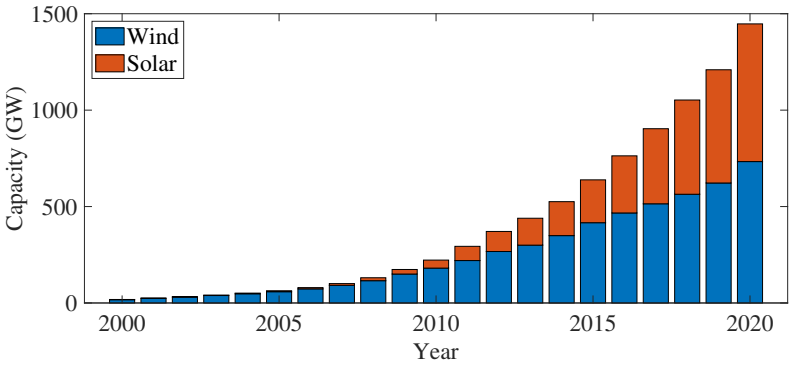

Fig. 1.1. Trends in the installed capacity of wind and solar power.

power capacities are expected to increase to 4474 GW and 2434 GW by 2050, respectively, accounting for 36% of total power generation [8]. Moreover, to make optimal use of VRE generation, battery energy storage systems (BESSs) are increasingly integrated as well. Specifically, the global energy capacity of stationary storage technologies is expected to expand from 30 GWh in 2019 to 3400 GWh in 2050 [8].

Besides BESSs, demand response can also be used to increase the flexibility of power system operation [9]. Demand response refers to intentional changes in electric energy consumption induced by changes in the price of electricity or by incentive payments as signals from the system operator [10]. With demand response, a range of services can be performed including peak demand reduction, congestion management, and assistance in emergency conditions [11]. In the Stated Policies Scenario of the International Energy Agency, demand response is a fast-rising source of flexibility, whose increased shares in the year 2040 in the US, the EU, China, and India compared with in 2018 are noticeable [12].

Despite numerous advantages they bring to power systems, however, VRE generation and demand response pose fundamental challenges in addressing the UC problem by adding to the uncertainties. In the presence of VRE generation or demand response, it might increase operating costs drastically or cause a power supply-demand imbalance to implement traditional UC models for any nominal scenario of VRE generation or demand response.

1.2 Literature Review

To deal with the uncertainty of VRE generation or demand response, many UC models are studied in the literature adopting stochastic optimization methods where possible scenarios of VRE generation or demand response are explicitly considered. In this section, such existing UC models are reviewed.

1.2.1 UC with Uncertain VRE Generation

Arguably the two most popular stochastic optimization methods for the UC problem under the uncertainty of VRE generation are stochastic programming and robust optimization [13], [14]. In this dissertation, UC models based on stochastic programming and robust optimization are referred to as *stochastic* and *robust* UC models, respectively. Both types of

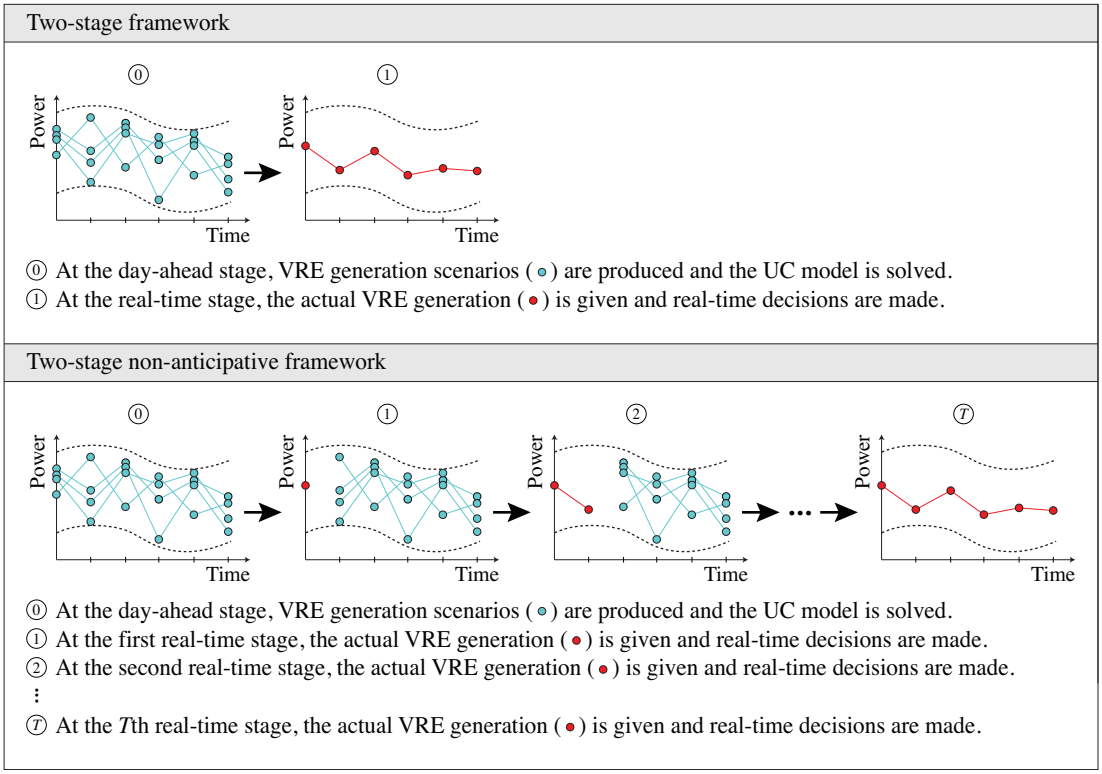

Fig. 1.2. Decision-makings in the two-stage and the two-stage non-anticipative frameworks.

UC models typically assume a series of two or more decision-making stages, among which the first and the other one or more are usually for day-ahead and real-time decisions, respectively. In this dissertation, UC models assuming one day-ahead plus one real-time stages and those assuming one day-ahead plus more than one real-time stages are referred to as *two-stage* and *two-stage non-anticipative* UC models, respectively.

Considering a single real-time stage, two-stage UC models optimize real-time decisions for all the time periods of the planning horizon simultaneously by solving a multi-period ED problem. In practice, however, as the VRE generation at different time periods cannot be observed at once, real-time decisions at different time periods have to be made sequentially with the future VRE generation unknown. To enable such non-anticipative real-time decision-making, two-stage non-anticipative UC models assume more than one real-time stages, each of which corresponds to each time period of the planning horizon. Differently from two-stage UC models, real-time decisions at each time period are made based on only the past or current, but not the future, VRE generation. In this regard, two-stage non-anticipative UC models are more practical than two-stage UC models. Fig. 1.2 illustrates the two-stage and the two-stage non-anticipative frameworks to address the uncertainty of VRE generation over the planning horizon of T time periods.

Regardless of the UC model, the objective of the real-time decision-making is mainly to minimize operating costs for the actual VRE generation. However, the day-ahead decision-making has different objectives depending on the stochastic optimization method. In general, stochastic UC models aim at minimizing the expected total operating cost or ensuring that the probability of failing to maintain power supply-demand balance is below

a specified level, under the assumption that a probability distribution of VRE generation is given [15]. To build representative scenarios of VRE generation that are explicitly considered, various scenario generation methods are also developed in the literature [16]. Stochastic UC models are well studied for both two-stage and two-stage non-anticipative frameworks, the latter of which is made possible by constructing a scenario tree [17].

Robust UC models, on the other hand, do not require a probability distribution of VRE generation. This is a major advantage because the accurate probability distribution of VRE generation is usually hard to infer. Instead, they use worst-case analyses for a set of VRE generation scenarios. Modeling techniques of the scenario set for robust UC models are extensively studied in the literature [18], [19]. The objective of a robust UC model may be to minimize the worst-case total operating cost [20], [21], a weighted sum of the worst-case and the expected total operating costs [22], [23], the maximum regret [24], the base-case total operating cost with the adaptivity of day-ahead decisions guaranteed [25], [26], and the variance of the total operating cost [27]. To reduce the intrinsic conservativeness of robust optimization, some models employ multiple scenario sets [28] or a single multi-band scenario set [29], [30]. Furthermore, the scenario set itself can be adjusted to minimize the base-case total operating cost with a limited operational risk [31], [32].

All the above-mentioned robust UC models are of the two-stage formulation. In contrast to stochastic programming, robust optimization is not easily applied within the two-stage non-anticipative framework as infinitely many scenarios of VRE generation are considered in general. Existing two-stage non-anticipative robust UC models include the ones in [33] and [34]. The model in [33] uses an affine policy [35], where the power output of each generator at each time period is modeled as an affine function of the current VRE generation. The coefficients of the function are determined so that power supply and demand are always balanced. The specific objective of this UC model is to minimize the worst-case total operating cost. The affine policy can also be used to plan operations of BESSs [36]. In [34], some VRE generation scenarios are preselected and the corresponding power outputs of each generator are first obtained to minimize a weighted sum of the total operating costs for the preselected scenarios. Subsequently, the power output of each generator for the actual VRE generation at each time period is computed as a linear combination of the predetermined power outputs for that time period.

Last but not least, it is noteworthy that a stochastic UC model is studied within a *three-stage* framework in [37]. The three decision-making stages in this model represent a day-ahead electricity market, an intra-day electricity market, and the real-time operation in the real world, respectively. The intra-day market, which is the newly added decision-making stage compared with two-stage stochastic UC models, makes adjustments to 24 hourly schedules settled at the day-ahead market and closes a few hours before the first power delivery on the planning horizon. The three-stage stochastic UC model is demonstrated to be superior to its two-stage counterpart through numerical simulations. To the best of the author's knowledge, no robust UC model based on the three-stage or the *three-stage non-anticipative* framework, which further enables the non-anticipative real-time decision-making, is found in the literature.

1.2.2 UC with Uncertain Demand Response

Similarly to the uncertainty of VRE generation, that of demand response can be addressed using stochastic programming and robust optimization [38]–[41]. The uncertainty considered in [38]–[41] is specifically that in the demand curve of each customer, which is dealt with more directly in the form of the utility function of power consumption. In [38], stochastic programming is applied within the two-stage framework; the UC model is solved under the uncertainty of demand response at the day-ahead stage, and the power output of each generator is determined simultaneously with the power consumption of each customer for the actual utility at the real-time stage. The objective of this model is to maximize the expected social welfare; the social welfare is defined in this dissertation as the total utility of power consumption by customers subtracted by the total operating cost of generators. The model in [39] uses robust optimization within the two-stage framework to maximize the worst-case social welfare. The models in [40] and [41] also employ robust optimization to maximize the worst-case social welfare, but assume only one decision-making stage in addressing the uncertainty of demand response; the power output of each generator and the power consumption of each customer are determined while the utility is uncertain, and not adjusted afterwards. Owing to its adaptivity, the two-stage framework used in [39] never achieves a lower social welfare than the single-stage one in [40] and [41].

1.3 Contributions and Organization

As its main contributions, this dissertation proposes three robust UC models to address the uncertainty of VRE generation or that of demand response. In this section, the three proposed models are briefly explained. Thereafter, the rest of this dissertation is outlined.

The first proposed model is a two-stage non-anticipative robust UC model for a power system of generators, BESSs, loads, and VRE generation systems under the uncertainty of VRE generation; the generators and the BESSs indicate fossil-fuel-based ones that cannot be turned on or off promptly and stationary ones, respectively. This model can be used to minimize the worst-case total operating cost. Although the affine-policy-based model in [33] has the same objective, which also enables the non-anticipative real-time decision-making, its solution might be too conservative. This is because the operating level is modeled as an affine function of the VRE generation. To balance power supply and demand in a less costly way, the first proposed model uses a novel approach where the operating level of each power source at each time period is optimized by solving a single-period ED problem for the actual VRE generation at the same time period. To this aim, the operating *range* of each power source at each time period is determined with the operating status at the day-ahead stage. The operating range is such that every element in it as a possible operating level is feasible for any operating level of the power source at the other time periods. The first proposed model is formulated as a two-stage robust optimization problem, which can be solved by using existing algorithms. It is shown via numerical simulations that this model is less conservative than the affine-policy-based model. In the meantime, this dissertation further provides two supplementary methods for the first proposed model to

reduce the actual total operating cost. Combining stochastic programming and robust optimization, the first supplementary method minimizes the expected total operating cost for some preselected scenarios of VRE generation with the worst-case total operating cost bounded by a specified value. By using the second supplementary method, the operating range of each power source at each time period obtained by solving the first proposed model is extended so that more economical real-time decisions can be made.

The second proposed model is a three-stage non-anticipative robust UC model for a power system of generators, BESSs, loads, and wind farms, among other VRE generation systems, under the uncertainty of wind power. This model can be used to minimize the worst-case total operating cost, which builds on the first proposed model. Although the first proposed model is directly applicable with the same objective, the solution may be unnecessarily costly if the scenario set of wind power is constructed too conservatively. To lessen the conservativeness of the first proposed model, the second proposed model exploits the fact that the uncertainty of wind power reduces over time and delays determining the operating range of each power source at each time period. To this end, an intermediate decision-making stage, namely the intra-day stage, is introduced between the day-ahead stage and the first real-time stage; the time scale of the intra-day stage is the same as that of the second decision-making stage in the three-stage stochastic UC model [37]. Consequently, in the second proposed model, the operating status, range, and level are optimized sequentially at the day-ahead, the intra-day, and each real-time stage, respectively, under different degrees of wind power uncertainty. This model is formulated as a three-stage robust optimization problem, for which existing algorithms are not applicable. To solve it, a suboptimal approach is developed where an additional constraint is imposed on the operating range so that one of the operational constraints in the power system of interest is temporarily ignorable. By this approach, the intractable three-stage robust optimization problem is reduced to a tractable two-stage robust optimization problem. It is numerically shown that the second proposed model outperforms the first one when the wind power uncertainty is severe at the day-ahead stage but reduces greatly at the intra-day stage.

The third proposed model is a two-stage robust UC model for a power system of generators and loads under the uncertainty of demand response. Each load has an associated customer. Integrating a demand response program where each customer is allowed to bid at the real-time stage for their flexible demand, this model maximizes the worst-case social welfare, i.e., the social welfare for worst-case bidding scenarios. While the model in [39] assumes the same number of decision-making stages with the same objective, it does not consider the winning status of each customer as a decision variable. The winning status of a customer indicates whether or not their bidding is accepted, which is a general modeling concept of demand response [42]. The third proposed model is novel in that it explicitly considers the winning status of each customer as a decision variable, enhancing the modeling capability and the flexibility of power system operation. This model is formulated as a two-stage robust optimization problem whose second-stage problem has integer variables and an uncertain objective function. To solve it, an algorithm is designed borrowing the concept of an existing one developed for a different class of problems. Numerical simulation

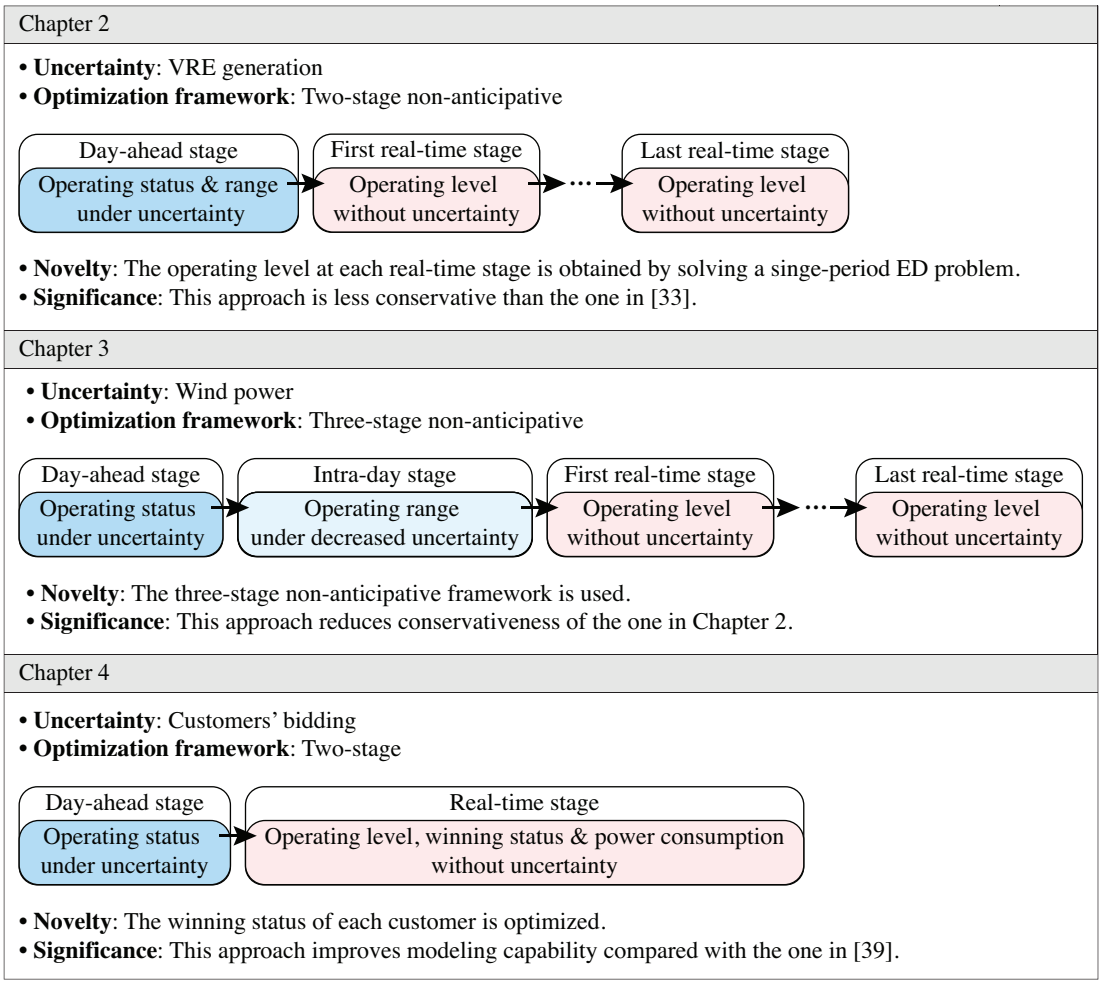

Fig. 1.3. Summary of the proposed models in Chapters 2–4.

results show the effectiveness of this model.

The rest of this dissertation comprises four chapters. Chapter 2 explains the first proposed model and the two supplementary methods in further detail. Chapters 3 and 4 study in depth the second and third proposed models, respectively. Each of Chapters 2–4 begins with an introductory section elucidating the motivation of the corresponding proposed model and ends with a section summing it up. Each of these chapters is also equipped with sections providing a mathematical formulation of the proposed model, a solution method, and numerical simulation results. Finally, Chapter 5 closes the dissertation. Fig. 1.3 summarizes the proposed models described in the three main chapters.

Remark 1.3.1. The core idea used in the first proposed model is also suggested in several existing research papers, e.g., [43] and [44], which are independent of this dissertation and not further mentioned.

Chapter 2

Two-stage Non-anticipative Robust UC with Uncertain VRE Generation

This chapter explains the novel two-stage non-anticipative robust UC model for addressing the uncertainty of VRE generation and the two supplementary methods. This chapter is organized as follows: Section 2.1 explains the motivation of the proposed model. Section 2.2 models the power system of interest. Section 2.3 presents a deterministic UC model without considering any uncertainty. Section 2.4 models the uncertainty of VRE generation. Section 2.5 gives the mathematical formulation of the proposed model. Section 2.6 describes a solution method. Section 2.7 discusses numerical simulation results. Sections 2.8 and 2.9 provide the first and second supplementary methods, respectively. Section 2.10 summarizes the chapter.

2.1 Motivation

For a system operator who wishes to minimize the worst-case total operating cost under the uncertainty of VRE generation, the affine-policy-based two-stage non-anticipative robust UC model studied in [33] yields a more practical solution than any two-stage robust UC model. However, because the operating level of each power source at each time period is modeled as an affine function of the VRE generation, the solution might be unnecessarily costly. To reduce the conservativeness in the affine policy, the proposed model uses a different approach to realizing the non-anticipative real-time decision-making. In the proposed model, a range of the operating level of each power source at each time period is determined at the day-ahead stage with the operating status so that the operating level can be obtained by solving a single-period ED problem parameterized with the VRE generation at the same time period. To give mathematical descriptions of the proposed model, the power system of interest is first modeled in the following subsection.

2.2 Power System Modeling

In the proposed model, a power system with I buses and L transmission lines is considered. The planning horizon is discretized with T time periods. The index set of the buses, that of the transmission lines, and that of the time periods are denoted by $\mathcal{I} := \{1, 2, \ldots, I\}$,

$\mathcal{L} := \{1, 2, \ldots, L\}$, and $\mathcal{T} := \{1, 2, \ldots, T\}$, respectively. To represent the transmission network, a DC power flow model is used, which is an approximation to a single-phase AC power flow model [45], [46]. In the latter model, each bus has four associated parameters, namely the voltage magnitude, the voltage angle, the active power injection, and the reactive power injection, yielding nonlinear equations describing the active and reactive power flow in each transmission line. In the DC power flow model, on the other hand, only the active power injection is addressed under the following assumptions: First, the resistance of each transmission line is small enough compared with its reactance. Second, the voltage magnitudes at all the buses are approximately equal. Lastly, the voltage angle difference between any two connected buses is small enough. By these assumptions, the nonlinear equations in the AC power flow model are linearized. The active power flow in a transmission line is then computed as a linear combination of the active power injections at all the buses, whose coefficients are called power transfer distribution factors [47]. As the reactive power injection is ignored, only the following two systemwide constraints are imposed on the entire transmission network: First, the active power injections at all the buses add to zero, which corresponds to the power supply-demand balance condition. Second, the amount of active power flow in a transmission line is limited by its capacity.

Without loss of generality, it is assumed that a generator, a BESS, a load, and a VRE generation system are connected to each bus, all with the same index as that of the bus. The decision variables of each generator at each time period are the operating status, which indicates whether it is turned on or off, and the operating level, i.e., its power output. The generators cannot start up or shut down instantly; once a generator starts up, a certain amount of time has to pass before it can be turned off again. This time length is called the minimum up time; the minimum down time is similarly defined. Furthermore, the power output of each generator in operation at each time period has to be greater than or equal to the minimum possible power output and be smaller than or equal to the maximum possible power output. The increase and decrease in the power output of each generator over two consecutive time periods are also limited by the ramp-up and ramp-down rates, respectively, if it is turned on at both time periods. If the generator starts up or shuts down at the second time period, then its start-up-ramp and shut-down-ramp rates are applied instead of the ramp-up and ramp-down rates, respectively. Moreover, the increase and decrease in the power output of each generator within each time period is limited by the maximum possible spinning reserve. The operating costs of each generator are divided into fixed and variable ones. The fixed operating cost of a generator is defined as the sum of its no-load, start-up, and shut-down costs, which are incurred when it is turned on, starts up, and shuts down, respectively, regardless of its power output. Depending on the power output, the variable operating cost of a generator is modeled as a linear function for the sake of simplicity. Modeling the variable operating cost more generally and practically as a piecewise linear function is straightforward [48].

The decision variables of each BESS at each time period are the operating status, which indicates whether it is charging or discharging, and the operating level, i.e., its power input or output. Differently from the generators, the operating status of the BESSs

can be quickly changed. However, there are maximum possible values of the power input and output, and more importantly, the amount of energy stored. While no fixed operating cost is incurred, the variable operating cost of a BESS is defined as the sum of the charging and discharging costs, each of which is modeled as a linear function of the operating level.

The power demand and VRE generation at each bus and time period are considered unadjustable. Load shedding and VRE generation curtailment are not modeled for the sake of simplicity. In the following section, the deterministic UC model for this power system is described where both power demand and VRE generation at each bus and time period are assumed precisely known.

2.3 Deterministic UC

Without considering any uncertainty, the deterministic UC model is formulated as the following mixed-integer linear programming (MILP) problem:

$$\min_{\mathbf{u}\in\{0,1\}^{4IT},\mathbf{x}\in\mathbb{R}^{3IT}} \sum_{t\in\mathcal{T}}\sum_{i\in\mathcal{I}} C_i^{\mathrm{n}} u_{it}^{\mathrm{n}} + C_i^{\mathrm{u}} u_{it}^{\mathrm{u}} + C_i^{\mathrm{d}} u_{it}^{\mathrm{d}} + C_i^{\mathrm{g}} x_{it}^{\mathrm{g}} + C_i^{\mathrm{i}} x_{it}^{\mathrm{i}} + C_i^{\mathrm{o}} x_{it}^{\mathrm{o}} \tag{2.1a}$$

$$\text{s.t.} \quad u_{it}^{\mathrm{n}} - u_{i(t-1)}^{\mathrm{n}} = u_{it}^{\mathrm{u}} - u_{it}^{\mathrm{d}}, \quad \forall i \in \mathcal{I}, \forall t \in \mathcal{T}, \tag{2.1b}$$

$$u_{it}^{\mathrm{n}} - u_{i(t-1)}^{\mathrm{n}} \leq u_{i\tau}^{\mathrm{n}}, \quad \tau = t, \ldots, \min\left\{t - 1 + T_i^{\mathrm{u}}, T\right\}, \forall i \in \mathcal{I}, \forall t \in \mathcal{T}, \tag{2.1c}$$

$$u_{i(t-1)}^{\mathrm{n}} - u_{it}^{\mathrm{n}} \leq 1 - u_{i\tau}^{\mathrm{n}}, \quad \tau = t, \ldots, \min\left\{t - 1 + T_i^{\mathrm{d}}, T\right\}, \forall i \in \mathcal{I}, \forall t \in \mathcal{T} \tag{2.1d}$$

$$\underline{X}_i u_{it}^{\mathrm{n}} \leq x_{it}^{\mathrm{g}} \leq \overline{X}_i u_{it}^{\mathrm{n}}, \quad \forall i \in \mathcal{I}, \forall t \in \mathcal{T}, \tag{2.1e}$$

$$x_{it}^{\mathrm{g}} - x_{i(t-1)}^{\mathrm{g}} \leq R_i^{\mathrm{u}} u_{i(t-1)}^{\mathrm{n}} + R_i^{\mathrm{su}} u_{it}^{\mathrm{u}}, \quad \forall i \in \mathcal{I}, \forall t \in \mathcal{T}, \tag{2.1f}$$

$$x_{i(t-1)}^{\mathrm{g}} - x_{it}^{\mathrm{g}} \leq R_i^{\mathrm{d}} u_{it}^{\mathrm{n}} + R_i^{\mathrm{sd}} u_{it}^{\mathrm{d}}, \quad \forall i \in \mathcal{I}, \forall t \in \mathcal{T} \tag{2.1g}$$

$$0 \leq y_{it}^{\mathrm{i}} \leq Y_i^{\mathrm{i}} \left(1 - u_{it}^{\mathrm{o}}\right), \quad \forall i \in \mathcal{I}, \forall t \in \mathcal{T}, \tag{2.1h}$$

$$0 \leq y_{it}^{\mathrm{o}} \leq Y_i^{\mathrm{o}} u_{it}^{\mathrm{o}}, \quad \forall i \in \mathcal{I}, \forall t \in \mathcal{T}, \tag{2.1i}$$

$$0 \leq S_{i0} + \sum_{\tau=1}^{t} \left(E_i^{\mathrm{i}} y_{it}^{\mathrm{i}} - \frac{1}{E_i^{\mathrm{o}}} y_{it}^{\mathrm{o}}\right) \leq S_i, \quad \forall i \in \mathcal{I}, \forall t \in \mathcal{T}, \tag{2.1j}$$

$$\sum_{i\in\mathcal{I}} \left(x_{it}^{\mathrm{g}} - x_{it}^{\mathrm{i}} + x_{it}^{\mathrm{o}} - d_{it} + s_{it}\right) = 0, \quad \forall t \in \mathcal{T}, \tag{2.1k}$$

$$-F_l \leq \sum_{i\in\mathcal{I}} F_{il} \left(x_{it}^{\mathrm{g}} - x_{it}^{\mathrm{i}} + x_{it}^{\mathrm{o}} - d_{it} + s_{it}\right) \leq F_l, \quad \forall l \in \mathcal{L}, \forall t \in \mathcal{T} \tag{2.1l}$$

where $\mathbf{u}$, $\mathbf{x}$, and $\mathbb{R}$ denote a vector of binary variables u_{it}^{n}, u_{it}^{u}, u_{it}^{d}, and u_{it}^{o} for all $i \in \mathcal{I}$ and $t \in \mathcal{T}$, a vector of real variables x_{it}^{g}, x_{it}^{i}, and x_{it}^{o} for all $i \in \mathcal{I}$ and $t \in \mathcal{T}$, and the set of real numbers, respectively. Variables u_{it}^{n}, u_{it}^{u}, and u_{it}^{d} denote the on/off, start-up, and shut-down status of generator i at time period t, respectively; u_{it}^{n} being equal to 0 and 1 indicates that it is turned on and off at time period t, respectively; if it starts up at time period t, then u_{it}^{u} is set to 1; if it shuts down at time period t, then u_{it}^{d} is set to 1. Variable x_{it}^{g} denotes the power output of generator i at time period t. Variable u_{it}^{o} denotes the operating status of BESS i at time period t; if it is charging and discharging at time

period t, then u^{o}_{it} is set to 0 and 1, respectively. Variables x^{i}_{it} and x^{o}_{it} denote the power input and output of BESS i at time period t, respectively.

Constraints (2.1b)–(2.1l) in problem (2.1) are explained as follows: First, constraints (2.1b)–(2.1g) correspond to the operational constraints of the generators; (2.1b) to the logical constraint on the operating status; (2.1c) to the minimum up time constraint with T^{u}_i denoting the minimum up time of generator i; (2.1d) to the minimum down time constraint with T^{d}_i denoting the minimum down time of generator i; (2.1e) to the possible range of the power output of each generator at each time period with $\underline{X}_i$ and $\overline{X}_i$ denoting the minimum and maximum possible power output of generator i, respectively; (2.1f) to the ramp-up constraint with R^{u}_i and R^{su}_i denoting the ramp-up and start-up-ramp rates of generator i, respectively; (2.1g) to the ramp-down constraint with R^{d}_i and R^{sd}_i denoting the ramp-down and shut-down-ramp rates of generator i, respectively. Note that the constraint on the adjustment of the power output from each generator within each time period is not considered in the deterministic UC model. Furthermore, constraints (2.1h)–(2.1j) correspond to the operational constraints of the BESSs; (2.1h) to the possible range of the power input at each time period with Y^{i}_i denoting the maximum possible power input of BESS i; (2.1i) to the possible range of the power output at each time period with Y^{o}_i denoting the maximum possible power output of BESS i; (2.1j) to the storage constraint at each time period with E^{i}_i, E^{o}_i, S_{i0}, and S_i denoting the charging efficiency, discharging efficiency, initially stored energy, and storage capacity of BESS i, respectively. Finally, constraints (2.1k) and (2.1l) correspond to the systemwide constraints; (2.1k) to the power supply-demand balance condition with d_{it} and s_{it} denoting the power demand and the VRE generation at bus i and time period t, respectively; (2.1l) to the transmission capacity constraint with F_l and F_{il} denoting the power flow capacity of transmission line l and the power transfer distribution factor of bus i and transmission line l, respectively.

The objective function (2.1a) of problem (2.1) is the total operating cost, i.e., the sum of the fixed and variable operating costs of the power sources, where C^{n}_i, C^{u}_i, C^{d}_i, C^{g}_i, C^{i}_i, and C^{o}_i denote the no-load cost of generator i, the start-up cost of generator i, the shut-down cost of generator i, the marginal power output cost of generator i, the marginal power input cost of BESS i, and the marginal power output cost of BESS i, respectively.

For the sake of notational simplicity, let problem (2.1) be rewritten compactly as follows:

$$\min_{\mathbf{u}\in\mathcal{U},\mathbf{x}\in\mathcal{F}^{\mathrm{u}}(\mathbf{u})\cap\mathcal{F}^{\mathrm{s}}(\mathbf{s})} \mathbf{c}_1^{\top}\mathbf{u} + \mathbf{c}_2^{\top}\mathbf{x} \tag{2.2}$$

where $\mathbf{s}$ is a vector of s_{it} for all $i \in \mathcal{I}$ and $t \in \mathcal{T}$. Sets $\mathcal{U}$, $\mathcal{F}^{\mathrm{u}}(\mathbf{u})$, and $\mathcal{F}^{\mathrm{s}}(\mathbf{s})$ are defined as follows:

$$\begin{aligned}
\mathcal{U} &:= \left\{\mathbf{u} \in \{0,1\}^{4IT} : \text{(2.1b)–(2.1d)}\right\},\\
\mathcal{F}^{\mathrm{u}}(\mathbf{u}) &:= \left\{\mathbf{x} \in \mathbb{R}^{3IT} : \text{(2.1e)–(2.1j)}\ \right\},\\
\mathcal{F}^{\mathrm{s}}(\mathbf{s}) &:= \left\{\mathbf{x} \in \mathbb{R}^{3IT} : \text{(2.1k) and (2.1l)}\right\}.
\end{aligned}$$

Vectors $\mathbf{c}_1$ and $\mathbf{c}_2$ are such that

$$\mathbf{c}_1^\top \mathbf{u} = \sum_{t\in\mathcal{T}} \sum_{i\in\mathcal{I}} C_i^{\mathrm{n}} u_{it}^{\mathrm{n}} + C_i^{\mathrm{u}} u_{it}^{\mathrm{u}} + C_i^{\mathrm{d}} u_{it}^{\mathrm{d}}$$

and

$$\mathbf{c}_2^\top \mathbf{x} = \sum_{t\in\mathcal{T}} \sum_{i\in\mathcal{I}} C_i^{\mathrm{g}} x_{it}^{\mathrm{g}} + C_i^{\mathrm{i}} x_{it}^{\mathrm{i}} + C_i^{\mathrm{o}} x_{it}^{\mathrm{o}}$$

represent the fixed and the variable operating costs of the power sources, respectively.

Problem (2.1) can readily be solved by using various off-the-shelf solvers [49]. However, the solution may not satisfy the systemwide constraints (2.1k) and (2.1l) when the power demand or VRE generation deviates from the predicted values. In the following section, the uncertainty of VRE generation is modeled. For the sake of simplicity, the power demand at each bus and time period is assumed to be precisely known.

2.4 Uncertainty Modeling

The proposed model uses a worst-case analysis, for which a set of possible VRE generation scenarios has to be built. In this chapter, it is assumed that the scenario set is constructed by using an interval prediction method for simplicity [50]–[53], which yields an upper and a lower limit of the VRE generation at each bus and time period; to model the spatiotemporal correlation of VRE generation, a finite number of linear may be added. Specifically, the scenario set is defined as follows:

$$\mathcal{S} := \left\{ \mathbf{s} \in \mathbb{R}^{IT} : \underline{s}_{it} \leq s_{it} \leq \overline{s}_{it}, \quad \forall i \in \mathcal{I}, \forall t \in \mathcal{T} \right\}$$

where $\underline{s}_{it}$ and $\overline{s}_{it}$ denote the lower and upper limits of s_{it}, respectively. By using the proposed model, the total operating cost associated with worst-case scenarios of VRE generation in $\mathcal{S}$ can be minimized. In the following section, the mathematical formulation of the proposed model is given.

2.5 Problem Formulation

The proposed model is based on the following existing two-stage robust UC model [21]:

$$\min_{\mathbf{u}\in\mathcal{U}} \left\{ \mathbf{c}_1^\top \mathbf{u} + \max_{\mathbf{s}\in\mathcal{S}} f^{\mathrm{a}}(\mathbf{u}, \mathbf{s}) \right\} \tag{2.3}$$

where the objective function is the worst-case total operating cost and $f^{\mathrm{a}}(\mathbf{u}, \mathbf{s})$ is defined as the optimal value of the following linear programming (LP) problem:

$$\min_{\mathbf{x}\in\mathcal{F}^{\mathrm{u}}(\mathbf{u})\cap\mathcal{F}^{\mathrm{s}}(\mathbf{s})} \mathbf{c}_2^\top \mathbf{x}. \tag{2.4}$$

This model is implemented as follows: First, problem (2.3) is solved at the day-ahead stage for the scenario set $\mathcal{S}$ to determine the operating status $\mathbf{u}$. Subsequently, problem

(2.4) is solved at the real-time stage to determine the operating level $\mathbf{x}$ for the actual VRE generation $\mathbf{s}$. Notably, problem (2.4) is a multi-period ED problem; the optimal operating level of each power source at each time period depends on the VRE generation at all the time periods, which hinders the non-anticipative real-time decision-making. More specifically, this is due to the dynamic constraints implied by $\mathcal{F}^{\mathrm{u}}(\mathbf{u})$, i.e., the ramp limit constraints (2.1f) and (2.1g) of the generators and the storage capacity constraint (2.1j) of the BESSs. To enable the non-anticipative real-time decision-making, the proposed model replaces $\mathcal{F}^{\mathrm{u}}(\mathbf{u})$ by another set without any dynamic constraint. This new set is defined by the minimum and maximum allowable operating levels of each power source at each time period, which are determined with the operating status at the day-ahead stage.

Let $\overline{x}^{\mathrm{g}}_{it}$, $\overline{x}^{\mathrm{i}}_{it}$, $\overline{x}^{\mathrm{o}}_{it}$, and $\overline{\mathbf{x}}$ denote the maximum allowable power output of generator i at time period t, the maximum allowable charging power of BESS i at time period t, the maximum allowable discharging power of BESS i at time period t, and a vector of $\overline{x}^{\mathrm{g}}_{it}$, $\overline{x}^{\mathrm{i}}_{it}$, and $\overline{x}^{\mathrm{o}}_{it}$ for all $i \in \mathcal{I}$ and $t \in \mathcal{T}$, respectively. Let also $\underline{x}^{\mathrm{g}}_{it}$, $\underline{x}^{\mathrm{i}}_{it}$, $\underline{x}^{\mathrm{o}}_{it}$, and $\underline{\mathbf{x}}$ denote the minimum allowable power output of generator i at time period t, the minimum allowable charging power of BESS i at time period t, the minimum allowable discharging power of BESS i at time period t, and a vector of $\underline{x}^{\mathrm{g}}_{it}$, $\underline{x}^{\mathrm{i}}_{it}$, and $\underline{x}^{\mathrm{o}}_{it}$ for all $i \in \mathcal{I}$ and $t \in \mathcal{T}$, respectively. The proposed model is formulated as follows:

$$\min_{\mathbf{u}\in\mathcal{U},(\overline{\mathbf{x}},\underline{\mathbf{x}})\in\mathcal{X}(\mathbf{u})} \left\{ \mathbf{c}_1^\top \mathbf{u} + \max_{\mathbf{s}\in\mathcal{S}} f\left(\overline{\mathbf{x}}, \underline{\mathbf{x}}, \mathbf{s}\right) \right\} \tag{2.5}$$

where the objective function is the worst-case total operating cost and $f\left(\overline{\mathbf{x}}, \underline{\mathbf{x}}, \mathbf{s}\right)$ is defined as the optimal value of the following LP problem:

$$\min_{\mathbf{x}\in[\underline{\mathbf{x}},\overline{\mathbf{x}}]\cap\mathcal{F}^{\mathrm{s}}(\mathbf{s})} \mathbf{c}_2^\top \mathbf{x}. \tag{2.6}$$

Note the difference of the feasible sets $\mathcal{F}^{\mathrm{u}}\left(\mathbf{u}\right) \cap \mathcal{F}^{\mathrm{s}}\left(\mathbf{s}\right)$ of problem (2.4) and $[\underline{\mathbf{x}}, \overline{\mathbf{x}}] \cap \mathcal{F}^{\mathrm{s}}\left(\mathbf{s}\right)$ of problem (2.6). Problem (2.6) is seemingly a multi-period ED problem associated with all the T time periods, but contains none of the dynamic constraints of the power sources. Thus, problem (2.6) can be considered as a series of temporally decoupled T single-period ED problems each of which is parameterized by the VRE generation at each time period. Consequently, the operating level of each power source at each time period can be determined based on the VRE generation only at the same time period.

Meanwhile, the constraints (2.1e)–(2.1j) of the operating level have to be satisfied in any case. That is to say, $\mathbf{x}$ still has to be in $\mathcal{F}^{\mathrm{u}}\left(\mathbf{u}\right)$. Therefore, set $\mathcal{X}\left(\mathbf{u}\right)$ is defined as follows:

$$\mathcal{X}\left(\mathbf{u}\right) := \Big\{ \left(\overline{\mathbf{x}}, \underline{\mathbf{x}}\right) \in \mathbb{R}^{3IT} \times \mathbb{R}^{3IT} : \underline{X}_i u^{\mathrm{n}}_{it} \le \underline{x}^{\mathrm{g}}_{it} \le \overline{x}^{\mathrm{g}}_{it} \le \overline{X}_i u^{\mathrm{n}}_{it}, \quad \forall i \in \mathcal{I}, \forall t \in \mathcal{T}, \tag{2.7a}$$

$$\overline{x}^{\mathrm{g}}_{it} - \underline{x}^{\mathrm{g}}_{i(t-1)} \le R^{\mathrm{u}}_i u^{\mathrm{n}}_{i(t-1)} + R^{\mathrm{su}}_i u^{\mathrm{u}}_{it}, \quad \forall i \in \mathcal{I}, \forall t \in \mathcal{T}, \tag{2.7b}$$

$$\overline{x}^{\mathrm{g}}_{i(t-1)} - \underline{x}^{\mathrm{g}}_{it} \le R^{\mathrm{d}}_i u^{\mathrm{n}}_{it} + R^{\mathrm{sd}}_i u^{\mathrm{d}}_{it}, \quad \forall i \in \mathcal{I}, \forall t \in \mathcal{T}, \tag{2.7c}$$

$$\overline{x}^{\mathrm{g}}_{it} - \underline{x}^{\mathrm{g}}_{it} \le X^{\mathrm{r}}_i, \quad \forall i \in \mathcal{I}, \forall t \in \mathcal{T}, \tag{2.7d}$$

$$0 \le \underline{x}^{\mathrm{i}}_{it} \le \overline{x}^{\mathrm{i}}_{it} \le X^{\mathrm{i}}_{i}\left(1-u^{\mathrm{o}}_{it}\right), \quad \forall i \in \mathcal{I}, \forall t \in \mathcal{T}, \tag{2.7e}$$

$$0 \le \underline{x}^{\mathrm{o}}_{it} \le \overline{x}^{\mathrm{o}}_{it} \le X^{\mathrm{o}}_{i} u^{\mathrm{o}}_{it}, \quad \forall i \in \mathcal{I}, \forall t \in \mathcal{T}, \tag{2.7f}$$

$$0 \le S_{i0} + \sum_{\tau=1}^{t}\left(E^{\mathrm{i}}_{i}\underline{x}^{\mathrm{i}}_{it} - \frac{1}{E^{\mathrm{o}}_{i}}\overline{x}^{\mathrm{o}}_{it}\right), \quad \forall i \in \mathcal{I}, \forall t \in \mathcal{T}, \tag{2.7g}$$

$$S^{\mathrm{s}}_{i0} + \sum_{\tau=1}^{t}\left(E^{\mathrm{i}}_{i}\overline{x}^{\mathrm{i}}_{it} - \frac{1}{E^{\mathrm{o}}_{i}}\underline{x}^{\mathrm{o}}_{it}\right) \le S_{i}, \quad \forall i \in \mathcal{I}, \forall t \in \mathcal{T}\Big\} \tag{2.7h}$$

where constraints (2.7a)–(2.7c), (2.7e)–(2.7h) enforce that any $\mathbf{x} \in [\underline{\mathbf{x}}, \overline{\mathbf{x}}]$ satisfies constraints (2.1e)–(2.1j). Specifically, (2.1e) is guaranteed to be met by (2.7a); (2.1f) by (2.7b); (2.1g) by (2.7c); (2.1h) by (2.7e); (2.1i) by (2.7f); (2.1j) by (2.7g) and (2.7h). In other words, if $(\overline{\mathbf{x}}, \underline{\mathbf{x}}) \in \mathcal{X}(\mathbf{u})$, then $[\underline{\mathbf{x}}, \overline{\mathbf{x}}] \subseteq \mathcal{F}^{\mathrm{u}}(\mathbf{u})$ and thus a solution to problem (2.6) meets all the operational constraints of the power sources and the systemwide constraints. Furthermore, constraint (2.7d) limits the adjustment of the operating level of each generator at each time period, where X^{r}_{i} denotes the maximum possible spinning reserve of generator i.

The proposed model is implemented as follows: First, problem (2.5) is solved at the day-ahead stage for the scenario set $\mathcal{S}$ to determine the operating status and range of the power sources. Subsequently, the T single-period ED problems contained in problem (2.6) are sequentially solved at the T real-time stages to determine the operating level for the actual VRE generation. Fortunately, problem (2.5) is a two-stage robust optimization problem, or more specifically a min-max-min problem, for which many existing algorithms are readily available. In the following section, one of the existing algorithms is described.

2.6 Solution Method

Many of the existing robust UC models considering the uncertainty of VRE generation are solved by using Benders decomposition [20]–[22], [54] or the column-and-constraint generation (C&CG) algorithm [28], [55], both of which are iterative decomposition algorithms. In this dissertation, problem (2.5) is solved by using the latter as it is reportedly faster than the former [55]. In the algorithm, a master problem and two subproblems are iteratively solved to obtain a transient solution and test its feasibility and optimality.

The algorithm is described as follows: For initialization, any $\mathbf{s}^{\mathrm{w}}_{1} \in \mathcal{S}$ is selected and the iteration step P is set to 1. At each iteration step $P \ge 1$, the master problem is solved, which is formulated as the following MILP problem:

$$\min_{\mathbf{u}\in\mathcal{U},(\overline{\mathbf{x}},\underline{\mathbf{x}})\in\mathcal{X}(\mathbf{u}),\eta\in\mathbb{R},\mathbf{x}_p\in[\underline{\mathbf{x}},\overline{\mathbf{x}}]\cap\mathcal{F}^{\mathrm{s}}\left(\mathbf{s}^{\mathrm{w}}_{p}\right)} \mathbf{c}_{1}^{\top}\mathbf{u} + \eta \quad \text{s.t.} \quad \eta \ge \mathbf{c}_{2}^{\top}\mathbf{x}_{p}, \quad p = 1, \ldots, P \tag{2.8}$$

where $\mathbf{x}_p$ corresponds to the decision vector of problem (2.6) for $\mathbf{s} = \mathbf{s}^{\mathrm{w}}_{p}$. Let $(\mathbf{u}_P, \overline{\mathbf{x}}_P, \underline{\mathbf{x}}_P)$ denote the solution of problem (2.8) corresponding to $(\mathbf{u}, \overline{\mathbf{x}}, \underline{\mathbf{x}})$. Let also L_P denote the optimal value of problem (2.8). Note that problem (2.8) is a relaxation of problem (2.5), i.e., L_P is a lower bound of the optimal value of problem (2.5). Subsequently, the feasibility of the transient solution is tested by solving the first subproblem, which is formulated as

follows:

$$\max_{\mathbf{s}\in\mathcal{S},\boldsymbol{\xi}^{\mathrm{f}}\in\Xi^{\mathrm{f}}} \pi^{\top}\left(\overline{\mathbf{x}}_P,\underline{\mathbf{x}}_P,\mathbf{s}\right)\boldsymbol{\xi}^{\mathrm{f}} \tag{2.9}$$

where $\boldsymbol{\xi}^{\mathrm{f}}$, Ξ^{f}, and $\pi\left(\overline{\mathbf{x}},\underline{\mathbf{x}},\mathbf{s}\right)$ are a vector of the dual variables, the feasible set of $\boldsymbol{\xi}^{\mathrm{f}}$, and a vector of the coefficients in the dual function, respectively, all associated with a minimization problem of the total amount of violation of the systemwide constraints in problem (2.6). This minimization problem is formulated as an LP problem based on problem (2.6), specifically, by introducing auxiliary variables and modifying the objective function. Then, it follows from strong duality that the optimal value of problem (2.9) is equal to the worst-case total amount of violence of the systemwide constraints [56].

Let $\mathbf{s}^{\mathrm{w}}_{P+1}$ and V_P denote the solution corresponding to $\mathbf{s}$ and the optimal value of problem (2.9), respectively. If $V_P > \epsilon^{\mathrm{f}}$, where ϵ^{f} is a predefined tolerance, then it is implied that implementing $[\underline{\mathbf{x}}_P,\overline{\mathbf{x}}_P]$ as the operating range at the real-time stages may lead to a power supply-demand imbalance. In this case, the iteration step increase to $P+1$ and the master problem (2.8) is solved again. Otherwise, the second subproblem is solved to test the optimality of the transient solution, which is formulated as follows:

$$\max_{\mathbf{s}\in\mathcal{S},\boldsymbol{\xi}^{\mathrm{o}}\in\Xi^{\mathrm{o}}} \rho^{\top}\left(\overline{\mathbf{x}}_P,\underline{\mathbf{x}}_P,\mathbf{s}\right)\boldsymbol{\xi}^{\mathrm{o}} \tag{2.10}$$

where $\boldsymbol{\xi}^{\mathrm{o}}$, Ξ^{o}, and $\rho\left(\overline{\mathbf{x}},\underline{\mathbf{x}},\mathbf{s}\right)$ denote a vector of the dual variables, the feasible set of $\boldsymbol{\xi}^{\mathrm{o}}$, and a vector of the coefficients in the dual function associated with problem (2.6), respectively. Due to strong duality, the optimal value of problem (2.10) is equal to the worst-case variable operating cost when $[\underline{\mathbf{x}}_P,\overline{\mathbf{x}}_P]$ is implemented as the operating range at the real-time stages.

Let $\left(\mathbf{s}^{\mathrm{w}}_{P+1},\boldsymbol{\xi}^{\mathrm{o}}_P\right)$ denote the solution of problem (2.10). Let also

$$U_P := \mathbf{u}_P^{\top} + \rho^{\top}\left(\overline{\mathbf{x}}_P,\underline{\mathbf{x}}_P,\mathbf{s}^{\mathrm{w}}_{P+1}\right)\boldsymbol{\xi}^{\mathrm{o}}_P,$$

which is an upper bound of the optimal value of problem (2.5). If $U_P - L_P > \epsilon^{\mathrm{o}}$, where ϵ^{o} is a predefined tolerance, then it is implied that the transient solution does not minimize the worst-case total operating cost within the acceptable error range. In this case, the iteration step increases to $P+1$ and the master problem (2.8) is solved again. Otherwise, the algorithm terminates and $(\mathbf{u}_P,\overline{\mathbf{x}}_P,\underline{\mathbf{x}}_P)$ is returned as a solution of problem (2.5). At each iteration step $P \geq 1$, if either $V_P > \epsilon^{\mathrm{f}}$ or $U_P - L_P > \epsilon^{\mathrm{o}}$, then it is implied that $\mathbf{s}^{\mathrm{w}}_{P+1}$ is not equal to $\mathbf{s}^{\mathrm{w}}_p$ for any $p \leq P$. This indicates that L_P increases with P and approaches the optimal value of problem (2.5).

Meanwhile, the objective functions of the subproblems (2.9) and (2.10) include bilinear terms and cannot be readily solved. Common approaches for solving such problems include the Big M method [57] and the outer approximation method [58], [59]. Using the Big M method, each subproblem is rewritten as an MILP problem with auxiliary binary variables introduced, guaranteeing the global optimality of the solution [20], [28], [55]. However, the scalability issue may be faced depending on the number of additional binary variables. In the outer approximation method, on the other hand, the bilinear terms are iteratively linearized around transient solutions. Although not guaranteeing the global optimality, this

method is shown to be computationally efficient in various power system planning models based on robust optimization [21], [27], [30], [60]. For this reason, in this dissertation, the two subproblems are addressed using the outer approximation method.

The outer approximation method for solving the first subproblem (2.9) is described as follows: For initialization, any $\mathbf{s}_1^{\mathrm{f}} \in \mathcal{S}$ is selected and the iteration step Q is set to 1. At each iteration step $Q \geq 1$, the following LP problem is solved:

$$\max_{\boldsymbol{\xi}^{\mathrm{f}} \in \Xi^{\mathrm{f}}} \phi^{\top}\left(\overline{\mathbf{x}}_P, \underline{\mathbf{x}}_P\right) \boldsymbol{\xi}^{\mathrm{f1}} + \left(\mathbf{s}_Q^{\mathrm{f}}\right)^{\top} \mathbf{A} \boldsymbol{\xi}^{\mathrm{f2}} \tag{2.11}$$

where subvectors $\boldsymbol{\xi}^{\mathrm{f1}}$ and $\boldsymbol{\xi}^{\mathrm{f2}}$ of $\boldsymbol{\xi}^{\mathrm{f}}$, vector $\phi\left(\overline{\mathbf{x}}, \underline{\mathbf{x}}\right)$, and matrix $\mathbf{A}$ are such that

$$\pi^{\top}\left(\overline{\mathbf{x}}, \underline{\mathbf{x}}, \mathbf{s}\right) \boldsymbol{\xi}^{\mathrm{f}} = \phi^{\top}\left(\overline{\mathbf{x}}, \underline{\mathbf{x}}\right) \boldsymbol{\xi}^{\mathrm{f1}} + \mathbf{s}^{\top} \mathbf{A} \boldsymbol{\xi}^{\mathrm{f2}}.$$

Let $\boldsymbol{\xi}_Q^{\mathrm{f}}$ and L_Q^{f} denote the solution and the optimal value of problem (2.11), respectively. Let also $\boldsymbol{\xi}_Q^{\mathrm{f2}}$ denote the subvector of $\boldsymbol{\xi}_Q^{\mathrm{f}}$ corresponding to $\boldsymbol{\xi}^{\mathrm{f2}}$ of $\boldsymbol{\xi}^{\mathrm{f}}$. Subsequently, the following LP problem is solved:

$$\max_{\mathbf{s} \in \mathcal{S}, \boldsymbol{\xi}^{\mathrm{f}} \in \Xi^{\mathrm{f}}, \zeta \in \mathbb{R}} \pi^{\top}\left(\overline{\mathbf{x}}_P, \underline{\mathbf{x}}_P\right) \boldsymbol{\xi}^{\mathrm{f1}} + \zeta \quad \text{s.t.} \quad \zeta \leq \lambda\left(\mathbf{s}, \mathbf{s}_q^{\mathrm{f}}, \boldsymbol{\xi}^{\mathrm{f2}}, \boldsymbol{\xi}_q^{\mathrm{f2}}\right), \quad q = 1, \ldots, Q \tag{2.12}$$

where

$$\lambda\left(\mathbf{s}, \mathbf{s}_q^{\mathrm{f}}, \boldsymbol{\xi}^{\mathrm{f2}}, \boldsymbol{\xi}_q^{\mathrm{f2}}\right) := \left(\mathbf{s}_q^{\mathrm{f}}\right)^{\top} \mathbf{A} \boldsymbol{\xi}^{\mathrm{f2}} + \mathbf{s}^{\top} \mathbf{A} \boldsymbol{\xi}_q^{\mathrm{f2}} - \left(\mathbf{s}_q^{\mathrm{f}}\right)^{\top} \mathbf{A} \boldsymbol{\xi}_q^{\mathrm{f2}}$$

is the linearization of the bilinear term $\mathbf{s}^{\top} \mathbf{A} \boldsymbol{\xi}^{\mathrm{f2}}$ around $\left(\mathbf{s}, \boldsymbol{\xi}^{\mathrm{f2}}\right) = \left(\mathbf{s}_q^{\mathrm{f}}, \boldsymbol{\xi}_q^{\mathrm{f2}}\right)$. Let $\mathbf{s}_{Q+1}^{\mathrm{f}}$ and U_Q^{f} denote the solution corresponding to $\mathbf{s}$ and the optimal value of problem (2.12), respectively. If $U_Q^{\mathrm{f}} - L_Q^{\mathrm{f}} > \varepsilon^{\mathrm{s}}$, where ε^{s} is a predefined tolerance, then the iteration step increases to $Q+1$ and problems (2.11) and (2.12) are solved again. Otherwise, the iteration terminates and $\mathbf{s}_{P+1}^{\mathrm{w}}$ is set to $\mathbf{s}_Q^{\mathrm{f}}$ as an acceptable solution to problem (2.9). The outer approximation method for the second subproblem (2.10) is applied in the same way.

Fig. 4.1 illustrates the C&CG algorithm combined with the outer approximation method for solving problem (2.5). In the following section, performances of the proposed model are examined through numerical simulations.

2.7 Numerical Simulations

This section tests performances of the proposed model via numerical simulations. In the simulations, the proposed model is compared with the affine-policy-based model in [33] with respect to the optimality on a 24-bus and a 300-bus test system. In the following subsection, the simulation scheme and results for the 24-bus test system are explained.

2.7.1 24-bus Test System

The 24-bus test system consists of 12 generators, 17 loads, three wind farms, three BESSs, and 34 transmission lines, the parameters of which are shown in Appendix A. The planning horizon is discretized with 24 hourly time periods. Each load and wind farm have

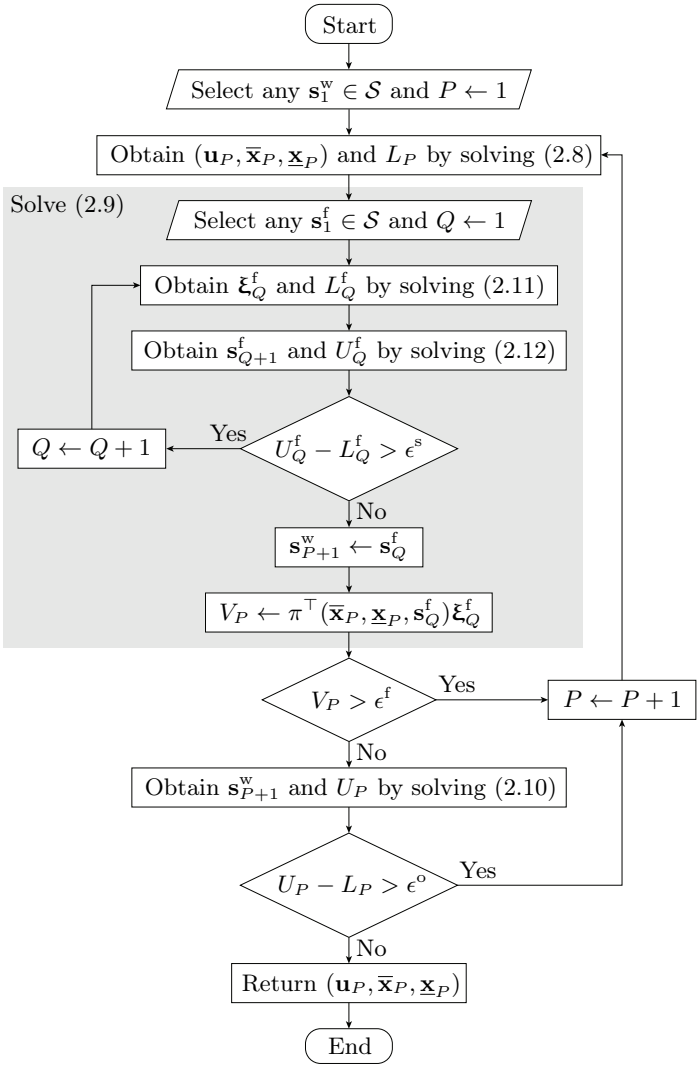

Fig. 2.1. Solution method for problem (2.5).

an associated demand profile and nominal wind power scenario, respectively. The wind penetration level of the test system, defined in this dissertation as the fraction of the total wind power capacity to the peak demand, is 22.64%. To build the scenario set, the upper and lower limits of the output from each wind farm at each time period are set above and below the nominal value, respectively, so that their difference is equal to $\alpha = 0.1, 0.2, \ldots, 1$ times the wind farm capacity. Fig. 2.2 shows the nominal wind power scenario and the scenario sets with the different values of α for wind farm 1.

For each value of α, the simulations are conducted as follows: First, the proposed and the affine-policy-based models are solved to calculate the worst-case total operating costs. Subsequently, the actual total operating costs for 100 wind power scenarios randomly chosen from the scenario set are calculated. The simulations are run on MATLAB R2020b with CPLEX 12.10 using a computer featuring an Intel Core i9 processor and 64 GB of RAM. The convergence tolerances in the C&CG algorithm are set to 10^{-6}; those in the MIP solver are set to the default values. Moreover, any initial guess required in the C&CG

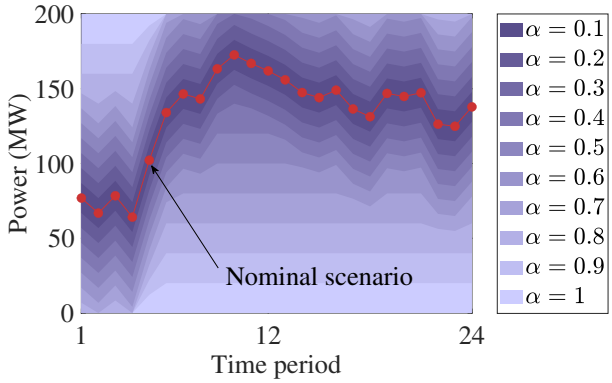

Fig. 2.2. Nominal scenario and scenario sets for wind farm 1 in the 24-bus test system.

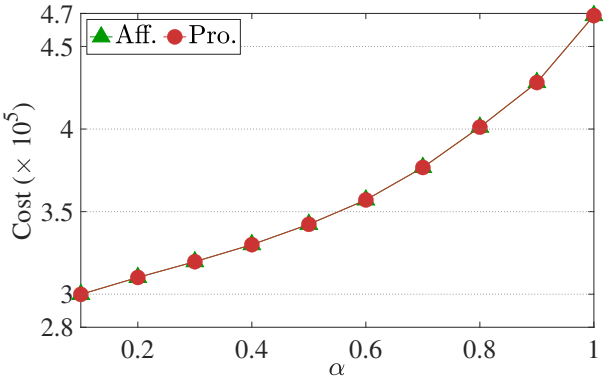

Fig. 2.3. Worst-case total operating costs of the 24-bus test system.

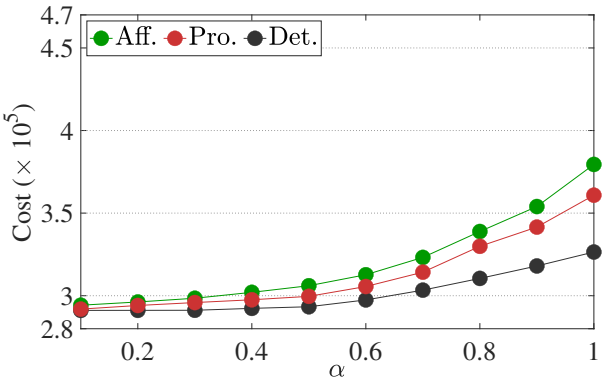

Fig. 2.4. Average actual total operating costs of the 24-bus test system.

algorithm is randomly selected. With these settings, the proposed and the affined-policy-based models are solved averagely in 2.88 s and 1.86 s, respectively.

The simulation results are presented in Figs. 2.3 to 2.5. Fig. 2.3 shows the worst-case total operating costs incurred by the proposed and the affined-policy-based models. It is observed that both models yield the same worst-case total operating cost for each value of α. Fig. 2.4 shows the average actual total operating costs incurred by the proposed and the affine-policy-based models. For reference, the minimum possible values of the average actual total operating cost are also plotted, obtained by solving the deterministic model (2.1). It is seen that the proposed model reduces the actual total operating cost

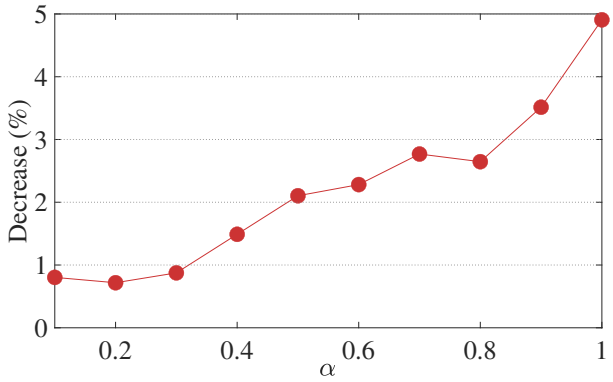

Fig. 2.5. Average percentage decreases in the actual total operating cost of the 24-bus test system.

in average compared with the affine-policy-based model for all the values of α. Fig. 2.5 shows the average percentage decreases from the actual total operating cost incurred by the affine-policy-based model to that incurred by the proposed model. The average percentage decrease tends to increase with α, implying that the more uncertain the VRE generation is, the more effective the proposed model is compared with the affine-policy-based model.

In this subsection, the scenario sets are built by setting the differences between the upper and lower limits of wind power equally for all the time periods. In the following subsection, a more practical setup is used with the 300-bus test system.

2.7.2 300-bus Test System

The 300-bus test system consists of 69 generators, 191 loads, 15 wind farms, 15 BESSs, and 411 transmission lines, the parameters of which are shown in Appendix B. The planning horizon is discretized with 24 hourly time periods. Each load and wind farm have an associated demand profile and nominal wind power scenario. The penetration level of wind power in this test system is 22.01%. In this subsection, the scenario set is constructed based on empirical data shown in Figure 20 in [61]. This figure illustrates how the fraction of the interval size, i.e., the difference between the upper and lower limits of wind power obtained by using the interval prediction method, to the wind farm capacity varies with look-ahead time from 2 h to 36 h. Based on these data, first, a profile of the fraction of the interval size to the wind farm capacity is generated as in Fig. 2.6, which is above the curves in Figure 20 in [61]. The upper and lower limits of wind power at each time period are then set so that the profile of the interval size over the planning horizon is identical to the profile in Fig. 2.6 for look-ahead times from 13 h to 36 h multiplied by the wind farm capacity. The largest look-ahead time of 36 h is chosen considering the values adopted by existing day-ahead electricity markets where the UC problem is solved [61], [62]. Fig. 2.7 shows the nominal scenario and the scenario set for wind farm 1.

For the resulting scenario set, the simulations are conducted in the same way as in the previous subsection with the optimality tolerance in the C&CG algorithm changed to 10^{-3} as a relative tolerance. As a consequence, the proposed and the affine-policy-based models are solved in 399.37 s and 50.78 s, respectively. The simulation results are as follows: Both

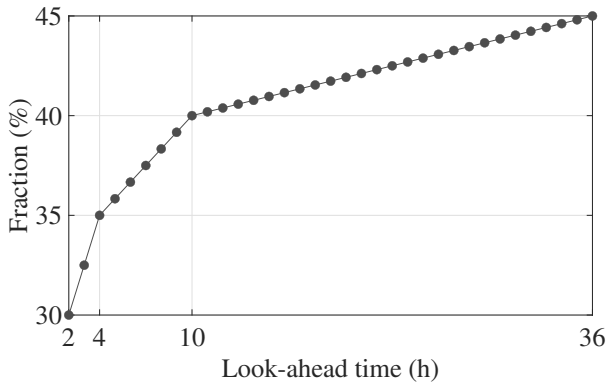

Fig. 2.6. Fraction of the interval size to the wind farm capacity in the 300-bus test system.

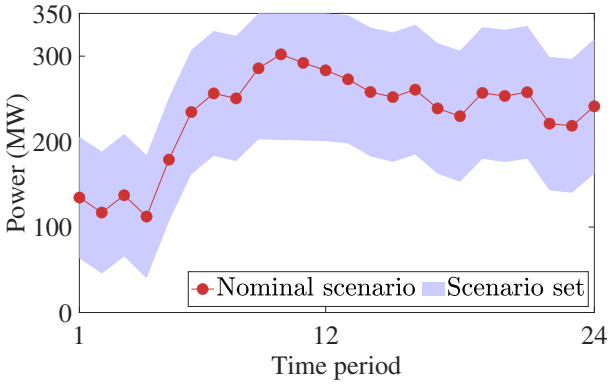

Fig. 2.7. Nominal scenario and scenario set for wind farm 1 in the 300-bus test system.

models yield the same worst-case total operating cost of 1.37×10^7. Furthermore, the average actual total operating costs incurred by the proposed, the affine-policy-based, and the deterministic models are equal to 1.19×10^7, 1.25×10^7, and 1.15×10^7, respectively. Notably, the proposed model lowers the actual total operating cost compared with the affine-policy-based model for all the 100 randomly chosen scenarios, averagely by 4.63%.

Through the numerical simulations on the two test systems, it is verified that the proposed model is more economical than the affine-policy-based model in terms of the actual total operating cost. However, as the objective of the proposed model is to minimize the worst-case total operating cost, the actual total operating cost might still be high. In the following two sections, the two supplementary methods for the proposed model are developed to reduce the actual total operating cost. The first method can be used to minimize the expected total operating cost for some representative VRE generation scenarios that are considered more probable, allowing an increase in the worst-case total operating cost up to a specified level. Integrating the framework of stochastic programming, this method requires modifications of the objective function of the proposed model and is thus explained in the form of another UC model, hereafter referred to simply as the modified model. Meanwhile, the second method seeks to increase the chance of reducing the actual total operating cost still minimizing the worst-case total operating cost. This method is applied after the proposed model, and thus explained independently.

2.8 Cost Reduction via Integration of Stochastic UC

In this section, the modified model as the first supplementary method for the proposed model is described. Combining the frameworks of stochastic programming and robust optimization, the modified model minimizes the expected total operating cost for some preselected VRE generation scenarios that are more probable with the worst-case total operating cost bounded by a predefined value. Another way of considering both the expected and the worst-case total operating costs is to minimize their weighted sum [22]. However, it is not easy to find proper weighting factors leading to an acceptable solution before actually solving the UC model [63]. In the modified model, the parameter affecting the trade-off between the expected and the worst-case total operating costs, i.e., the maximum allowable worst-case total operating cost, is in a monetary unit and thus can be set more intuitively.

Let $\mathcal{J} := \{1, \ldots, J\}$ and $\mathbf{s}_j \in \mathcal{S}$ for each $j \in \mathcal{J}$ denote the index set for the preselected scenarios of VRE generation and scenario j, respectively. Based on the proposed model (2.5), the modified model is formulated as follows:

$$\min_{\mathbf{u}\in\mathcal{U},(\overline{\mathbf{x}},\underline{\mathbf{x}})\in\mathcal{X}(\mathbf{u})} \mathbf{c}_1^\top \mathbf{u} + \sum_{j\in\mathcal{J}} W_j f\left(\overline{\mathbf{x}}, \underline{\mathbf{x}}, \mathbf{s}_j\right) \tag{2.13a}$$

$$\text{s.t.} \quad \overline{\eta} \geq \mathbf{c}_1^\top \mathbf{u} + \max_{\mathbf{s}\in\mathcal{S}} f\left(\overline{\mathbf{x}}, \underline{\mathbf{x}}, \mathbf{s}\right) \tag{2.13b}$$

where the objective function (2.13a) is the expected total operating cost for the preselected scenarios with W_j denoting the probability associated with scenario j. Constraint (2.13b) ensures that the worst-case total operating cost never exceeds $\overline{\eta} \in \mathbb{R}$ set by the system operator.

One straightforward way to solve problem (2.13) is to introduce a decision vector corresponding to $\mathbf{x}$ for each preselected scenario and apply the C&CG algorithm. However, this approach may cause memory shortage as the number of preselected scenarios increases. To avoid this computational issue, problem (2.13) is solved by using the C&CG algorithm combined with Benders decomposition. In Benders decomposition for a two-stage robust optimization problem, similarly to the C&CG algorithm, a master problem and one or more subproblems are iteratively solved. However, differently from the C&CG algorithm, only one or more of the most violated constraints, but not decision variables, are added to the master problem. Benders decomposition is widely studied for not only robust UC models [20]–[22] but stochastic UC models [64], [65]. To further apply Benders decomposition, problem (2.13) is first rewritten as follows:

$$\begin{aligned}
&\min_{\mathbf{u}\in\mathcal{U},(\overline{\mathbf{x}},\underline{\mathbf{x}})\in\mathcal{X}(\mathbf{u}),\eta_j} \mathbf{c}_1^\top \mathbf{u} + \sum_{j\in\mathcal{J}} W_j \eta_j \\
&\text{s.t.} \quad \overline{\eta} \geq \mathbf{c}_1^\top \mathbf{u} + f\left(\overline{\mathbf{x}}, \underline{\mathbf{x}}, \mathbf{s}\right), \quad \forall \mathbf{s} \in \mathcal{S}, \\
&\eta_j \geq \rho^\top \left(\overline{\mathbf{x}}, \underline{\mathbf{x}}, \mathbf{s}_j\right) \boldsymbol{\xi}, \quad \forall \boldsymbol{\xi} \in \Xi^{\mathrm{o}}, \forall j \in \mathcal{J}
\end{aligned} \tag{2.14}$$

where η_j is an auxiliary variable introduced to minimize $f\left(\overline{\mathbf{x}}, \underline{\mathbf{x}}, \mathbf{s}_j\right)$. Note that, due to strong duality, the last constraint in problem (2.14) is rewritten as follows:

$$\eta_j \geq f\left(\overline{\mathbf{x}}, \underline{\mathbf{x}}, \mathbf{s}_j\right), \quad \forall j \in \mathcal{J}.$$

The solution method for problem (2.14) combining the C&CG algorithm and Benders decomposition is described as follows: For initialization, any $\mathbf{s}_1^{\mathrm{w}} \in \mathcal{S}$ and $\boldsymbol{\xi}_1^j \in \Xi$ for all $j \in \mathcal{J}$ are selected. Furthermore, R, P_1, and Q_1^j for all $j \in \mathcal{J}$ are set to 1. At each iteration step $R \geq 1$, the following master problem is solved:

$$\begin{aligned} \min_{\mathbf{u}\in\mathcal{U},(\overline{\mathbf{x}},\underline{\mathbf{x}})\in\mathcal{X}(\mathbf{u}),\eta_j\in\mathbb{R},\mathbf{x}_p\in[\underline{\mathbf{x}},\overline{\mathbf{x}}]\cap\mathcal{F}^{\mathrm{s}}\left(\mathbf{s}_p^{\mathrm{w}}\right)} & \mathbf{c}_1^\top \mathbf{u} + \sum_{j\in\mathcal{J}} W_j \eta_j \\ \text{s.t.} \quad & \overline{\eta} \geq \mathbf{c}_1^\top \mathbf{u} + \mathbf{c}_2^\top \mathbf{x}_p, \quad p = 1, \ldots, P_R, \\ & \eta_j \geq \rho^\top \left(\overline{\mathbf{x}}, \underline{\mathbf{x}}, \mathbf{s}_j\right) \boldsymbol{\xi}_q^j, \quad q = 1, \ldots, Q_R^j, \ \forall j \in \mathcal{J} \end{aligned} \tag{2.15}$$

where $\mathbf{x}_p$ corresponds to the decision vector of problem (2.6) for $\mathbf{s} = \mathbf{s}_p^{\mathrm{w}}$. Let L_R denote the optimal value of problem (2.15), which is a lower bound of the optimal value of problem (2.14). Let also $(\mathbf{u}_R, \overline{\mathbf{x}}_R, \underline{\mathbf{x}}_R, \eta_R^j)$ denote the solution corresponding to $(\mathbf{u}, \overline{\mathbf{x}}, \underline{\mathbf{x}}, \eta^j)$ of problem (2.15). Subsequently, the first subproblem of the problem (2.14) is solved to check the feasibility of $(\overline{\mathbf{x}}_R, \underline{\mathbf{x}}_R)$ with respect to the systemwide constraints. As in the case of the proposed model (2.5), the first subproblem is formulated as problem (2.9). Let V_R and $\mathbf{s}_p^{\mathrm{w}}$ for $p = P_{R+1}$ denote the optimal value and the solution corresponding to $\mathbf{s}$ of problem (2.9), respectively. If $V_R > 0$, then the iteration step increases to $R + 1$ and the master problem (2.15) is solved again with $P_{R+1} = P_R + 1$ and $Q_{R+1}^j = Q_R^j$ for all $j \in \mathcal{J}$. If $V_R = 0$, then the second subproblem of problem (2.14) is solved to check the feasibility of $(\overline{\mathbf{x}}_R, \underline{\mathbf{x}}_R)$ with respect to constraint (2.13b), which is formulated as problem (2.10). If

$$\overline{\eta} < \mathbf{c}_1^\top \mathbf{u}_R + f\left(\overline{\mathbf{x}}_R, \underline{\mathbf{x}}_R, \mathbf{s}_p^{\mathrm{w}}\right), \quad p = P_{R+1} \tag{2.16}$$

where $\mathbf{s}_p^{\mathrm{w}}$ for $p = P_{R+1}$ is defined as the solution of problem (2.10) corresponding to $\mathbf{s}$, then the iteration step increases to $R + 1$ and the master problem (2.15) is solved again with $P_{R+1} = P_R + 1$ and $Q_{R+1}^j = Q_R^j$ for all $j \in \mathcal{J}$. Otherwise, the following subproblem of problem (2.14) is solved for each $j \in \mathcal{J}$ to check the optimality of $(\overline{\mathbf{x}}_R, \underline{\mathbf{x}}_R)$ in terms of the actual total operating cost associated with scenario j:

$$\max_{\boldsymbol{\xi}\in\Xi^{\mathrm{o}}} \rho^\top \left(\overline{\mathbf{x}}_R, \underline{\mathbf{x}}_R, \mathbf{s}_j\right) \boldsymbol{\xi} \tag{2.17}$$

whose optimal value is equal to $f\left(\overline{\mathbf{x}}_R, \underline{\mathbf{x}}_R, \mathbf{s}_j\right)$. Let $\boldsymbol{\xi}_q^j$ for $q = Q_{R+1}^j$ denote the solution of problem (2.17). Let also

$$\mathcal{J}_R^{\mathrm{v}} := \left\{ j \in \mathcal{J} : U_R^j - L_R^j > \epsilon^{\mathrm{e}} \right\}$$

where

$$\begin{aligned} U_R^j &:= \mathbf{c}_1^\top \mathbf{u}_R + \rho^\top \left(\overline{\mathbf{x}}_R, \underline{\mathbf{x}}_R, \mathbf{s}_j\right) \boldsymbol{\xi}_q^j, \quad q = Q_{R+1}^j, \\ L_R^j &:= \mathbf{c}_1^\top \mathbf{u}_R + \eta_R^j, \end{aligned}$$

and ϵ^{e} is a predefined tolerance. If $\mathcal{J}_R^{\mathrm{v}}$ is non-empty, then it is implied that the following constraint in problem (2.14) is violated for each $j \in \mathcal{J}_R^{\mathrm{v}}$:

$$\eta_j \geq \rho^\top (\overline{\mathbf{x}}, \underline{\mathbf{x}}, \mathbf{s}_j)\, \boldsymbol{\xi}_q^j, \quad q = Q_{R+1}^j.$$

In this case, the iteration step increase to $R+1$ and the master problem (2.15) is solved again with $P_{R+1} = P_R$, $Q_{R+1}^j = Q_R^j$ for all $j \in \mathcal{J} \setminus \mathcal{J}_R^{\mathrm{v}}$, and $Q_{R+1}^j = Q_R^j + 1$ for all $j \in \mathcal{J}_R^{\mathrm{v}}$. If $\mathcal{J}_R^{\mathrm{v}}$ is empty, then it is implied that all the constraints in problem (2.14) are satisfied. In this case, the algorithm terminates and $(\mathbf{u}_R, \underline{\mathbf{x}}_R, \overline{\mathbf{x}}_R)$ is returned as a solution of problem (2.13).

At each iteration step $R \geq 1$, if $V_R > 0$ or inequality (2.16) holds, then it is implied that $\mathbf{s}_p^{\mathrm{w}}$ for $p = P_{R+1}$ is not equal to $\mathbf{s}_p^{\mathrm{w}}$ for any $p \leq P_R$. Moreover, if $\mathcal{J}_R^{\mathrm{v}}$ is non-empty, then it is implied that, for each $j \in \mathcal{J}_R^{\mathrm{v}}$, $\boldsymbol{\xi}_q^j$ for $q = Q_{R+1}^j$ is not equal to $\boldsymbol{\xi}_q^j$ for any $q \leq Q_R^j$. This indicates that the optimal value of problem (2.15) increases with R and approaches the optimal value of problem (2.14). Note that other convergence criteria may be used instead to deal with the optimality of the expected total operating cost. For example, the difference of an upper and a lower bound of problem (2.14) may be evaluated, which can be computed by solving problems (2.15) and (2.17) for all $j \in \mathcal{J}$, respectively.

To examine performances of the modified model, numerical simulations are conducted on the 24-bus test system used in Section 2.7 with the scenario set for $\alpha = 0.3$. As the preselected scenarios, $J = 5, 10, 15, 20$ randomly chosen wind power scenarios are used. Each preselected scenario is assumed to have the same probability, i.e., $W_j = 1/J$ for all $j \in \mathcal{J}$. In the simulations, three UC models are implemented as follows: First, the proposed model (2.5) is solved. Subsequently, another UC model is solved to minimize the expected total operating cost with the feasibility of problem (2.6) guaranteed for any scenario in the scenario set; the worst-case total operating is not explicitly considered. Finally, the modified model (2.13) is solved with $\overline{\eta}$ set to the middle point of the worst-case total operating costs incurred by the first two models. In solving the modified model, the optimality tolerance ϵ^{e} for the actual total operating cost associated with each preselected scenario is set to 10^{-3} as a relative tolerance. For each value of J, the worst-case and the expected total operating costs incurred by the three models are compared.

Figs. 2.8 and 2.9 show the worst-case and the expected total operating costs, respectively, incurred by the three UC models. It is observed that the modified model yields a lower expected total operating cost than the proposed model by allowing an increase in the worst-case total operating cost up to the maximum allowable value. Meanwhile, the modified model requires much higher computation time than the proposed model; specifically, the modified model is solved in 4191.80 s, 7747.56 s, 9981.91 s, and 13151.79 s for $J = 5, 10, 15, 20$, respectively. This is due to the relatively slow convergence of the actual total operating costs associated with the preselected scenarios, which necessitates a novel technique to accelerate the algorithm.

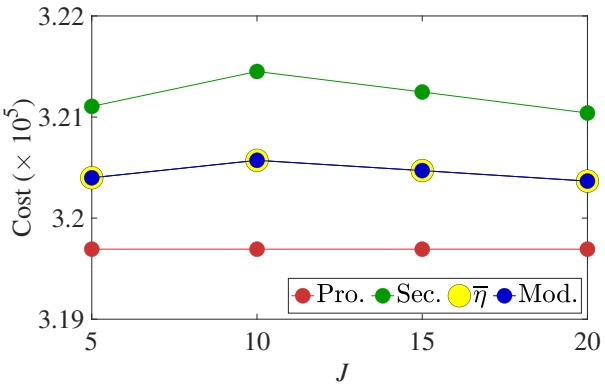

Fig. 2.8. Worst-case total operating costs incurred by the proposed, second tested, and modified models.

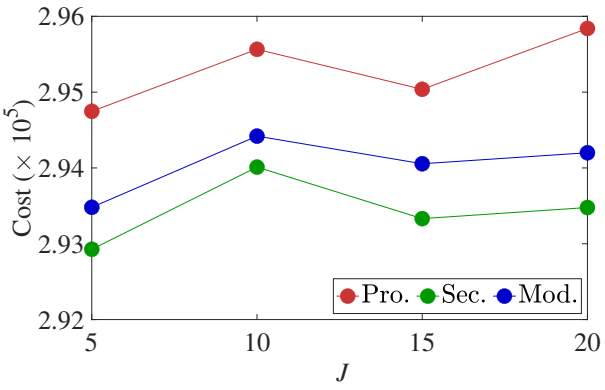

Fig. 2.9. Expected total operating costs incurred by the proposed, second tested, and modified models.

2.9 Cost Reduction via Interval Extension

In this section, the second supplementary method for the proposed model is described. The objective of this method is to increase the chance of reducing the actual total operating cost, or more precisely, the actual variable operating cost, while still minimizing the worst-case total operating cost. The idea is to extend the operating range of each power source at each time period obtained by solving the proposed model. As the optimal value of a minimization problem is equal to or smaller than that of the same problem but with another feasible set containing the original one, this method may well decrease the actual variable operating cost.

Let $(\mathbf{u}^{\mathrm{b}}, \overline{\mathbf{x}}^{\mathrm{b}}, \underline{\mathbf{x}}^{\mathrm{b}})$ denote the solution of the proposed model (2.5). In the second supplementary method, set $[\underline{\mathbf{x}}^{\mathrm{b}}, \overline{\mathbf{x}}^{\mathrm{b}}]$, which serves as part of the feasible set of the operating level $\mathbf{x}$ in problem (2.6), is expanded. The expanded set is also designed based on constraints (2.7a)–(2.7h) to enable the non-anticipative real-time decision-making. Specifically, the expanded set is modeled as a set $[\underline{\mathbf{x}}^{\mathrm{a}}, \overline{\mathbf{x}}^{\mathrm{a}}]$ such that $(\overline{\mathbf{x}}^{\mathrm{a}}, \underline{\mathbf{x}}^{\mathrm{a}}) \in \mathcal{X}(\mathbf{u}^{\mathrm{b}})$, where $\underline{\mathbf{x}}^{\mathrm{a}}$ and $\overline{\mathbf{x}}^{\mathrm{a}}$ are the decision vectors. Furthermore, to still minimize the worst-case total operating cost, $(\overline{\mathbf{x}}^{\mathrm{a}}, \underline{\mathbf{x}}^{\mathrm{a}})$ is determined so that $[\underline{\mathbf{x}}^{\mathrm{b}}, \overline{\mathbf{x}}^{\mathrm{b}}] \subseteq [\underline{\mathbf{x}}^{\mathrm{a}}, \overline{\mathbf{x}}^{\mathrm{a}}]$. This leads to $f(\overline{\mathbf{x}}^{\mathrm{a}}, \underline{\mathbf{x}}^{\mathrm{a}}, \mathbf{s}) \leq f(\overline{\mathbf{x}}^{\mathrm{b}}, \underline{\mathbf{x}}^{\mathrm{b}}, \mathbf{s})$ for any $\mathbf{s} \in \mathcal{S}$, increasing the chance of reducing the actual variable operating cost.

Notably, the larger any entry in $(\overline{\mathbf{x}}^{\mathrm{a}} - \underline{\mathbf{x}}^{\mathrm{a}}) \in \mathbb{R}^{3IT}$ is, the lower the actual variable

operating cost $f(\overline{\mathbf{x}}^{\mathrm{a}}, \underline{\mathbf{x}}^{\mathrm{a}}, \mathbf{s})$ is likely to be for any $\mathbf{s} \in \mathcal{S}$. However, it is impossible to maximize all the entires in $(\overline{\mathbf{x}}^{\mathrm{a}} - \underline{\mathbf{x}}^{\mathrm{a}})$ to the fullest as $(\overline{\mathbf{x}}^{\mathrm{a}}, \underline{\mathbf{x}}^{\mathrm{a}})$ has to be in $\mathcal{X}\left(\mathbf{u}^{\mathrm{b}}\right)$. Thus, the second supplementary method to determine $(\overline{\mathbf{x}}^{\mathrm{a}}, \underline{\mathbf{x}}^{\mathrm{a}})$ is formulated first as the following multi-objective optimization problem:

$$\max_{(\overline{\mathbf{x}}^{\mathrm{a}}, \underline{\mathbf{x}}^{\mathrm{a}}) \in \mathcal{X}\left(\mathbf{u}^{\mathrm{b}}\right)} \overline{\mathbf{x}}^{\mathrm{a}} - \underline{\mathbf{x}}^{\mathrm{a}} \tag{2.18a}$$

$$\text{s.t.} \quad \underline{\mathbf{x}}^{\mathrm{a}} \leq \underline{\mathbf{x}}^{\mathrm{b}} \text{ and } \overline{\mathbf{x}}^{\mathrm{b}} \leq \overline{\mathbf{x}}^{\mathrm{a}} \tag{2.18b}$$

where the objective vector (2.18a) include $3IT$ objective functions each of which is the width of the operating range of each power source at each time period. Constraint (2.18b) implies $[\underline{\mathbf{x}}^{\mathrm{b}}, \overline{\mathbf{x}}^{\mathrm{b}}] \subseteq [\underline{\mathbf{x}}^{\mathrm{a}}, \overline{\mathbf{x}}^{\mathrm{a}}]$.

As a multi-objective optimization problem, problem (2.18) can be addressed based on various criteria [66], [67]. In this dissertation, the problem is solved using the method of global criterion [68], which does not require any preference information on each objective function [69]. In the method of global criterion, the distance of the objective vector and the ideal objective vector is minimized in terms of, e.g., the p-norm where $1 \leq p \leq \infty$. The ideal objective vector refers to the vector each entry of which is the maximum possible value of the corresponding entry in the objective vector. In this dissertation, with the 2-norm chosen as the distance metric, problem (2.18) is converted to the following single-objective optimization problem:

$$\min_{(\overline{\mathbf{x}}^{\mathrm{a}}, \underline{\mathbf{x}}^{\mathrm{a}}) \in \mathcal{X}\left(\mathbf{u}^{\mathrm{b}}\right)} \|\mathbf{f}^{\star} - (\overline{\mathbf{x}}^{\mathrm{a}} - \underline{\mathbf{x}}^{\mathrm{a}})\|_2 \quad \text{s.t.} \quad (2.18\text{b}) \tag{2.19}$$

where $\|\cdot\|_2$ and $\mathbf{f}^{\star}$ represent the 2-norm and the ideal objective vector associated with problem (2.18), respectively. For $k = 1, 2, \ldots, 3IT$, the kth entry of $\mathbf{f}^{\star}$ is equal to the optimal value of the following LP problem:

$$\max_{(\overline{\mathbf{x}}^{\mathrm{a}}, \underline{\mathbf{x}}^{\mathrm{a}}) \in \mathcal{X}\left(\mathbf{u}^{\mathrm{b}}\right)} \overline{x}_k^{\mathrm{a}} - \underline{x}_k^{\mathrm{a}} \quad \text{s.t.} \quad (2.18\text{b})$$

where $\overline{x}_k^{\mathrm{a}}$ and $\underline{x}_k^{\mathrm{a}}$ denote the kth entries of $\overline{\mathbf{x}}^{\mathrm{a}}$ and $\underline{\mathbf{x}}^{\mathrm{a}}$, respectively. The solution of problem (2.19) is obtained by solving the following convex quadratic programming problem:

$$\min_{(\overline{\mathbf{x}}^{\mathrm{a}}, \underline{\mathbf{x}}^{\mathrm{a}}) \in \mathcal{X}\left(\mathbf{u}^{\mathrm{b}}\right)} \|\mathbf{f}^{\star} - (\overline{\mathbf{x}}^{\mathrm{a}} - \underline{\mathbf{x}}^{\mathrm{a}})\|_2^2 \quad \text{s.t.} \quad (2.18\text{b}). \tag{2.20}$$

Let $(\overline{\mathbf{x}}^{a\star}, \underline{\mathbf{x}}^{a\star})$ denote the solution of problem (2.20). By implementing $[\underline{\mathbf{x}}^{a\star}, \overline{\mathbf{x}}^{a\star}]$ instead of $\left[\underline{\mathbf{x}}^{\mathrm{b}}, \overline{\mathbf{x}}^{\mathrm{b}}\right]$ as the operating range at the real-time stages, the chance of reducing the actual total operating cost increases with the worst-case total operating cost still minimized.

To test performances of this supplementary method, numerical simulations are conducted on the 24-bus test system used in Section 2.7 with the scenario set for $\alpha = 0.3$. In the simulations, the proposed model (2.5) is first solved. Subsequently, the actual total operating costs for 100 randomly chosen wind power scenarios are calculated before and after the method. By using the method, the operating ranges of generators 1, 2, 6, 7, 11,

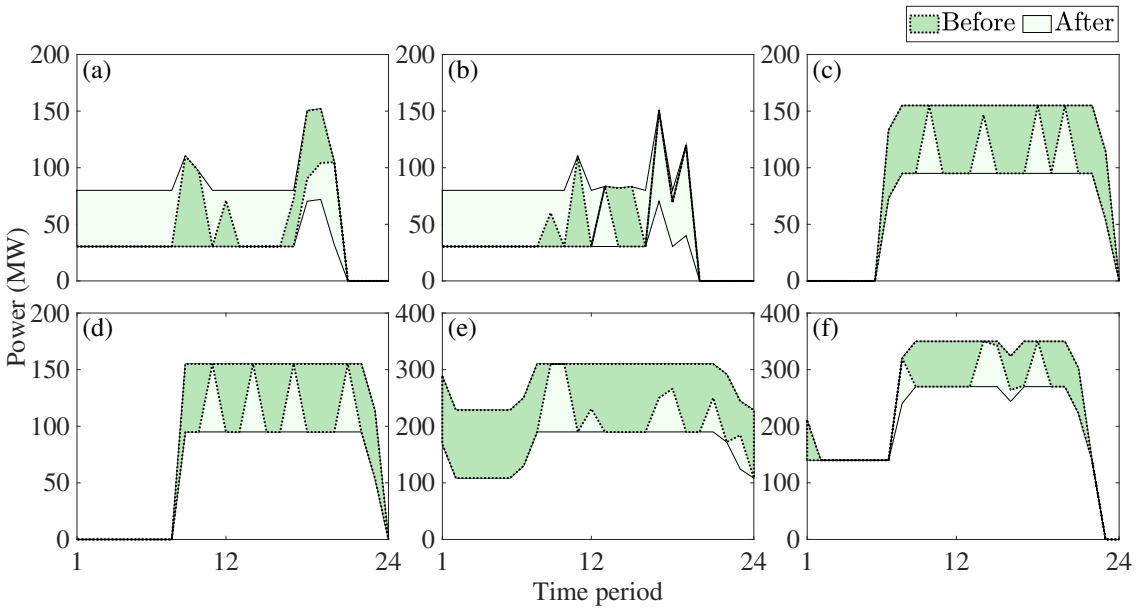

Fig. 2.10. Operating ranges of generators (a) 1, (b) 2, (c) 6, (d) 7, (e) 11, and (f) 12.

and 12 at some time periods are indeed extended as shown in Fig. 2.10; those of the other generators and the BESSs do not change. As a result, the actual total operating cost for each of the 100 scenarios is reduced averagely by 0.27%. Meanwhile, problem (2.20) is solved in 8.55 s. The computation time can be shortened by solving the problem separately for each power source, as it does not impose any coupling constraint on the decision variables for different power sources.

2.10 Summary

In this chapter, the novel two-stage non-anticipative robust UC model and the two supplementary methods were studied to deal with the uncertainty of VRE generation. The proposed model enables the non-anticipative real-time decision-making by confining the operating range of each power source at each time period. The simulation results verified that this strategy is less conservative than the affine policy. It was also shown that the two supplementary methods can further lower the actual total operating cost.

However, the proposed model itself might be overly conservative and show a poor worst-case performance if the uncertainty is too huge; notably, the supplementary methods cannot reduce the worst-case total operating cost. This issue is addressed in the following chapter.

Chapter 3

Three-stage Non-anticipative Robust UC with Uncertain Wind Power

This chapter studies the novel robust UC model considering the decreasing uncertainty in wind power forecasting. This chapter is organized as follows: Section 3.1 explains the motivation. Section 3.2 overviews the optimization framework. Section 3.3 models uncertainties considered in the proposed model. Section 3.4 gives the mathematical formulation. Section 3.5 presents a solution method. Section 3.6 discusses numerical simulation results. Section 3.7 summarizes the chapter.

3.1 Motivation

One of the intrinsic issues of the two-stage non-anticipative robust UC model proposed in the previous chapter is that it may yield a costly solution or even not be feasible if the scenario set is built too conservatively. Meanwhile, the forecasting accuracy of wind power, among other types of VRE generation, improves with time as more observation data, which are temporally more correlated to the actual wind power, are available [70], [71]. Indeed, it is shown in [61], [72], [73] that wind power forecasting errors grow with look-ahead time. Considering that the model in the previous chapter assumes only one scheduling stage, it may solve the issue to add another so that the decreasing wind power uncertainty can be exploited. Based on this idea, to achieves less conservative scheduling of power sources under severe wind power uncertainty, the model proposed in this chapter introduces an intermediate decision-making stage, namely the intra-day stage, between the day-ahead and the first real-time stages. The new decision-making stage corresponds to the intra-day market considered in the three-stage stochastic model [37]; the time gap between the day-ahead and the intra-day stages is thus assumed to be around 10 h.

In this chapter, the power system described in Section 2.2 is considered with each VRE generation system assumed to be a wind farm; the symbols are used without change except those for the VRE generation systems. For descriptive purposes, the models proposed in the previous and this chapter are hereafter referred to as the two-stage and the three-stage models, respectively. Furthermore, the real-time stages assumed in both the two-stage and the three-stage models are described as a single decision-making stage for the sake of

brevity. In the following section, the optimization framework in the three-stage model is overviewed.

3.2 Overview

The biggest difference of the two-stage and the three-stage models is that the former assumes one scheduling stage, whereas the latter does two. In the two-stage model, the operating status and range are optimized simultaneously at the day-ahead stage for a given scenario set. Subsequently, the operating level is determined at the real-time stage for the actual wind power. In the three-stage model, on the other hand, the operating range is optimized at the intra-day stage. That is to say, the operating status, range, and level are optimized sequentially at the day-ahead, intra-day, and real-time stages, respectively. To exploit the fact that the uncertainty in wind power forecasting decreases over time, the scenario set is constructed at the intra-day stage, not the day-ahead stage, using the interval prediction method. The scenario set constructed at the day-ahead stage for the two-stage model and that at the intra-day stage for the three-stage model are hereafter referred to as the day-ahead and the intra-day scenario sets, respectively.

The objective of the three-stage model is the same as that of the two-stage model, i.e., to minimize the worst-case total operating cost. Therefore, both operating status and range are optimized using the minimax criterion. When determining the operating status at the day-ahead stage, there are two uncertainties resolved at the two subsequent decision-making stages: the uncertainty in predicting the intra-day scenario set resolved at the intra-day stage and that in predicting the actual wind power for a given intra-day scenario set resolved at the real-time stage. This implies that the operating status has to be determined assuming worst-case wind power scenarios in worst-case intra-day scenario sets. With this aim, a collection of possible intra-day scenario sets is constructed at the day-ahead stage. In this dissertation, the collection of possible intra-day scenario sets is referred to as the vaguity set. As the intra-day scenario set is built using the interval prediction method, the vaguity set is constructed by setting a lower limit to the lower limit in, and an upper limit to the upper limit in each interval of the intra-day scenario set. Furthermore, the size of each interval is bounded above to model the largest projected wind power uncertainty at the intra-day stage [52], [53]. These parameters of the vaguity set can be determined practically in various ways. For example, the lower (upper) limit of the lower (upper) limit in each interval of the intra-day scenario set can be set to the lower (upper) limit in each interval of the day-ahead scenario set. Moreover, the upper limit of the interval size of the intra-day scenario set can be set based on historical data on the interval size obtained for different look-ahead times. At the intra-day stage, the uncertainty in predicting the actual wind power is the only uncertainty. The operating range is thus optimized assuming worst-case wind power scenarios in the actual intra-day scenario set. Finally, at the real-time stage, the operating level is optimized to minimize the variable operating cost for the actual wind power.

Considering the three decision-making stages, the three-stage model is formulated as a three-stage robust optimization problem. This problem is suboptimally addressed by solving instead a tractable two-stage robust optimization problem. Before going into detail on the mathematical formulation, the two uncertainties in the three-stage model are modeled in the following section.

3.3 Uncertainty Modeling

To exploit the decreasing uncertainty of wind power, the three-stage model uses the intra-day scenario set instead of the day-ahead scenario set. The intra-day scenario set is built by using the interval prediction method and denoted by $\tilde{\mathbf{w}} := [\underline{\mathbf{w}}, \overline{\mathbf{w}}] \subset \mathbb{R}^{IT}$ where $\underline{\mathbf{w}}$ and $\overline{\mathbf{w}}$ represent the vector of $\underline{w}_{it}$ and that of $\overline{w}_{it}$ for all $i \in \mathcal{I}$ and $t \in \mathcal{T}$, respectively; $\underline{w}_{it}$ and $\overline{w}_{it}$ denote the lower and upper limits of the power output w_{it} from wind farm i at time period t, respectively, both set at the intra-day stage and unknown at the day-ahead stage.

Meanwhile, to consider worst-case intra-day scenario sets, the vaguity set is also constructed at the day-ahead stage. The vaguity set is equivalently represented by the following set of pairs of $\overline{\mathbf{w}}$ and $\underline{\mathbf{w}}$:

$$\mathcal{W} := \left\{ (\overline{\mathbf{w}}, \underline{\mathbf{w}}) \in \mathbb{R}^{IT} \times \mathbb{R}^{IT} : \underline{\mathbf{w}}^{\mathrm{d}} \leq \underline{\mathbf{w}} \leq \overline{\mathbf{w}} \leq \overline{\mathbf{w}}^{\mathrm{d}} \quad \text{and} \quad \overline{\mathbf{w}} - \underline{\mathbf{w}} \leq \hat{\mathbf{w}}^{*} \right\}$$

where $\underline{\mathbf{w}}^{\mathrm{d}}$, $\overline{\mathbf{w}}^{\mathrm{d}}$, and $\hat{\mathbf{w}}^{*}$ denote the vectors of $\underline{w}^{\mathrm{d}}_{it}$, $\overline{w}^{\mathrm{d}}_{it}$, and $\hat{w}^{*}_{it}$ for all $i \in \mathcal{I}$ and $t \in \mathcal{T}$, respectively; $\underline{w}^{\mathrm{d}}_{it}$, $\overline{w}^{\mathrm{d}}_{it}$, and $\hat{w}^{*}_{it}$ denote the lower limit of $\underline{w}_{it}$, the upper limit of $\overline{w}_{it}$, and the upper limit of the difference $(\overline{w}_{it} - \underline{w}_{it})$ of $\overline{w}_{it}$ and $\underline{w}_{it}$, respectively, all of which are set at the day-ahead stage. Notably, $(\overline{w}_{it} - \underline{w}_{it})$ can be interpreted as the degree of wind power uncertainty at the intra-day stage and is bounded by $\hat{w}^{*}_{it}$. In the following subsection, the mathematical formulation of the three-stage model is given.

3.4 Problem Formulation

For the vaguity set $\mathcal{W}$, the three-stage model is formulated as follows:

$$\min_{\mathbf{u} \in \mathcal{U}} \left\{ \mathbf{c}_1^{\top} \mathbf{u} + \max_{(\overline{\mathbf{w}}, \underline{\mathbf{w}}) \in \mathcal{W}} g\left(\mathbf{u}, \overline{\mathbf{w}}, \underline{\mathbf{w}}\right) \right\} \tag{3.1}$$

where $g\left(\mathbf{u}, \overline{\mathbf{w}}, \underline{\mathbf{w}}\right)$ denotes the minimum variable operating cost for worst-case wind power scenarios in a given intra-day scenario set $\tilde{\mathbf{w}}$. Specifically, $g\left(\mathbf{u}, \overline{\mathbf{w}}, \underline{\mathbf{w}}\right)$ is defined as the optimal value of the following problem:

$$\min_{(\overline{\mathbf{x}}, \underline{\mathbf{x}}) \in \mathcal{X}(\mathbf{u})} \max_{\mathbf{w} \in \tilde{\mathbf{w}}} f\left(\overline{\mathbf{x}}, \underline{\mathbf{x}}, \mathbf{w}\right) \tag{3.2}$$

where $\mathbf{w}$ is the vector of w_{it} for all $i \in \mathcal{I}$ and $t \in \mathcal{T}$. Moreover, $f\left(\overline{\mathbf{x}}, \underline{\mathbf{x}}, \mathbf{w}\right)$ represents the minimum variable operating cost for a given wind power scenario $\mathbf{w}$, i.e., the optimal value of problem (2.6) for $\mathbf{s} = \mathbf{w}$.

The three-stage decision-making framework in the three-stage model is realized ideally by solving problem (3.1) to determine the operating status at the day-ahead stage, problem (3.2) to determine the operating range at the intra-day stage, and problem (2.6) to determine the operating level at the real-time stage. However, problem (3.1) is a three-stage robust optimization problem, or more specifically, a min-max-min-max-min problem, for which no standard algorithm exists; problem (3.2) is a two-stage robust optimization problem that can be solved using well-studied cutting-plane methods, e.g., Benders decomposition and the C&CG algorithm, as explained in the previous chapter. In the following section, the suboptimal solution method for problem (3.1) is suggested.

3.5 Solution Method

In this section, the two-stage robust optimization problem is formulated to obtain a suboptimal solution to problem (3.1). While there is no standard algorithm that exactly solves the three-stage model (3.1), for the single-bus version of the power system of interest, i.e., the power system of interest without the transmission capacity constraint (2.1l), the three-stage model is formulated as a tractable two-stage robust optimization problem. To show this, let the three-stage model for the single-bus system be written as follows:

$$\min_{\mathbf{u}\in\mathcal{U}} \left\{ \mathbf{c}_1^\top \mathbf{u} + \max_{(\overline{\mathbf{w}},\underline{\mathbf{w}})\in\mathcal{W}} g^{\mathrm{s}}\left(\mathbf{u},\overline{\mathbf{w}},\underline{\mathbf{w}}\right) \right\} \tag{3.3}$$

where $g^{\mathrm{s}}\left(\mathbf{u},\overline{\mathbf{w}},\underline{\mathbf{w}}\right)$ is the minimum variable total operating cost for worst-case wind power scenarios in a given intra-day scenario set $\tilde{\mathbf{w}}$. Specifically, $g^{\mathrm{s}}\left(\mathbf{u},\overline{\mathbf{w}},\underline{\mathbf{w}}\right)$ is defined as the optimal value of the following problem:

$$\min_{(\overline{\mathbf{x}},\underline{\mathbf{x}})\in\mathcal{X}(\mathbf{u})} \max_{\mathbf{w}\in\tilde{\mathbf{w}}} f^{\mathrm{s}}\left(\overline{\mathbf{x}},\underline{\mathbf{x}},\mathbf{w}\right) \tag{3.4}$$

where $f^{\mathrm{s}}\left(\overline{\mathbf{x}},\underline{\mathbf{x}},\mathbf{w}\right)$ denotes the minimum variable operating cost for a given wind power scenario $\mathbf{w}$. Specifically, $f^{\mathrm{s}}\left(\overline{\mathbf{x}},\underline{\mathbf{x}},\mathbf{w}\right)$ is defined as the optimal value of the following problem:

$$\min_{\mathbf{x}\in[\underline{\mathbf{x}},\overline{\mathbf{x}}]} \mathbf{c}_2^\top \mathbf{x} \quad \text{s.t.} \quad (2.1\mathrm{k}) \tag{3.5}$$

where the power supply-demand balance condition is the only systemwide constraint.

Problem (3.5) is a series of single-period ED problems for the single-bus system, implying that the merit-order dispatch is possible at each time period. This further means that the all-maximum and all-minimum wind power scenarios can be considered as the possible worst-case ones at each time period. Therefore, problem (3.4) is rewritten as the following LP problem:

$$\begin{aligned} &\min_{(\overline{\mathbf{x}},\underline{\mathbf{x}})\in\mathcal{X}(\mathbf{u}),\boldsymbol{\eta}\in\mathbb{R}^T} \mathbf{1}^\top \boldsymbol{\eta} \\ &\text{s.t.} \quad \eta_t \geq \sum_{i\in\mathcal{I}} \left(C_i^{\mathrm{g}} \overline{x}_{it} + C_i^{\mathrm{i}} \underline{x}_{it}^{\mathrm{i}} + C_i^{\mathrm{o}} \overline{x}_{it}^{\mathrm{o}} \right), \quad \forall t \in \mathcal{T}, \end{aligned} \tag{3.6a}$$

$$\eta_t \geq \sum_{i\in\mathcal{I}} \left(C_i^{\mathrm{g}} \underline{x}_{it} + C_i^{\mathrm{i}} \overline{x}_{it}^{\mathrm{i}} + C_i^{\mathrm{o}} \underline{x}_{it}^{\mathrm{o}}\right), \quad \forall t \in \mathcal{T}, \tag{3.6b}$$

$$\sum_{i\in\mathcal{I}} \left(\overline{x}_{it} - \underline{x}_{it}^{\mathrm{i}} + \overline{x}_{it}^{\mathrm{o}} - d_{it} + \underline{w}_{it}\right) = 0, \quad \forall t \in \mathcal{T}, \tag{3.6c}$$

$$\sum_{i\in\mathcal{I}} \left(\underline{x}_{it} - \overline{x}_{it}^{\mathrm{i}} + \underline{x}_{it}^{\mathrm{o}} - d_{it} + \overline{w}_{it}\right) = 0, \quad \forall t \in \mathcal{T} \tag{3.6d}$$

where $\boldsymbol{\eta}$ and $\mathbf{1}$ represent a vector of η_t for all $t \in \mathcal{T}$ and the T-dimensional all-ones vector, respectively; η_t denotes the worst-case variable operating cost at time period t. The right-hand sides of constraints (3.6a) and (3.6b) correspond to the variable operating costs for the all-minimum and all-maximum wind power scenarios, respectively. Constraints (3.6c) and (3.6d) specify the operating levels for the all-minimum and all-maximum wind power scenarios, respectively. Since problem (3.4) is rewritten as an LP minimization problem, problem (3.3) can be considered as a tractable two-stage robust optimization problem.

Although the three-stage models (3.1) for the power system of interest and (3.3) for the single-bus system have seemingly the same structure, only the latter is tractable. This is due to the difference in the scales of problems (3.2) and (3.4). In fact, problem (3.2) is rewritten as an LP minimization problem using the duality principle. However, the number of variables or constraints in it is too large for problem (3.1) to be solved using the cutting-plane methods. By contrast, problem (3.4) is rewritten as a much more small-scale LP minimization problem as shown above, thus making problem (3.3) solvable.

The basic idea of the suboptimal approach for problem (3.1) is to impose a constraint on the operating range for each possible intra-day scenario set so that the power system of interest can be considered as the single-bus system. The constraint is written as follows:

$$\begin{aligned} &-F_l \leq \sum_{i\in\mathcal{I}} \left(x_{it}^{\mathrm{g}-} - x_{it}^{\mathrm{i}+} + x_{it}^{\mathrm{o}-} - F_{il} d_{it} + w_{it}^{-}\right), \quad \forall l \in \mathcal{L}, \forall t \in \mathcal{T}, \\ &\sum_{i\in\mathcal{I}} \left(x_{it}^{\mathrm{g}+} - x_{it}^{\mathrm{i}-} + x_{it}^{\mathrm{o}+} - F_{il} d_{it} + w_{it}^{+}\right) \leq F_l, \quad \forall l \in \mathcal{L}, \forall t \in \mathcal{T} \end{aligned} \tag{3.7}$$

where

$$\begin{aligned} x_{it}^{\mathrm{g}+} &:= \max\left\{F_{il}\underline{x}_{it}^{\mathrm{g}}, F_{il}\overline{x}_{it}^{\mathrm{g}}\right\}, \quad x_{it}^{\mathrm{g}-} := \min\left\{F_{il}\underline{x}_{it}^{\mathrm{g}}, F_{il}\overline{x}_{it}^{\mathrm{g}}\right\}, \\ x_{it}^{\mathrm{i}+} &:= \max\left\{F_{il}\underline{x}_{it}^{\mathrm{i}}, F_{il}\overline{x}_{it}^{\mathrm{i}}\right\}, \quad x_{it}^{\mathrm{i}-} := \min\left\{F_{il}\underline{x}_{it}^{\mathrm{i}}, F_{il}\overline{x}_{it}^{\mathrm{i}}\right\}, \\ x_{it}^{\mathrm{o}+} &:= \max\left\{F_{il}\underline{x}_{it}^{\mathrm{o}}, F_{il}\overline{x}_{it}^{\mathrm{o}}\right\}, \quad x_{it}^{\mathrm{o}-} := \min\left\{F_{il}\underline{x}_{it}^{\mathrm{o}}, F_{il}\overline{x}_{it}^{\mathrm{o}}\right\}, \\ w_{it}^{+} &:= \max\left\{F_{il}\underline{w}_{it}, F_{il}\overline{w}_{it}\right\}, \quad w_{it}^{-} := \min\left\{F_{il}\underline{w}_{it}, F_{il}\overline{w}_{it}\right\}. \end{aligned}$$

Regarding problem (3.2), if $(\overline{\mathbf{x}}, \underline{\mathbf{x}}) \in \mathcal{X}(\mathbf{u})$ further meets constraint (3.7), then the power system of interest can be considered as the single-bus system for the intra-day scenario set $\tilde{\mathbf{w}}$ as constraint (2.1l) will be satisfied for any $\mathbf{x} \in [\underline{\mathbf{x}}, \overline{\mathbf{x}}]$ and $\mathbf{w} \in \tilde{\mathbf{w}}$ at the real-time stage. The two-stage robust optimization problem to obtain a suboptimal solution to problem (3.1) is formulated by adding constraint (3.7) to problem (3.2) as follows:

$$\min_{\mathbf{u}\in\mathcal{U}} \left\{\mathbf{c}_1^{\top}\mathbf{u} + \max_{(\overline{\mathbf{w}},\underline{\mathbf{w}})\in\mathcal{W}} f^{\dagger}(\mathbf{u}, \overline{\mathbf{w}}, \underline{\mathbf{w}})\right\} \tag{3.8}$$

where

$$f^{\dagger}\left(\mathbf{u}, \overline{\mathbf{w}}, \underline{\mathbf{w}}\right) := \min_{(\overline{\mathbf{x}}, \underline{\mathbf{x}}) \in \mathcal{X}(\mathbf{u}), \boldsymbol{\eta} \in \mathbb{R}^T} \mathbf{1}^{\top} \boldsymbol{\eta} \quad \text{s.t.} \quad (3.6), (3.7) \tag{3.9}$$

is equal to the optimal value of problem (3.2) with the additional constraint (3.7). Note that constraint (3.7) is rewritten as $2LT$ linear inequalities and thus problem (3.9) is recast as an LP minimization problem. The LP reformulation of problem (3.9) has a significantly small number of variables or constraints compared with a duality-based LP reformulation of problem (3.2). Consequently, problem (3.8) can be solved by using Benders decomposition or the C&CG algorithm similarly to problem (3.3). In this dissertation, problem (3.8) is solved in the same way as problem (2.5), which has the same structure. To avoid repetition, the algorithm for problem (3.8) is not described in detail.

To sum up, the three-stage decision-making framework of the three-stage model can be realized practically by solving problem (3.8) at the day-ahead stage, problem (3.2) at the intra-day stage, and problem (2.6) at the real-time stage. In the following section, performances of the proposed approach is tested via numerical simulations.

3.6 Numerical Simulations

This section test performances of the three-stage model via numerical simulations. In the simulations, the three-stage model is compared with the two-stage model with respect to the optimality on the 24-bus and 300-bus test systems used in Section 2.7. In the following subsection, the simulation scheme and results for the 24-bus test system are explained.

3.6.1 24-bus Test System

In this subsection, the relationship between performances of the three-stage model and the degrees of wind power uncertainty at the two scheduling stages is analyzed on the 24-bus test system. To build the day-ahead scenario set for the two-stage model and the vaguity set for the three-stage model, two simulation parameters $\beta = 0.2, 0.4, \ldots, 1$ and $\gamma = 0.1, 0.2 \ldots, 1$ are introduced. Regarding the day-ahead scenario set, the upper and lower limits of the output from each wind farm at each time period are set above and below the nominal value, respectively, so that their difference is equal to β times the wind farm capacity. As for the vaguity set, the upper (lower) limit of the upper (lower) limit in the intra-day scenario set is set to the upper (lower) limit in the day-ahead scenario set. Furthermore, the upper limit of the interval size of the intra-day scenario set is set to γ times the interval size of the day-ahead scenario set. Notably, β and γ can be interpreted as the degree of uncertainty at the day-ahead stage and the maximum degree of uncertainty at the intra-day stage, respectively.

For each pair of β and γ, which defines the day-ahead scenario set and the vaguity set, the simulations are conducted as follows: First, the two-stage and the three-stage models are solved for the day-ahead scenario set and the vaguity set, respectively. Subsequently, 10 intra-day scenario sets of the largest interval size are randomly chosen from the vaguity set. For each intra-day scenario set, problem (3.2) is solved with the operating status fixed

to the one obtained by solving three-stage model. For fair comparisons, the operating range for the two-stage model is updated by solving problem (3.2) with the operating status fixed to the one obtained by solving the two-stage model. Furthermore, 10 wind power scenarios are randomly chosen from each intra-day scenario set. For each wind power scenario and each model, problem (2.6) is solved. Meanwhile, the worst-case total operating cost assumed at the day-ahead stage (DA-TOC), the worst-case total operating cost for each of the 10 intra-day scenario sets assumed at the intra-day stage (ID-TOC), and the actual total operating cost for each of the 100 wind power scenarios incurred at the real-time stage (RT-TOC) are calculated for each model.

The simulations are run on MATLAB R2020b with CPLEX 12.10 using a computer featuring an Intel Core i9 processor and 64 GB of RAM. The convergence tolerances in the C&CG algorithm are set to 10^{-6}; those in the MIP solver are set to the default values. Any initial guess required in the C&CG algorithm is randomly selected. With these settings, the two-stage and the three-stage models are solved averagely in 3.18 s and 2.71 s, respectively. Moreover, problem (3.2) for both models is solved averagely in 1.38 s.

The simulation results are presented in Fig. 3.1 and 3.2. Fig. 3.1 shows the DA-TOCs, the average ID-TOCs, and the average RT-TOCs incurred by the two-stage and the three-stage models. For reference, the minimum average RT-TOCs are also plotted, which are calculated by solving the deterministic model (2.1). It is observed that the three indices associated with the three-stage model increase with γ for each β and become more sensitive to change in γ as β grows. This indicates that the worst-case or actual total operating cost at each decision-making stage can be reduced by improving the worst-case forecasting accuracy at the intra-day stage, especially when the wind power uncertainty is severe at the day-ahead stage. Fig. 3.2 shows the average percentage decreases from the DA-TOC, ID-TOC, and RT-TOC incurred by the two-stage model to those incurred by the three-stage model. It is seen that the larger β is and the smaller γ is, the higher the average percentage decrease tends to be. This implies that the three-stage model can be particularly effective when the uncertainty is large at the day-ahead stage and expected to reduce greatly at the intra-day stage.

In the simulations above, each randomly chosen intra-day scenario set is of the maximum interval size. To investigate the sensitivity and uncertainty of the relative performance of the three-stage model with regard to the actual degree of uncertainty at the intra-day stage and the actual wind power, percentage decreases from the RT-TOC incurred by the two-stage model to that incurred by the three-stage model for another 5000 wind power scenarios are further calculated. The 5000 wind power scenarios are randomly selected from 50 intra-day scenario sets, 100 scenarios from each set, which are generated around the nominal scenario so that the interval sizes are equal to $\delta = 0.02, 0.04, \ldots, 1$ times the largest value assumed in the vaguity set for $(\beta, \gamma) = (1, 0.8)$. Fig. 3.3 shows box plots of all the 5000 percentage decreases and 100 out of them associated with each value of δ. It is observed that the percentage decrease varies over a far smaller range for a fixed value of δ. This implies that the relative performance of the three-stage model is more sensitive to change in the actual degree of uncertainty at the intra-day stage than to that in the actual

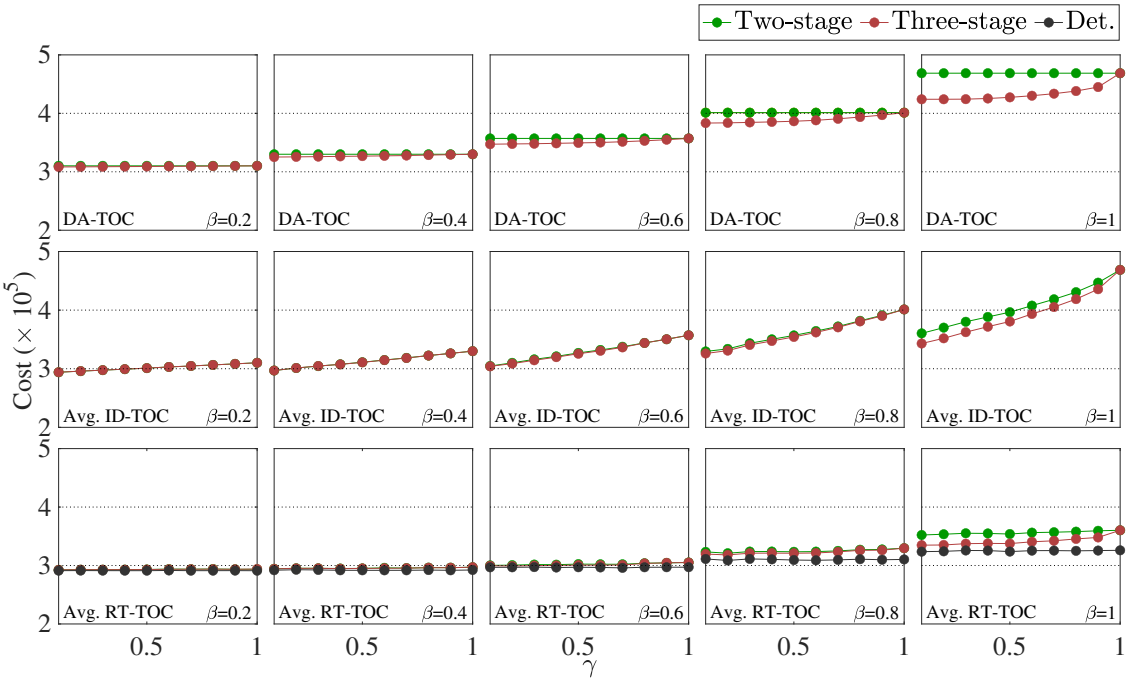

Fig. 3.1. DA-TOCs, average ID-TOCs, and average RT-TOCs of the 24-bus test system.

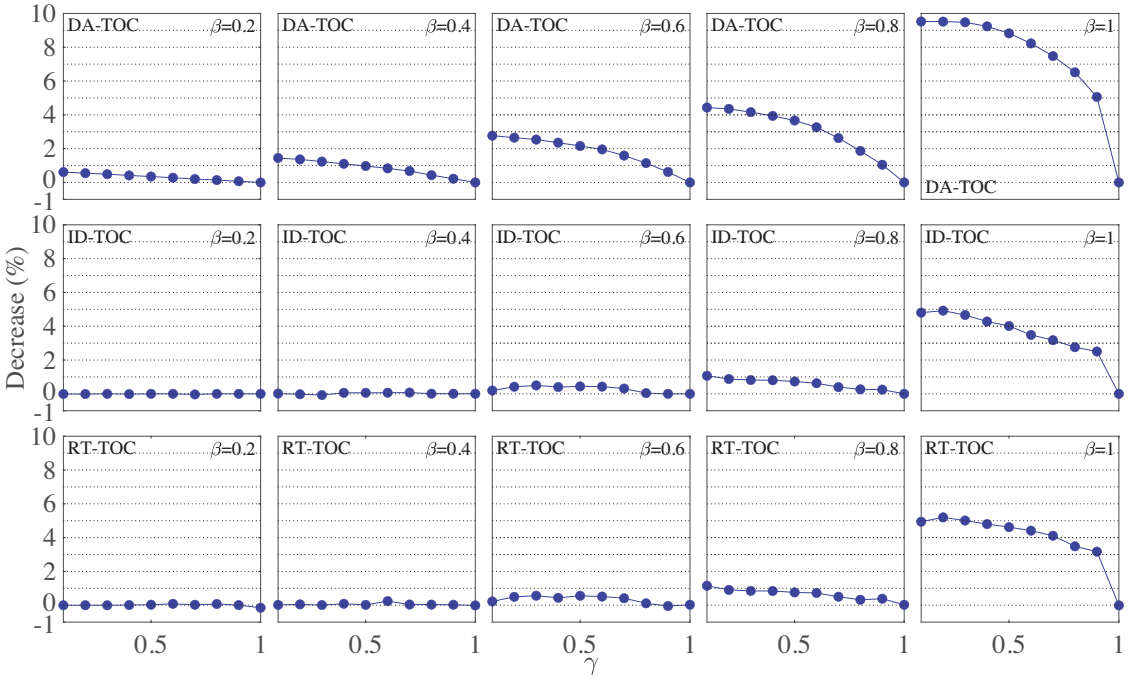

Fig. 3.2. Average percentage decreases in the DA-TOC, ID-TOC, and RT-TOC of the 24-bus test system achieved by the three-stage model compared with the two-stage model.

wind power.

In this subsection, the differences between the upper and lower limits of wind power in the scenario sets are set equally for all the time periods. In the following subsection, a more practical setup is used with the 300-bus test system.

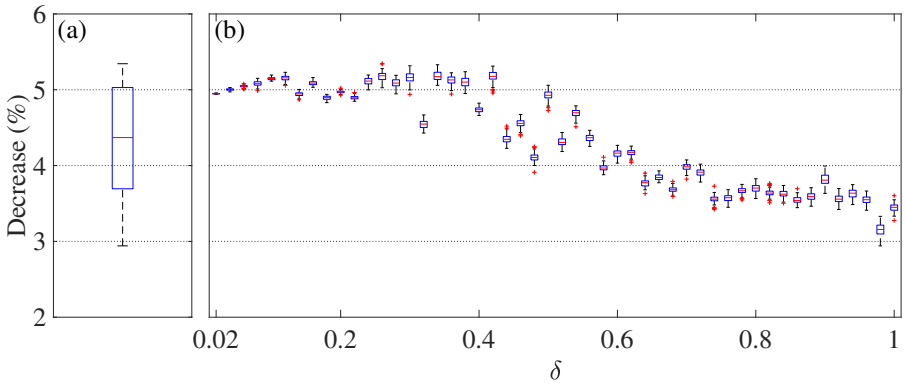

Fig. 3.3. Box plots of (a) the 5000 percentage decreases in the RT-TOC of the 24-bus test system achieved by the three-stage model and (b) 100 out of them associated with each value of δ.

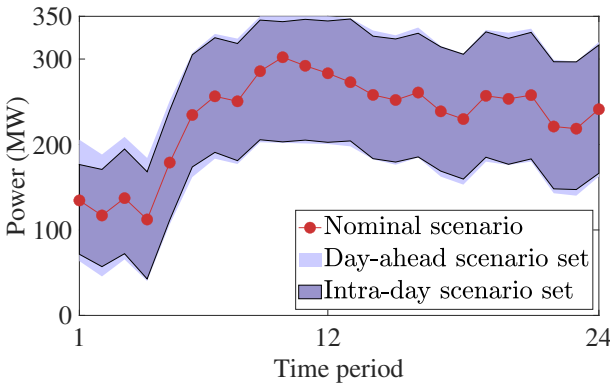

Fig. 3.4. Construction of the vaguity set for wind farm 1 in the 300-bus test system.

3.6.2 300-bus Test System

In this subsection, the performances of the two-stage and the three-stage models are compared on the 300-bus test system. To build the day-ahead scenario set and the vaguity set, the empirical data used for this test system in Section 2.7 are revisited. Specifically, it is supposed that a profile of the maximum fraction of the interval size to the wind farm capacity for look-ahead time from 2 h to 36 h is given as in Fig. 2.6. The day-ahead scenario set is then generated around the nominal scenario so that the profile of the interval size over the planning horizon is identical to the profile in Fig. 2.6 for look-ahead time from 13 h to 36 h multiplied by the wind farm capacity. Regarding the vaguity set, the upper (lower) limit of the upper (lower) limit in the intra-day scenario set at each time period is set to the upper (lower) limit in the day-ahead scenario set. Furthermore, the profile of the upper limit of the interval size of the intra-day scenario set over the planning horizon is set to the profile in Fig. 2.6 for look-ahead time from 2 h to 25 h multiplied by the wind farm capacity. To help understanding the construction of the vaguity set, Fig. 3.4 shows the nominal wind power scenario, the day-ahead scenario set, and an intra-day scenario set with the maximum interval size in the vaguity set for wind farm 1.

For the resulting pair of the day-ahead scenario set and the vaguity set, the simulations are conducted in the same way as in the previous subsection with the optimality tolerance in the C&CG algorithm changed to 10^{-3} as a relative tolerance. As a consequence, the

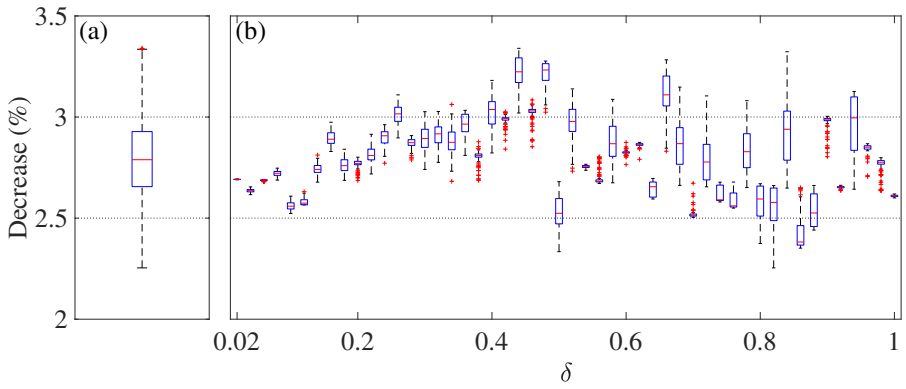

Fig. 3.5. Box plots of (a) the 5000 percentage decreases in the RT-TOC of the 300-bus test system achieved by the three-stage model and (b) 100 out of them for each value of δ.

two-stage and the three-stage models are solved in 444.51 s and 921.67 s, respectively. Moreover, problem (3.2) for both models is solved averagely in 89.38 s.

The simulation results are shown in TABLE 3.1, where the figures in parentheses indicate the average percentage decreases from the DA-TOC, ID-TOC, and RT-TOC incurred by the two-stage model to those incurred by the three-stage model. It is observed that the three-stage model averagely lowers the total operating costs at all the decision-making stages. Meanwhile, the sensitivity and uncertainty analysis are performed in the same way as in the previous subsection. Fig. 3.5 shows the results, from which the same interpretation can be made as in the previous subsection.

3.7 Summary

In this chapter, the three-stage non-anticipative robust UC model under the uncertainty of wind power was studied. Utilizing the fact that the uncertainty of wind power decreases with time, the three-stage model optimizes the operating status, range, and level of each power source at the day-ahead, the intra-day, and each real-time stage, respectively, under different degrees of wind power uncertainty. The simulation results showed that this model can outperform the two-stage model with respect to not only the actual total operating cost but the worst-case total operating cost. Its relative performances improve with the worst-case accuracy of wind power forecasting at the intra-day stage.

In Chapters 2 and 3, the uncertainty of VRE generation was addressed. In the following chapter, that of demand response is considered.

TABLE 3.1. Simulation results for the 300-bus test system.

Index	Two-stage	Three-stage	Deterministic
DA-TOC ($\times 10^7$)	1.37	1.27 (7.71%)	-
Avg. ID-TOC ($\times 10^7$)	1.29	1.26 (2.48%)	-
Avg. RT-TOC ($\times 10^7$)	1.20	1.16 (2.91%)	1.15

Chapter 4

Two-stage Robust UC with Uncertain Demand Response

This chapter describes the novel two-stage robust UC model for addressing the uncertainty of demand response. This chapter is organized as follows: Section 4.1 explains the motivation. Section 4.2 overviews the proposed model. Section 4.3 models the uncertainty. Section 4.4 gives the mathematical formulation. Section 4.5 presents a solution method. Section 4.6 discusses numerical simulation results. Section 4.7 summarizes the chapter.

4.1 Motivation

To enhance the flexibility of power system operation, a UC model can integrate a demand response program where customers are allowed to bid for their flexible demand [74]. However, the utility of power consumption, which a bid price represents, may vary with time. Thus, a solution to the UC model with a fixed bid price might lead to an unexpectedly low social welfare. Under the uncertain utility of power consumption, the two-stage robust UC model studied in [39] maximizes the worst-case social welfare. In this model, however, the winning status of a customer, which indicates whether their bid is accepted, is not dealt with as a decision variable. The winning status is a general modeling concept in demand response that enables considering more diverse constraints, e.g., the minimum level of flexible demand at each time period and that of the total flexible demand [42]. The novelty of the proposed model, which is also based on the two-stage robust optimization framework, is that it explicitly considers the winning status of each customer as a decision variable.

The power system of interest in this chapter is modeled as the one described in Section 2.2 without the VRE generation systems and BESSs; $\mathbf{u}$, $\mathbf{x}$, $\mathbf{c}_1$, $\mathbf{c}_2$, and $\mathcal{U}$ are redefined accordingly. Furthermore, in the context of the bidding process, each load has an associated customer with the same index; additional variables for each customer are introduced later in this chapter. In the following section, the proposed model is overviewed.

4.2 Overview

The proposed model considers a bid-based demand response program over the day-ahead and the real-time stages, at the latter of which the bidding takes place. Specifically, the

following optimization framework is used: At the day-ahead stage, each customer submits a set of flexible demand profiles and that of bid price profiles over the planning horizon. The utility associated with the flexible demand at each time period is modeled as a linear function, and a bid price at each time period indicates the marginal utility. Without loss of generality, the inflexible demand of each customer at each time period, which must be fully met regardless of its utility, is set to zero [42]. At the real-time stage, each customer reports the actual bid price profile, i.e., the actual marginal utility profile, which is assumed to be in the set submitted at the day-ahead stage. Meanwhile, based on the customers' reports, the operating status of the generators are optimized at the day-ahead stage. Subsequently, the operating levels of the generators are determined at the real-time stage with the winning status and the power consumption profiles of the customers. The winning status of a customer in the proposed model indicates whether their bid is accepted, i.e., whether they are served for their flexible demand at all. The power consumption profile of each customer is chosen from the set of flexible demand profiles only if their bid is accepted.

The objective of the proposed model is to maximize the worst-case social welfare under the uncertainty of the customers' real-time bidding. Thus, the proposed model is formulated as a two-stage robust optimization problem where the second-stage problem is an MILP problem whose objective function includes uncertain parameters. Before going into detail on the mathematical formulation, the set of bid price profiles submitted by the customers is modeled. Note that only the bid price profile, i.e., the marginal utility profile, of each customer is uncertain; their power consumption profile is not. To clarify this, the set of bid price profiles is hereafter referred to as the scenario set.

4.3 Uncertainty Modeling

Let θ_{it} and $\boldsymbol{\theta}$ denote the bid price associated with the flexible demand of customer i at time period t, and a vector of θ_{it} for all $i \in \mathcal{I}$ and $t \in \mathcal{T}$, respectively. Although the marginal utility is uncertain at the day-ahead stage, customer i is required to submit the following parameters, which are available from their own historical data: the lower limit $\underline{\theta}_{it}$ of θ_{it} for all $t \in \mathcal{T}$, the upper limit $\overline{\theta}_{it}$ of θ_{it} for all $t \in \mathcal{T}$, the lower limit $\underline{\theta}^{\mathrm{s}}_{i}$ of the sum $\sum_{t\in\mathcal{T}} \theta_{it}$ of the bid prices, the upper limit $\overline{\theta}^{\mathrm{s}}_{i}$ of $\sum_{t\in\mathcal{T}} \theta_{it}$, the lower limit $\underline{\theta}^{\mathrm{r}}_{it}$ of the temporal change $(\theta_{it} - \theta_{i(t-1)})$ in the bid price over two consecutive time periods for all $t \in \mathcal{T}$, and the upper limit $\overline{\theta}^{\mathrm{r}}_{it}$ of $(\theta_{it} - \theta_{i(t-1)})$ for all $t \in \mathcal{T}$. Then, the scenario set Θ is defined as follows:

$$
\begin{aligned}
\Theta := \Big\{ \boldsymbol{\theta} \in \mathbb{R}^{IT} : \; & \underline{\theta}_{it} \leq \theta_{it} \leq \overline{\theta}_{it}, \quad \forall i \in \mathcal{I}, \forall t \in \mathcal{T}, \\
& \underline{\theta}^{\mathrm{s}}_{i} \leq \sum_{t\in\mathcal{T}} \theta_{it} \leq \overline{\theta}^{\mathrm{s}}_{i}, \quad \forall i \in \mathcal{I}, \\
& \underline{\theta}^{\mathrm{r}}_{it} \leq \theta_{it} - \theta_{i(t-1)} \leq \overline{\theta}^{\mathrm{r}}_{it}, \quad \forall i \in \mathcal{I}, \forall t \in \mathcal{T} \Big\}
\end{aligned}
$$

Note that any constraint on $\boldsymbol{\theta}$ can be added, if it is written as a linear (in)equality. In the following section, the mathematical formulation of the proposed model is given.

4.4 Problem Formulation

To maximize the worst-case social welfare under the uncertainty of demand response, the proposed model is formulated as follows:

$$\max_{\mathbf{u}\in\mathcal{U}} \left\{ -\mathbf{c}_1^\top \mathbf{u} + \min_{\boldsymbol{\theta}\in\Theta} h\left(\mathbf{u}, \boldsymbol{\theta}\right) \right\} \tag{4.1}$$

where $h\left(\mathbf{u}, \boldsymbol{\theta}\right)$ is defined as the optimal value of the following MILP problem:

$$\max_{\mathbf{z}\in\{0,1\}^I, (\mathbf{x},\mathbf{y})\in\mathcal{Y}(\mathbf{u},\mathbf{z})} -\mathbf{c}_2^\top \mathbf{x} + \boldsymbol{\theta}^\top \mathbf{y} \tag{4.2}$$

where $\mathbf{z}$ and $\mathbf{y}$ denote a vector of binary variables z_i for all $i \in \mathcal{I}$ and that of real variables y_{it} for all $i \in \mathcal{I}$ and $t \in \mathcal{T}$, respectively; z_i and y_{it} denote the winning status of customer i and their power consumption at time period t, respectively. Furthermore, $\mathbf{y}$ is such that

$$\boldsymbol{\theta}^\top \mathbf{y} = \sum_{i\in\mathcal{I}} \sum_{t\in\mathcal{T}} \theta_{it} y_{it}$$

represents the total utility. The feasible set $\mathcal{Y}\left(\mathbf{u}, \mathbf{z}\right)$ of $(\mathbf{x}, \mathbf{y})$ is defined as follows:

$$\begin{aligned}
&\mathcal{Y}\left(\mathbf{u}, \mathbf{z}\right) := \Big\{ (\mathbf{x}, \mathbf{y}) \in \mathbb{R}^{IT} \times \mathbb{R}^{IT} : \text{(2.1e)–(2.1g)}, \\
&\underline{Y}_{it} z_i \le y_{it} \le \overline{Y}_{it} z_i, \quad \forall i \in \mathcal{I}, \forall t \in \mathcal{T}, && \text{(4.3a)} \\
&\underline{Y}_i^{\mathrm{s}} z_i \le \sum_{t\in\mathcal{T}} y_{it} \le \overline{Y}_i^{\mathrm{s}} z_i, \quad \forall i \in \mathcal{I}, && \text{(4.3b)} \\
&-F_l \le \sum_{i\in\mathcal{I}} F_{il} \left(x_{it}^{\mathrm{g}} - y_{it}\right) \le F_l, \quad \forall l \in \mathcal{L}, \forall t \in \mathcal{T}, && \text{(4.3c)} \\
&\sum_{i\in\mathcal{I}} \left(x_{it}^{\mathrm{g}} - y_{it}\right) = 0, \quad \forall t \in \mathcal{T} \Big\} && \text{(4.3d)}
\end{aligned}$$

where constraints (4.3a) and (4.3b) represent the lower and upper limits of the power consumption by each customer at each time period and those of the total power consumption by each customer, respectively; the parameters $\underline{Y}_{it}$ for all $t \in \mathcal{T}$, $\overline{Y}_{it}$ for all $t \in \mathcal{T}$, $\underline{Y}_i^{\mathrm{s}}$, and $\overline{Y}_i^{\mathrm{s}}$ are submitted by customer i at the day-ahead stage wth those defining the scenario set. Constraints (4.3c) and (4.3d) represent the transmission capacity constraint and the power supply-demand balance condition, respectively. The objective function of problem (4.2) is the variable net utility, i.e., the total utility subtracted by the variable operating cost. Constraints (4.3a) and (4.3b) imply that $y_{it} = 0$ for all $t \in \mathcal{T}$ if $z_i = 0$ for each $i \in \mathcal{I}$; customer i may not be served if their marginal contribution to the variable net utility is negative. This is the most distinguishable feature of the proposed model compared with the existing model in [39]; the existing model can be considered the proposed model with z_i fixed to 1 for all $i \in \mathcal{I}$. While it is straightforward to decide whether to serve customer i at each time period with T binary variables introduced, only z_i is used for simplicity.

The proposed model is implemented as follows: First, problem (4.1) is solved at the day-ahead stage for the scenario set Θ to determine the operating status of the generators.

Subsequently, problem (4.2) is solved at the real-time stage to determine the winning status and the power consumption profiles of the customers as well as the power output profiles of the generators for the actual bid price profile $\boldsymbol{\theta}$. Problem (4.1) is a two-stage robust optimization problem whose second-stage problem (4.2) is an MILP problem. The solution method for problem (4.1) is described in the following section.

4.5 Solution Method

The proposed model cannot be solved using Benders decomposition or the C&CG algorithm in the same way as problems (2.5) and (3.8), due to the non-concavity of the second-stage problem. To solve the proposed model, the C&CG algorithm is applied in a nested fashion, the concept of which is developed in [75]. The solution method is overviewed as follows: First, the C&CG algorithm is applied to problem (4.1), which is decomposed into a master problem and a subproblem that are iteratively solved. The master problem and the subproblem of problem (4.1) are written as an MILP problem and a minimax problem, respectively. Subsequently, the C&CG algorithm is applied to the subproblem of problem (4.1), which itself is decomposed into a master problem and a subproblem that are iteratively solved. In other words, the C&CG algorithm is used twice in a nested fashion. Hereafter, the iteration involving the master problem and the subproblem of problem (4.1) and that dealing with the master problem and the subproblem of the subproblem of problem (4.1) are referred to as the outer and the inner iterations, respectively.

The outer iteration is described as follows: First, for initialization, any $\boldsymbol{\theta}_1 \in \Theta$ is selected and P is set to 1. At each iteration step $P \geq 1$, the master problem of problem (4.1) is solved, which is formulated as the following MILP problem:

$$\begin{aligned} \max_{\mathbf{u}\in\mathcal{U},\eta\in\mathbb{R},\mathbf{z}_p\in\{0,1\}^I,(\mathbf{x}_p,\mathbf{y}_p)\in\mathcal{X}(\mathbf{u},\mathbf{z}_p)} \quad & -\mathbf{c}_1^\top \mathbf{u} + \eta \\ \text{s.t.} \quad \eta \leq -\mathbf{c}_2^\top \mathbf{x}_p + \boldsymbol{\theta}_p^\top \mathbf{y}_p, \quad & p = 1, \ldots, P. \end{aligned} \tag{4.4}$$

Let $\mathbf{u}_P$ and U_P denote the solution corresponding to $\mathbf{u}$ and the optimal value of problem (4.4), respectively. Note that U_P is an upper bound of the optimal value of problem (4.1). Subsequently, the subproblem of problem (4.1) is solved, which is formulated as follows:

$$\min_{\boldsymbol{\theta}\in\Theta} h\left(\mathbf{u}_P, \boldsymbol{\theta}\right). \tag{4.5}$$

Problem (4.5) is solved via the inner iteration. Let $\boldsymbol{\theta}_{P+1}$ denote the solution of problem (4.5). Let also

$$L_P := -\mathbf{c}_1^\top \mathbf{u}_P + h\left(\mathbf{u}_P, \boldsymbol{\theta}_{P+1}\right),$$

which is a lower bound of the optimal value of problem (4.1). If $(U_P - L_P)$ is greater than a predefined tolerance ε, then the iteration step increases to $P+1$ and problem (4.4) is solved again. Otherwise, the outer iteration terminates and $\mathbf{u}_P$ is returned as a solution to problem (4.1). At each iteration step $P \geq 1$, if L_P is less than U_P, then $\boldsymbol{\theta}_{P+1}$ is not equal

to $\boldsymbol{\theta}_p$ for any $p \leq P$. This implies that U_P decreases with P, approaching the optimal value of problem (4.1).

While problem (4.4) is an MILP problem that can be solved by using off-the-shelf solvers, problem (4.5) cannot. In this dissertation, the C&CG algorithm is used again to solve problem (4.5). Before the inner iteration is described, problem (4.2) is first rewritten as follows:

$$\max_{\mathbf{z}\in\{0,1\}^I} h^{\mathrm{p}}(\mathbf{u},\boldsymbol{\theta},\mathbf{z})$$

where

$$h^{\mathrm{p}}(\mathbf{u},\boldsymbol{\theta},\mathbf{z}) := \max_{(\mathbf{x},\mathbf{y})\in\mathcal{X}(\mathbf{u},\mathbf{z})} -\mathbf{c}_2^\top\mathbf{x} + \boldsymbol{\theta}^\top\mathbf{y}. \tag{4.6}$$

Also, the dual optimal value of problem (4.6) is denoted by

$$h^{\mathrm{d}}(\mathbf{u},\boldsymbol{\theta},\mathbf{z}) := \min_{\boldsymbol{\xi}\in\Xi(\boldsymbol{\theta})} \pi^\top(\mathbf{u},\mathbf{z})\,\boldsymbol{\xi} \tag{4.7}$$

where $\boldsymbol{\xi}$, $\Xi(\boldsymbol{\theta})$, and $\pi(\mathbf{u},\mathbf{z})$ denote a vector of dual variables, the feasible set of $\boldsymbol{\xi}$, and a vector of coefficients of dual variables associated with problem (4.6), respectively. Set $\Xi(\boldsymbol{\theta})$ is described by a finite number of linear inequalities whose coefficients are linear in $\boldsymbol{\theta}$. Each entry in $\pi(\mathbf{u},\mathbf{z})$ is an affine function of $\mathbf{u}$ or $\mathbf{z}$. Then, it follows from strong duality that

$$h(\mathbf{u}_P,\boldsymbol{\theta}) = \max_{\mathbf{z}\in\mathcal{Z}(\mathbf{u}_P)} h^{\mathrm{d}}(\mathbf{u}_P,\boldsymbol{\theta},\mathbf{z})$$

where

$$\mathcal{Z}(\mathbf{u}) := \left\{ z\in\{0,1\}^I : \mathcal{X}(\mathbf{u},\mathbf{z}) \neq \emptyset \right\}.$$

This indicates that problem (4.5) itself can be considered as a two-stage robust optimization problem where $\mathbf{z}$ and problem (4.7) correspond to the uncertainty and the second-stage problem, respectively. The C&CG algorithm is now applicable to problem (4.5).

The inner iteration is describe as follows: First, for initialization, any $\mathbf{z}_1^{\mathrm{s}} \in \mathcal{Z}(\mathbf{u}_P)$ is selected and Q is set to 1. At each iteration step $Q \geq 1$, the master problem of problem (4.5) is solved, which is formulated as the following LP problem:

$$\min_{\boldsymbol{\theta}\in\Theta,\boldsymbol{\xi}_q\in\Xi(\boldsymbol{\theta}),\eta\in\mathbb{R}} \eta \quad \text{s.t.} \quad \eta \geq \pi^\top\left(\mathbf{u}_P,\mathbf{z}_q^{\mathrm{s}}\right)\boldsymbol{\xi}_q, \quad q=1,\ldots,Q. \tag{4.8}$$

Let $\boldsymbol{\theta}_Q^{\mathrm{s}}$ and L_Q^{s} denote the solution corresponding to $\boldsymbol{\theta}$ and the optimal value of problem (4.8), respectively. Note that L_Q^{s} is a lower bound of the optimal value of problem (4.5). Subsequently, the subproblem of problem (4.5) is solved, which is formulated as the following MILP problem:

$$\max_{\mathbf{z}\in\{0,1\}^I,(\mathbf{x},\mathbf{y})\in\mathcal{X}(\mathbf{u}_P,\mathbf{z})} -\mathbf{c}_2^\top\mathbf{x} + \left(\boldsymbol{\theta}_Q^{\mathrm{s}}\right)^\top\mathbf{y}. \tag{4.9}$$

Let $\mathbf{z}_{Q+1}^{\mathrm{s}}$ and U_Q^{s} denote the solution corresponding to $\mathbf{z}$ and the optimal value of problem (4.9), respectively. Note that U_Q^{s} is an upper bound of the optimal value of problem (4.5). If $U_Q^{\mathrm{s}} - L_Q^{\mathrm{s}}$ is greater than a predefined optimality tolerance ε^{s}, the iteration step increases

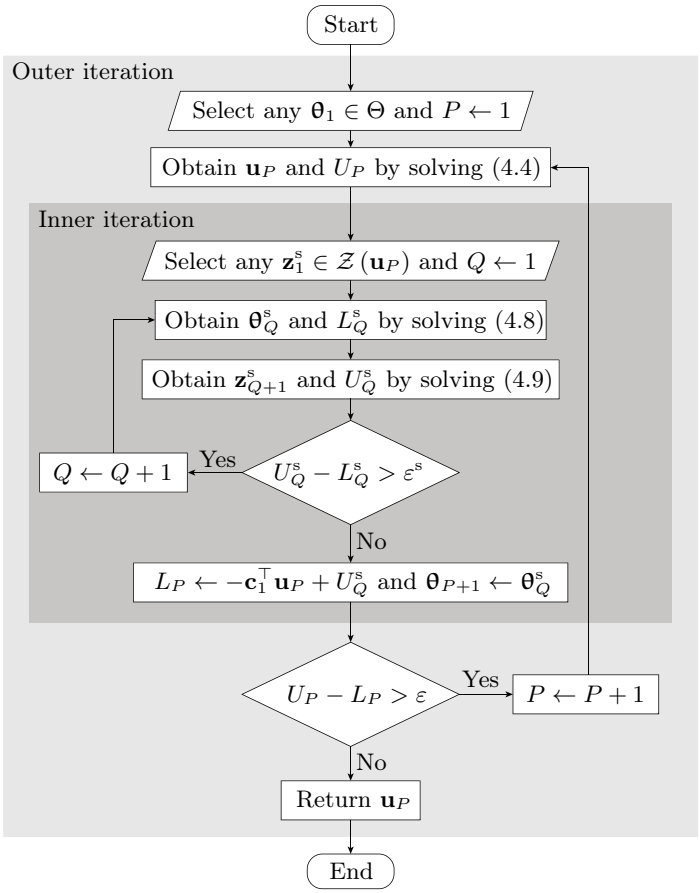

Fig. 4.1. Solution method for problem (4.1).

to $Q+1$ and problem (4.8) is solved again. Otherwise, the inner iteration terminates and $\boldsymbol{\theta}_Q^{\mathrm{s}}$ is returned as a solution to problem (4.5). At each iteration step $Q \geq 1$, if U_Q^{s} is greater than L_Q^{s} at any iteration step Q, then $\mathbf{z}_{Q+1}^{\mathrm{s}}$ is not equal to $\mathbf{z}_q^{\mathrm{s}}$ for any $q \leq Q$. This implies that L_Q^{s} increases with Q, approaching the optimal value of problem (4.5). The inner iteration stops in a finite number of iterations as the feasible set $\mathcal{Z}(\mathbf{u}_P)$ of $\mathbf{z}$ is finite.

Combining the outer and the inner iterations, the solution method for problem (4.1) is illustrated in Fig. 4.1. The effectiveness of the proposed model is examined in the following section.

Remark 4.5.1. Problem (4.5) can also be solved by using another cutting-plane method [76]. In this case, at each iteration step $R \geq 1$, the master problem of problem (4.5) is formulated as the following LP problem:

$$\min_{\boldsymbol{\theta} \in \Theta, \eta \in \mathbb{R}} \eta \quad \text{s.t.} \quad \eta \geq -\mathbf{c}_2^\top \mathbf{x}_r' + \boldsymbol{\theta}^\top \mathbf{y}_r', \quad r = 1, \ldots, R$$

where $(\mathbf{x}_r', \mathbf{y}_r')$ denotes the solution of the subproblem corresponding to $(\mathbf{x}, \mathbf{y})$ at the iteration step r. The subproblem is formulated as problem (4.2) with $\mathbf{u}$ and $\boldsymbol{\theta}$ set to $\mathbf{u}_P$ and the solution corresponding to $\boldsymbol{\theta}$ of the master problem, respectively. However, as could be expected by the fact that a two-stage robust optimization problem whose second-stage problem is an LP problem with an uncertain feasible region is solved in general more

efficiently by the C&CG algorithm than by Benders decomposition [55], it was checked through some pretests that the C&CG algorithm solves problem (4.5) much faster than this alternative algorithm. Thus, only the C&CG algorithm is used in this dissertation.

Remark 4.5.2. The original nested C&CG algorithms in [75] target a two-stage robust optimization problem whose second-stage problem is an MILP problem with an uncertain feasible region. The algorithms include some complicated computational steps to linearize bilinear terms. Notably, the solution method for the proposed model, where only the objective function of the second-stage problem is uncertain, works without such steps.

4.6 Numerical Simulations

To test performances of the proposed model, numerical simulations are conducted on the 24-bus and 300-bus test systems used in Section 2.7 without considering the BESSs and wind farms. To model the set of flexible demand profiles, the upper and lower limits of power consumption by each load at each time period are set to 1.5 and 0.5 times the nominal value, respectively; the upper and lower limits of the total power consumption by each load are set to 1.2 and 0.8 times the nominal value, respectively. Meanwhile, to model the scenario set, first, a profile of nominal bid prices $\hat{\theta}_{it}$ for all $i \in \mathcal{I}$ and $t \in \mathcal{T}$ is generated by scaling that of the nominal demand values so that the maximum nominal bid price is equal to the maximum marginal generation cost. Subsequently, the parameters of the scenario set are set as follows:

$$
\begin{aligned}
&\overline{\theta}_{it} = 1.5\ \hat{\theta}_{it}, \quad \forall i \in \mathcal{I}, \forall t \in \mathcal{T}, \\
&\underline{\theta}_{it} = 0.5\ \hat{\theta}_{it}, \quad \forall i \in \mathcal{I}, \forall t \in \mathcal{T}, \\
&\overline{\theta}^{\mathrm{r}}_{it} = 0.8 \left(\overline{\theta}_{it} - \underline{\theta}_{i(t-1)} \right) + 0.2 \left(\underline{\theta}_{it} - \overline{\theta}_{i(t-1)} \right), \quad \forall i \in \mathcal{I}, \forall t \in \mathcal{T}, \\
&\underline{\theta}^{\mathrm{r}}_{it} = 0.8 \left(\underline{\theta}_{it} - \overline{\theta}_{i(t-1)} \right) + 0.2 \left(\overline{\theta}_{it} - \underline{\theta}_{i(t-1)} \right), \quad \forall i \in \mathcal{I}, \forall t \in \mathcal{T}, \\
&\overline{\theta}^{\mathrm{s}}_{i} = 0.8 \sum_{t \in \mathcal{T}} \overline{\theta}_{it}, \quad \forall i \in \mathcal{I}, \\
&\underline{\theta}^{\mathrm{s}}_{i} = 1.2 \sum_{t \in \mathcal{T}} \underline{\theta}_{it}, \quad \forall i \in \mathcal{I}.
\end{aligned}
$$

The simulation scheme is explained as follows: First, problem (4.1) is solved. Subsequently, the deterministic model

$$
\max_{\mathbf{u} \in \mathcal{U}, \mathbf{z} \in \{0,1\}^I, (\mathbf{x}, \mathbf{y}) \in \mathcal{X}(\mathbf{u}, \mathbf{z})} -\mathbf{c}_1^\top \mathbf{u} - \mathbf{c}_2^\top \mathbf{x} + \boldsymbol{\theta}^\top \mathbf{y}
$$

is solved to maximize the social welfare for three scenarios of $\boldsymbol{\theta}$; two are selected from the scenario set by maximizing and minimizing the sum of the bid prices, while the other is set to the nominal profile. These three deterministic models are referred to as MAX, MIN, and NOM, respectively. Based on the operating status of the generators obtained by solving each model, the maximum variable net utility is calculated for 100 scenarios randomly selected from the scenario set. The four UC models are compared in terms of

the worst-case social welfare for the scenario set and the average social welfare for the randomly selected scenarios. In solving problem (4.1), both outer and inner optimality tolerances are set to 10^{-3} as a relative tolerance. The simulations are run on MATLAB R2020a with CPLEX 12.10 using a computer featuring an Intel Core i9 processor and 64 GB of RAM. As a consequence, for the 24-bus and the 300-bus test systems, the proposed model is solved in 27.68 s and 201.74 s, respectively. The three deterministic models are solved averagely in 0.24 s and 5.82 s, respectively.

The simulation results are shown in TABLE 4.1; the figures in parentheses indicate percentage increases from the indices associated with each deterministic model to those associated with the proposed model. It is observed that the proposed model yields the highest worst-case social welfare for both test systems. In the meantime, the relative performance of the proposed model regarding the average social welfare varies depending on the test system and the deterministic model. To explicitly consider the trade-off between the worst-case and the average social welfares within the proposed framework, the method suggested in Section 2.8 may be used.

4.7 Summary

In this chapter, the novel two-stage robust UC model under the uncertainty of demand response was studied. By explicitly considering the winning status of each customer as a decision variable, the proposed model can integrate more generalized constraints in demand response than the existing model with the same objective.

TABLE 4.1. Simulation results for the 24-bus and the 300-bus test systems.

Index (24-bus)	Proposed	MIN	NOM	MAX
Worst-case social welfare ($\times 10^4$)	4.13	3.82 (+8.05%)	3.70 (+11.49%)	3.13 (+31.88%)
Average social welfare ($\times 10^5$)	1.18	0.98 (+20.39%)	1.34 (−12.26%)	1.25 (−5.57%)
Index (300-bus)	Prop.	MIN	NOM	MAX
Worst-case social welfare ($\times 10^6$)	9.31	9.29 (+0.16%)	9.12 (+2.08%)	9.07 (+2.61%)
Average social welfare ($\times 10^7$)	3.43	3.43 (+0.01%)	3.42 (+0.39%)	3.41 (+0.53%)

Chapter 5

Conclusion

In this dissertation, the three robust UC models were proposed to address the uncertainty of VRE generation or that of demand response. Chapters 2–4 are summarized as follows:

In Chapter 2, the novel two-stage non-anticipative robust UC model under the uncertainty of VRE generation was explained. Considering a power system of generators, BESSs, loads, and VRE generation systems, this model minimizes the worst-case total operating cost for a set of VRE generation scenarios. To this end, the operating range of each power source at each time period of the planning horizon is determined at the day-ahead stage with the operating status. Subsequently, the operating level of each power source is optimized at each real-time stage within the predetermined range for the actual VRE generation. This model is formulated as a two-stage robust optimization problem, which was solved by using the C&CG algorithm and the outer approximation method. The simulation results showed that this model can be more economical than the affine-policy-based model. Meanwhile, in this chapter, the two cost reduction techniques for the UC model were also suggested. The first supplementary method modifies the model so that the expected total operating cost is minimized with the worst-case total operating cost allowed to increase up to a specified level. The modified model was solved by using the algorithm for the original model combined with Benders decomposition. The second supplementary method extends the operating range of each power source at each time period obtained by solving the model. This method is formulated as a multi-objective optimization problem, which was solved by using the method of global criterion with the 2-norm.

In Chapter 3, the three-stage non-anticipative robust UC model under the uncertainty of wind power was explained. Considering a power system of generators, BESSs, loads, and wind farms, this model minimizes the worst-case total operating cost for a set of wind power scenarios. Based on the first proposed model, to exploit the fact that the wind power uncertainty decreases over time, this model delays determining the operating range until the intra-day stage introduced between the day-ahead and the first real-time stage. This model is formulated as a three-stage robust optimization problem, for which no exact algorithm exists. The intractable problem was reduced to a tractable two-stage robust optimization problem by adding a constraint on the operating range such that the transmission line capacity constraint can be ignored. The resulting problem was solved by using the C&CG algorithm and the outer approximation method. The simulation results demonstrated that this model can outperform the first proposed model under the currently

severe but decreasing wind power uncertainty.

In Chapter 4, the novel two-stage robust UC model under the uncertainty of demand response was explained. Considering a power system of generators and loads with a demand response program where each customer bids for their flexible demand, this model maximizes the worst-case social welfare for a set of bidding scenarios. The novelty of this model is that it explicitly considers the winning status of each customer as a decision variable, which improves the modeling capability of demand response. This model is formulated as a two-stage robust optimization problem whose second-stage problem has integer decision variables and an uncertain objective function. This problem was solved by applying the C&CG algorithm in a nested way. The simulation results verified its effectiveness.

The studies in this dissertation have the following four issues among others to be solved in the future work: First, the class of intra-day scenario sets for the second proposed model is technically restricted to those obtained by using the interval prediction method, which thus might be overly conservative. This is because the constraint added to the operating range assumes the spatiotemporal independence of wind power. Second, the solution of the second proposed model is suboptimal, which is also due to the additional constraint. As a result, this model might incur a higher worst-case total operating cost than the first proposed model, especially when the biggest assumption does not hold, i.e., when the wind power uncertainty is not expected to decrease at the intra-day stage. Therefore, it is recommended that both models are pretested so that the one with a lower worst-case total operating cost can be used. Furthermore, finding a suboptimality bound for the second proposed model would be an interesting research topic. Third, the optimization framework of the third proposed model is unrealistic in that the non-anticipative real-time decision-making is not considered. Notably, the temporal decomposition technique in the first proposed model is not viable because of the binary variables in the second-stage problem. Finally, the suggested algorithms for the three proposed models may not be computationally efficient for practical power systems. This is due to the following two aspects of the algorithms: First, a set of decision variables and constraints are iteratively added to the master problems. With this feature, the algorithms cannot straightforwardly handle relatively large-scale power systems, e.g., those with a few thousand buses, in the real world. Second, they are centralized; it is assumed that a single system operator collects all the information needed, e.g., the operational parameters of generators and the scenario sets of VRE generation systems, and solves the models. However, modern power systems feature various distributed energy resources managed by local communities, whose data privacy is not preserved by the algorithms. To resolve the scalability and privacy concerns simultaneously, novel distributed algorithms will need to be developed.

Appendix A

Parameters of 24-bus Test System

The 24-bus test system used in this dissertation is a modified version of the one studied in [77]. In the following sections, the parameters of the generators, the BESSs, and the wind farms are listed. Regarding the buses, loads, and transmission lines, the parameters in [77] are used without change.

A.1 Generator Data

TABLE A.1 shows the operating parameters of the generators. Furthermore, TABLE A.2 shows the cost parameters and initial status of the generators. The generators are assumed to be initially turned on and off for longer than the minimum up and down times, respectively.

TABLE A.1. Operating parameters of the generators in the 24-bus test system.

Generator	Bus	$\overline{X}_i$ (MW)	$\underline{X}_i$ (MW)	X_i^{r} (MW)	X_i^{u}, X_i^{su}, X_i^{d}, X_i^{sd} (MW/h)	T^{u} (h)	T^{d} (h)
1	1	152	30.4	80	120	8	4
2	2	152	30.4	80	120	8	4
3	7	350	75	140	350	8	8
4	13	591	206.85	360	240	12	10
5	15	60	12	48	60	4	2
6	15	155	54.25	60	155	8	8
7	16	155	54.25	60	155	8	8
8	18	400	100	0	280	1	1
9	21	400	100	0	280	1	1
10	22	300	300	0	300	1	1
11	23	310	108.5	120	180	8	8
12	23	350	140	80	240	8	8

TABLE A.2. Cost parameters and initial status of the generators in the 24-bus test system.

Generator	Bus	C_i^{n} (/h)	C_i^{u}	C_i^{d}	C_i^{g} (/MWh)	u_{i0}^{n}	x_{i0}^{g} (MW)
1	1	0	1430.4	0	13.32	1	76

2	2	0	1430.4	0	13.32	1	76
3	7	0	1725	0	20.7	0	0
4	13	0	3056.7	0	20.93	0	0
5	15	0	437	0	26.11	0	0
6	15	0	312	0	10.52	0	0
7	16	0	312	0	10.52	1	124
8	18	0	0	0	6.02	1	240
9	21	0	0	0	5.47	1	240
10	22	0	0	0	0	1	240
11	23	0	624	0	10.52	1	248
12	23	0	2298	0	10.89	1	280

A.2 BESS Data

TABLE A.3 shows the parameters of the BESSs.

TABLE A.3. Parameters of the BESSs in the 24-bus test system.

BESS	Bus	$\overline{X}_i^{\mathrm{i}}$, $\overline{X}_i^{\mathrm{o}}$ (MW)	C_i^{i}, C_i^{o} ($/MWh)	E_i^{i}, E_i^{o}	S_i (MW)	S_{0i} (MWh)
1	3	20	0	0.9	200	0
2	7	20	0	0.9	200	0
3	5	20	0	0.9	200	0

A.3 Wind Power Data

TABLE A.4 and A.5 show the parameters and the nominal scenarios of the wind farms, respectively. The nominal scenarios are based on data in [78].

TABLE A.4. Parameters of the wind farms in the 24-bus test system.

Wind farm	Bus	Capacity (MW)
1	3	200
2	5	200
3	7	200

TABLE A.5. Nominal wind power scenarios in the 24-bus test systems.

Time period	Power output (MW)		
	Wind farm 1	Wind farm 2	Wind farm 3
1	76.8921	112.6747	72.5227
2	66.8277	111.2854	105.5854

3	78.4220	124.0128	106.7157
4	64.1437	113.1810	123.8305
5	102.2196	132.5925	137.2258
6	134.0390	134.4096	141.9488
7	146.5166	136.7111	144.1148
8	143.1758	138.1363	142.1095
9	163.2967	141.2391	142.9034
10	172.6347	131.1882	136.2534
11	166.9354	136.8023	141.5592
12	161.9205	140.3817	134.2399
13	155.9409	141.4847	126.6948
14	147.4501	141.0267	137.1150
15	144.0457	148.9593	138.3782
16	149.0420	152.6110	148.6890
17	136.4638	145.5098	139.0087
18	131.2970	139.1727	131.5645
19	146.8513	144.9506	154.5557
20	144.8147	154.3495	160.4212
21	147.2976	164.8713	167.0224
22	126.3128	156.5771	165.0386
23	124.8788	163.0162	164.2696
24	137.8622	150.3954	154.5532

Appendix B

Parameters of 300-bus Test System

The 300-bus test system used in this dissertation is a modified version of the one studied in [79]. In the following sections, the parameters of the generators, the BESSs, and the wind farms are listed. Regarding the buses, loads, and transmission lines, the parameters in [79] are used without change.

B.1 Generator Data

TABLE B.1 shows the operating parameters of the generators. Furthermore, TABLE B.2 shows the cost parameters and initial status of the generators. Each generator is assumed to be initially turned on for longer than the minimum up time.

TABLE B.1. Operating parameters of the generators in the 300-bus test system.

Generator	Bus	$\overline{X}_i$ (MW)	$\underline{X}_i$ (MW)	X_i^{r} (MW)	X_i^{u}, X_i^{su}, X_i^{d}, X_i^{sd} (MW/h)	T^{u}, T^{d} (h)
1	8	130	20	33.33	100	5
2	10	130	20	33.33	100	5
3	20	130	20	33.33	100	5
4	63	130	20	33.33	100	5
5	76	450	50	100	300	8
6	84	450	25	33.33	100	6
7	91	200	20	33.33	100	5
8	92	350	20	33.33	100	5
9	98	130	20	33.33	100	5
10	108	130	20	33.33	100	5
11	119	2500	150	100	300	8
12	124	450	50	100	300	8
13	125	130	20	33.33	100	5
14	138	130	20	33.33	100	5
15	141	350	20	33.33	100	5
16	143	900	20	33.33	100	5
17	146	130	20	33.33	100	5
18	147	300	20	33.33	100	5

19	149	130	20	33.33	100	5
20	152	500	20	33.33	100	5
21	153	450	150	100	300	8
22	156	162	25	33.33	100	6
23	170	300	20	33.33	100	5
24	171	130	20	33.33	100	5
25	176	300	25	33.33	100	6
26	177	162	25	33.33	100	6
27	185	300	20	33.33	100	5
28	186	1500	150	100	300	8
29	187	1500	150	100	300	8
30	190	600	150	100	300	8
31	191	2300	20	33.33	100	5
32	198	500	20	33.33	100	5
33	213	350	20	33.33	100	5
34	220	130	20	33.33	100	5
35	221	500	20	33.33	100	5
36	222	300	20	33.33	100	5
37	227	450	50	100	300	8
38	230	400	20	33.33	100	5
39	233	500	20	33.33	100	5
40	236	700	50	100	300	8
41	238	300	20	33.33	100	5
42	239	700	20	33.33	100	5
43	241	700	20	33.33	100	5
44	242	300	20	33.33	100	5
45	243	450	50	100	300	8
46	7001	600	20	33.33	100	5
47	7002	700	20	33.33	100	5
48	7003	1500	100	33.33	100	5
49	7011	300	20	33.33	100	5
50	7012	400	20	33.33	100	5
51	7017	400	20	33.33	100	5
52	7023	200	20	33.33	100	5
53	7024	500	20	33.33	100	5
54	7039	800	20	33.33	100	5
55	7044	130	20	33.33	100	5
56	7049	130	20	33.33	100	5
57	7055	130	20	33.33	100	5
58	7057	300	20	33.33	100	5
59	7061	450	50	100	300	8
60	7062	500	25	50	150	6

61	7071	130	20	33.33	100	5
62	7130	1500	20	33.33	100	5
63	7139	900	20	33.33	100	5
64	7166	700	20	33.33	100	5
65	9002	450	50	100	300	8
66	9051	450	50	100	300	8
67	9053	130	20	33.33	100	5
68	9054	130	20	33.33	100	5
69	9055	130	20	16.67	50	5

TABLE B.2. Cost parameters and initial status of the generators in the 300-bus test system.

Generator	Bus	C_i^{n} (/h)	C_i^{u}	C_i^{d}	C_i^{g} (/MWh)	u_{i0}^{n}	x_{i0}^{g} (MW)
1	8	0	550	0	27.5	1	20
2	10	0	550	0	27.5	1	20
3	20	0	550	0	27.5	1	20
4	63	0	550	0	27.5	1	20
5	76	0	4500	0	225	1	50
6	84	0	900	0	45	1	25
7	91	0	550	0	27.5	1	20
8	92	0	550	0	27.5	1	20
9	98	0	550	0	27.5	1	20
10	108	0	550	0	27.5	1	20
11	119	0	4500	0	225	1	150
12	124	0	4500	0	225	1	50
13	125	0	550	0	27.5	1	20
14	138	0	550	0	27.5	1	20
15	141	0	550	0	27.5	1	20
16	143	0	550	0	27.5	1	20
17	146	0	550	0	27.5	1	20
18	147	0	550	0	27.5	1	20
19	149	0	550	0	27.5	1	20
20	152	0	550	0	27.5	1	20
21	153	0	4500	0	225	1	150
22	156	0	900	0	45	1	25
23	170	0	550	0	27.5	1	20
24	171	0	550	0	27.5	1	20
25	176	0	900	0	45	1	25
26	177	0	900	0	45	1	25
27	185	0	550	0	27.5	1	20
28	186	0	4500	0	225	1	150
29	187	0	4500	0	225	1	150

30	190	0	4500	0	225	1	150
31	191	0	550	0	27.5	1	20
32	198	0	550	0	27.5	1	20
33	213	0	550	0	27.5	1	20
34	220	0	550	0	27.5	1	20
35	221	0	550	0	27.5	1	20
36	222	0	550	0	27.5	1	20
37	227	0	4500	0	225	1	50
38	230	0	550	0	27.5	1	20
39	233	0	550	0	27.5	1	20
40	236	0	4500	0	225	1	50
41	238	0	550	0	27.5	1	20
42	239	0	550	0	27.5	1	20
43	241	0	550	0	27.5	1	20
44	242	0	550	0	27.5	1	20
45	243	0	4500	0	225	1	50
46	7001	0	550	0	27.5	1	20
47	7002	0	550	0	27.5	1	20
48	7003	0	550	0	27.5	1	100
49	7011	0	550	0	27.5	1	20
50	7012	0	550	0	27.5	1	20
51	7017	0	550	0	27.5	1	20
52	7023	0	550	0	27.5	1	20
53	7024	0	550	0	27.5	1	20
54	7039	0	550	0	27.5	1	20
55	7044	0	550	0	27.5	1	20
56	7049	0	550	0	27.5	1	20
57	7055	0	550	0	27.5	1	20
58	7057	0	550	0	27.5	1	20
59	7061	0	4500	0	225	1	50
60	7062	0	900	0	45	1	25
61	7071	0	550	0	27.5	1	20
62	7130	0	550	0	27.5	1	20
63	7139	0	550	0	27.5	1	20
64	7166	0	550	0	27.5	1	20
65	9002	0	4500	0	225	1	50
66	9051	0	4500	0	225	1	50
67	9053	0	550	0	27.5	1	20
68	9054	0	550	0	27.5	1	20
69	9055	0	550	0	27.5	1	20

B.2 BESS Data

TABLE A.3 shows the parameters of the BESSs.

TABLE B.3. Parameters of the BESSs in the 300-bus test system.

BESS	Bus	$\overline{X}_i^{\mathrm{i}}$, $\overline{X}_i^{\mathrm{o}}$ (MW)	C_i^{i}, C_i^{o} ($/MWh)	E_i^{i}, E_i^{o}	S_i (MW)	S_{0i} (MWh)
1	19	35	13.75	1	350	0
2	39	35	13.75	1	350	0
3	43	35	13.75	1	350	0
4	100	35	13.75	1	350	0
5	114	35	13.75	1	350	0
6	121	35	13.75	1	350	0
7	145	35	13.75	1	350	0
8	153	35	13.75	1	350	0
9	172	35	13.75	1	350	0
10	179	35	13.75	1	350	0
11	213	35	13.75	1	350	0
12	221	35	13.75	1	350	0
13	248	35	13.75	1	350	0
14	319	35	13.75	1	350	0
15	7024	35	13.75	1	350	0

B.3 Wind Power Data

TABLE B.4 and B.5 show the parameters and the nominal scenarios of the wind farms, respectively. The nominal scenarios are based on data in [78].

TABLE B.4. Parameters of the wind farms in the 300-bus test system.

Wind farm	Bus	Capacity (MW)	Wind farm	Bus	Capacity (MW)
1	19	350	9	172	350
2	39	350	10	179	350
3	43	350	11	213	350
4	100	350	12	221	350
5	114	350	13	248	350
6	121	350	14	319	350
7	145	350	15	7024	350
8	153	350			

TABLE B.5. Nominal wind power scenario in the 300-bus test systems.

Time period	Power output (MW)			
	Wind farm 1	Wind farm 2	Wind farm 3	Wind farm 4
1	134.5612	197.1806	126.9148	70.7233
2	116.9484	194.7495	184.7745	109.9931
3	137.2386	217.0225	186.7525	151.3217
4	112.2515	198.0667	216.7034	158.2608
5	178.8842	232.0369	240.1452	204.6654
6	234.5683	235.2167	248.4104	190.7862
7	256.404	239.2445	252.2009	219.7115
8	250.5577	241.7385	248.6916	213.0525
9	285.7693	247.1684	250.0809	243.9737
10	302.1107	229.5793	238.4434	255.6491
11	292.137	239.404	247.7287	258.3902
12	283.3609	245.668	234.9198	237.4107
13	272.8965	247.5982	221.716	206.0808
14	258.0377	246.7968	239.9512	216.5924
15	252.0799	260.6788	242.1618	217.1874
16	260.8236	267.0693	260.2058	226.2602
17	238.8117	254.6422	243.2652	230.379
18	229.7697	243.5522	230.2379	206.91
19	256.9897	253.6635	270.4724	239.5389
20	253.4258	270.1115	280.7371	247.7054
21	257.7707	288.5248	292.2891	252.8171
22	221.0474	274.0099	288.8176	255.3889
23	218.5379	285.2783	287.4717	257.7769
24	241.2589	263.1919	270.4682	248.2101

Time period	Power output (MW)			
	Wind farm 5	Wind farm 6	Wind farm 7	Wind farm 8
1	195.3915	163.8661	142.7711	174.7102
2	192.0929	193.8261	198.1291	226.4174
3	212.5226	200.9765	201.0225	236.902
4	213.3869	212.6324	245.4862	245.9996
5	232.2957	241.3968	251.3885	245.7554
6	224.6407	245.3729	225.9542	207.9511
7	234.8057	251.8407	216.1643	228.5029
8	230.4488	256.2326	219.1438	253.4331
9	246.0792	251.1609	225.6417	253.0894
10	215.2703	224.294	219.6467	254.1349
11	220.977	230.6477	218.5153	234.9262
12	206.2955	239.3252	222.2887	236.8665

13	204.1448	187.4016	189.9258	219.4849
14	211.9889	186.8643	183.0864	187.2984
15	231.5888	219.0176	183.9271	196.6775
16	253.5596	231.9011	179.4701	208.8072
17	237.5188	200.3306	181.3227	220.9022
18	230.1904	182.3051	161.5731	190.8079
19	263.6601	254.0486	250.3484	241.0639
20	256.1009	251.5917	268.9723	255.6376
21	253.3738	231.509	259.0887	248.4399
22	251.002	221.2766	260.5103	249.4324
23	234.3438	219.8513	273.6409	253.1659
24	198.7378	193.444	245.0852	222.438

Time period	Power output (MW)			
	Wind farm 9	Wind farm 10	Wind farm 11	Wind farm 12
1	123.975	188.0991	149.5832	170.0304
2	142.1535	179.443	165.8351	175.3373
3	142.4474	181.3469	198.9748	187.5721
4	160.6539	201.9071	203.5112	210.9148
5	159.165	226.7748	214.9212	221.0134
6	147.0418	186.2466	190.6261	209.1112
7	149.6856	203.2511	213.1871	202.0189
8	152.621	212.0134	228.5942	213.573
9	153.3347	224.679	247.3293	207.1608
10	149.3942	221.0235	230.4046	215.8965
11	139.9038	216.4689	224.5139	200.3778
12	141.6738	215.68	224.7272	224.4912
13	124.4952	185.8278	192.8043	202.5309
14	123.8046	146.264	167.266	191.7899
15	121.4486	166.8798	171.5415	207.8409
16	135.0239	212.9267	174.6226	200.6781
17	141.6114	228.7373	189.7633	221.7965
18	139.4991	231.4452	218.3078	212.4794
19	151.2933	258.1086	262.0748	261.6054
20	146.8222	244.4596	250.3501	254.4634
21	144.5201	227.2293	207.9921	233.2617
22	140.6239	218.8905	210.4615	225.5793
23	137.5553	215.4578	208.6413	196.1795
24	113.4379	193.1604	191.8606	184.531

Time period	Power output (MW)			
	Wind farm 13	Wind farm 14	Wind farm 15	
1	164.2808	165.6102	129.8909	
2	186.1338	188.8418	125.4783	

3	209.0641	208.6881	138.325	
4	236.6788	228.9113	187.9145	
5	230.4269	228.0154	177.186	
6	229.1293	229.5299	152.5638	
7	224.5629	222.8846	164.6137	
8	222.4579	218.357	181.3251	
9	220.637	212.3715	151.232	
10	218.9739	214.8295	181.6424	
11	206.9621	224.9194	188.3402	
12	209.6244	225.3978	169.2179	
13	201.7264	186.1185	155.0621	
14	197.2707	162.8914	127.9684	
15	215.8607	153.8296	115.6978	
16	218.5506	179.8426	132.3953	
17	240.4426	202.2974	199.5338	
18	250.9076	198.6045	175.201	
19	272.4957	247.4696	245.173	
20	254.1918	238.7793	228.3933	
21	256.1075	191.0244	220.4843	
22	257.1801	179.3709	221.4655	
23	248.3541	177.7513	225.2509	
24	245.9429	161.0885	208.0504	

Bibliography

[1] A. von Meier, "Integration of renewable generation in California: Coordination challenges in time and space," *11th International Conference on Electrical Power Quality and Utilisation*, 2011, pp. 1–6, doi: 10.1109/EPQU.2011.6128888.

[2] B. Saravanan, S. Das, S. Sikri, and D. Kothari, "A solution to the unit commitment problem—a review," *Frontiers in Energy*, vol. 7, no. 2, pp. 223–236, 2013, doi: 10.1007/s11708-013-0240-3.

[3] S. Sen and D. Kothari, "Optimal thermal generating unit commitment: A review," *International Journal of Electrical Power & Energy Systems*, vol. 20, no. 7, pp. 443–451, 1998, doi: 10.1016/S0142-0615(98)00013-1.

[4] N. P. Padhy, "Unit commitment-a bibliographical survey," *IEEE Transactions on power systems*, vol. 19, no. 2, pp. 1196–1205, 2004, doi: 10.1109/TPWRS.2003.821611.

[5] R. Billinton and R. Karki, "Capacity reserve assessment using system well-being analysis," *IEEE Transactions on Power Systems*, vol. 14, no. 2, pp. 433–438, 1999, doi: 10.1109/59.761861.

[6] D. Gielen, F. Boshell, D. Saygin, M. D. Bazilian, N. Wagner, and R. Gorini, "The role of renewable energy in the global energy transformation," *Energy Strategy Reviews*, vol. 24, pp. 38–50, 2019, doi: 10.1016/j.esr.2019.01.006.

[7] IRENA, "Statistics time series," *International Renewable Energy Agency: IRENA*, n.d. [Online]. Available: https://www.irena.org/Statistics/View-Data-by-Topic/Capacity-and-Generation/Statistics-Time-Series. [Accessed: Jun. 25, 2021].

[8] IRENA, "Global renewables outlook: Energy transformation 2050 (edition: 2020)," International Renewable Energy Agency, Abu Dhabi, 2020.

[9] N. G. Paterakis, O. Erdinç, and J. P. Catalão, "An overview of demand response: Key-elements and international experience," *Renewable and Sustainable Energy Reviews*, vol. 69, pp. 871–891, 2017, doi: 10.1016/j.rser.2016.11.167.

[10] M. H. Albadi and E. F. El-Saadany, "Demand response in electricity markets: An overview," *2007 IEEE Power Engineering Society General Meeting*, 2007, pp. 1–5, doi: 10.1109/PES.2007.385728.

[11] P. Du, N. Lu, and H. Zhong, *Demand Response in Smart Grids*, Springer, Cham, 2019, doi: 10.1007/978-3-030-19769-8.

[12] IEA, *World Energy Outlook 2019*, OECD Publishing, 2019.

[13] Q. P. Zheng, J. Wang, and A. L. Liu, "Stochastic optimization for unit commitment—a review," *IEEE Transactions on Power Systems*, vol. 30, no. 4, pp. 1913–1924, 2015, doi: 10.1109/TPWRS.2014.2355204.

[14] M. Tahanan, W. van Ackooij, A. Frangioni, and F. Lacalandra, "Large-scale unit commitment under uncertainty," *4OR*, vol. 13, no. 2, pp. 115–171, 2015, doi: 10.1007/s10288-014-0279-y.

[15] M. Håberg, "Fundamentals and recent developments in stochastic unit commitment," *International Journal of Electrical Power & Energy Systems*, vol. 109, pp. 38–48, 2019, doi: 10.1016/j.ijepes.2019.01.037.

[16] A Zakaria, F. B. Ismail, M. H. Lipu, and M. A. Hannan, "Uncertainty models for stochastic optimization in renewable energy applications," *Renewable Energy*, vol. 145, pp. 1543–1571, 2020, doi: 10.1016/j.renene.2019.07.081.

[17] H. Heitsch and W. Römisch, "Scenario tree modeling for multistage stochastic programs," *Mathematical Programming*, vol. 118, no. 2, pp. 371–406, 2009, doi: 10.1007/s10107-007-0197-2.

[18] Y. Guan and J. Wang, "Uncertainty sets for robust unit commitment," *IEEE Transactions on Power Systems*, vol. 29, no. 3, pp. 1439–1440, 2013, doi: 10.1109/TPWRS.2013.2288017.

[19] A. Lorca and X. A. Sun, "Adaptive robust optimization with dynamic uncertainty sets for multi-period economic dispatch under significant wind," *IEEE Transactions on Power Systems*, vol. 30, no. 4, pp. 1702–1713, 2014, doi: 10.1109/TPWRS.2014.2357714.

[20] R. Jiang, J. Wang, and Y. Guan, "Robust unit commitment with wind power and pumped storage hydro," *IEEE Transactions on Power Systems*, vol. 27, no. 2, pp. 800–810, 2011, doi: 10.1109/TPWRS.2011.2169817.

[21] D. Bertsimas, E. Litvinov, X. A. Sun, J. Zhao, and T. Zheng, "Adaptive robust optimization for the security constrained unit commitment problem," *IEEE Transactions on Power Systems*, vol. 28, no. 1, pp. 52–63, 2012, doi: 10.1109/TPWRS.2012.2205021.

[22] C. Zhao and Y. Guan, "Unified stochastic and robust unit commitment," *IEEE Transactions on Power Systems*, vol. 28, no. 3, pp. 3353–3361, 2013, doi: 10.1109/TPWRS.2013.2251916.

[23] G. Morales-España, Á. Lorca, and M. M. de Weerdt, "Robust unit commitment with dispatchable wind power," *Electric Power Systems Research*, vol. 155, pp. 58–66, 2018, doi: 10.1016/j.epsr.2017.10.002.

[24] R. Jiang, J. Wang, M. Zhang, and Y. Guan, "Two-stage minimax regret robust unit commitment," *IEEE Transactions on Power Systems*, vol. 28, no. 3, pp. 2271–2282, 2013, doi: 10.1109/TPWRS.2013.2250530.

[25] B. Hu, L. Wu, and M. Marwali, "On the robust solution to SCUC with load and wind uncertainty correlations," *IEEE Transactions on Power Systems*, vol. 29, no. 6, pp. 2952–2964, 2014, doi: 10.1109/TPWRS.2014.2308637.

[26] B. Hu and L. Wu, "Robust SCUC considering continuous/discrete uncertainties and quick-start units: A two-stage robust optimization with mixed-integer recourse," *IEEE Transactions on Power Systems*, vol. 31, no. 2, pp. 1407–1419, 2016, doi: 10.1109/TPWRS.2015.2418158.

[27] B. Hu, L. Wu, X. Guan, F. Gao, and Q. Zhai, "Comparison of variant robust SCUC models for operational security and economics of power systems under uncertainty," *Electric Power Systems Research*, vol. 133, pp. 121–131, 2016, doi: 10.1016/j.epsr.2015.11.016.

[28] Y. An and B. Zeng, "Exploring the modeling capacity of two-stage robust optimization: Variants of robust unit commitment model," *IEEE transactions on Power Systems*, vol. 30, no. 1, pp. 109–122, 2015, doi: 10.1109/TPWRS.2014.2320880.

[29] B. Hu and L. Wu, "Robust SCUC with multi-band nodal load uncertainty set," *IEEE Transactions on Power Systems*, vol. 31, no. 3, pp. 2491–2492, 2016, doi: 10.1109/TPWRS.2015.2449764.

[30] C. Dai, L. Wu, and H. Wu, "A multi-band uncertainty set based robust SCUC with spatial and temporal budget constraints," *IEEE Transactions on Power Systems*, vol. 31, no. 6, pp. 4988–5000, 2016, doi: 10.1109/TPWRS.2016.2525009.

[31] C. Wang, F. Liu, J. Wang, W. Wei, and S. Mei, "Risk-based admissibility assessment of wind generation integrated into a bulk power system," *IEEE Transactions on Sustainable Energy*, vol. 7, no. 1, pp. 325–336, 2016, doi: 10.1109/TSTE.2015.2495299.

[32] C. Wang, F. Liu, J. Wang, F. Qiu, W. Wei, S. Mei, and S. Lei, "Robust risk-constrained unit commitment with large-scale wind generation: An adjustable uncertainty set approach," *IEEE Transactions on Power Systems*, vol. 32, no. 1, pp. 723–733, 2017, doi: 10.1109/TPWRS.2016.2564422.

[33] Á. Lorca, X. A. Sun, E. Litvinov, and T. Zheng, "Multistage adaptive robust optimization for the unit commitment problem," *Operations Research*, vol. 64, no. 1, pp. 32–51, 2016, doi: 10.1287/opre.2015.1456.

[34] Q. Zhai, X. Li, X. Lei, and X. Guan, "Transmission constrained UC with wind power: An all-scenario-feasible MILP formulation with strong nonanticipativity," *IEEE Transactions on Power Systems*, vol. 32, no. 3, pp. 1805–1817, 2017, doi: 10.1109/TPWRS.2016.2592507.

[35] D. Bertsimas, D. A. Iancu, and P. A. Parrilo, "Optimality of affine policies in multistage robust optimization," *Mathematics of Operations Research*, vol. 35, no. 2, pp. 363–394, 2010, doi: 10.1287/moor.1100.0444.

[36] A. Lorca and X. A. Sun, "Multistage robust unit commitment with dynamic uncertainty sets and energy storage," *IEEE Transactions on Power Systems*, vol. 32, no. 3, pp. 1678–1688, 2017, doi: 10.1109/TPWRS.2016.2593422.

[37] F. Abbaspourtorbati, A. J. Conejo, J. Wang, and R. Cherkaoui, "Three- or two-stage stochastic market-clearing algorithm?," *IEEE Transactions on Power Systems*, vol. 32, no. 4, pp. 3099–3110, 2017, doi: 10.1109/TPWRS.2016.2621069.

[38] Q. Wang, J. Wang, and Y. Guan, "Stochastic unit commitment with uncertain demand response," *IEEE Transactions on Power Systems*, vol. 28, no. 1, pp. 562–563, 2013, doi: 10.1109/TPWRS.2012.2202201.

[39] C. Zhao, Q. Wang, and Y. Guan, "Two-stage robust optimization for power grid with uncertain demand response," *62nd Annual Conference and Expo of the Institute of Industrial Engineers 2012*, 2012, pp. 426–434.

[40] C. Zhao, J. Wang, J.-P. Watson, and Y. Guan, "Multi-stage robust unit commitment considering wind and demand response uncertainties," *IEEE Transactions on Power Systems*, vol. 28, no. 3, pp. 2708–2717, 2013, doi: 10.1109/TPWRS.2013.2244231.

[41] G. Liu and K. Tomsovic, "Robust unit commitment considering uncertain demand response," *Electric Power Systems Research*, vol. 119, pp. 126–137, 2015, doi: 10.1016/j.epsr.2014.09.006.

[42] C. Su and D. Kirschen, "Quantifying the effect of demand response on electricity markets," *IEEE Transactions on Power Systems*, vol. 24, no. 3, pp. 1199–1207, 2009, doi: 10.1109/TPWRS.2009.2023259.

[43] N. G. Cobos, J. M. Arroyo, N. Alguacil, and A. Street, "Network-constrained unit commitment under significant wind penetration: A multistage robust approach with non-fixed recourse," *Applied Energy*, vol. 232, pp. 489–503, 2018, doi: 10.1016/j.apenergy.2018.09.102.

[44] X. Li and Q. Zhai, "Multi-stage robust transmission constrained unit commitment: A decomposition framework with implicit decision rules," *International Journal of Electrical Power & Energy Systems*, vol. 108, pp. 372–381, 2019, doi: 10.1016/j.ijepes.2019.01.020.

[45] B. Stott, J. Jardim, and O. Alsaç, "DC power flow revisited," *IEEE Transactions on Power Systems*, vol. 24, no. 3, pp. 1290–1300, 2009, doi: 10.1109/TPWRS.2009.2021235.

[46] D. K. Molzahn, F. Dörfler, H. Sandberg, S. H. Low, S. Chakrabarti, R. Baldick, and J. Lavaei, "A survey of distributed optimization and control algorithms for electric

power systems," *IEEE Transactions on Smart Grid*, vol. 8, no. 6, pp. 2941–2962, 2017, doi: 10.1109/TSG.2017.2720471.

[47] H. Ronellenfitsch, M. Timme, and D. Witthaut, "A dual method for computing power transfer distribution factors," *IEEE Transactions on Power Systems*, vol. 32, no. 2, pp. 1007–1015, 2016, doi: 10.1109/TPWRS.2016.2589464.

[48] L. Wu, "A tighter piecewise linear approximation of quadratic cost curves for unit commitment problems," *IEEE Transactions on Power Systems*, vol. 26, no. 4, pp. 2581–2583, 2011, doi: 10.1109/TPWRS.2011.2148370.

[49] J. T. Linderoth and A. Lodi, "MILP software," in *Wiley Encyclopedia of Operations Research and Management Science* (ed. J. J. Cochran), Wiley, 2011, doi: 10.1002/9780470400531.eorms0524.

[50] R. Marquez and C. F. Coimbra, "Forecasting of global and direct solar irradiance using stochastic learning methods, ground experiments and the NWS database," *Solar Energy*, vol. 85, no. 5, pp. 746–756, 2011, doi: 10.1016/j.solener.2011.01.007.

[51] K. Li, R. Wang, H. Lei, T. Zhang, Y. Liu, and X. Zheng, "Interval prediction of solar power using an improved bootstrap method," *Solar Energy*, vol. 159, pp. 97–112, 2018, doi: 10.1016/j.solener.2017.10.051.

[52] P. Pinson, G. Kariniotakis, H. A. Nielsen, T. S. Nielsen, and H. Madsen, "Properties of quantile and interval forecasts of wind generation and their evaluation," *Proceedings of the European Wind Energy Conference & Exhibition*, 2006, pp. 1–10.

[53] H. Quan, D. Srinivasan, and A. Khosravi, "Short-term load and wind power forecasting using neural network-based prediction intervals," *IEEE Transactions on Neural Networks and Learning Systems*, vol. 25, no. 2, pp. 303–315, 2014, doi: 10.1109/TNNLS.2013.2276053.

[54] J. F. Benders, "Partitioning procedures for solving mixed-variables programming problems," *Numerische Mathematik*, vol. 4, no. 1, pp. 238–252, 1962, doi: 10.1007/BF01386316.

[55] B. Zeng and L. Zhao, "Solving two-stage robust optimization problems using a column-and-constraint generation method," *Operations Research Letters*, vol. 41, no. 5, pp. 457–461, 2013, doi: 10.1016/j.orl.2013.05.003.

[56] R. J. Vanderbei, *Linear Programming: Foundations and Extensions*, 5th ed., International Series in Operations Research & Management Science, vol. 285, Springer International Publishing, 2020, doi: 10.1007/978-3-030-39415-8.

[57] A. Gupte, S. Ahmed, M. S. Cheon, and S. Dey, "Solving mixed integer bilinear problems using MILP formulations," *SIAM Journal on Optimization*, vol. 23, no. 2, pp. 721–744, 2013, doi: 10.1137/110836183.

[58] M. A. Duran and I. E. Grossmann, "An outer-approximation algorithm for a class of mixed-integer nonlinear programs," *Mathematical Programming*, vol. 36, no. 3, pp. 307–339, 1986, doi: 10.1007/BF02592064.

[59] R. Fletcher and S. Leyffer, "Solving mixed integer nonlinear programs by outer approximation," *Mathematical Programming*, vol. 66, no. 1, pp. 327–349, 1994, doi: 10.1007/BF01581153.

[60] R. Chen, H. Sun, Q. Guo, Z. Li, T. Deng, W. Wu, and B. Zhang, "Reducing generation uncertainty by integrating CSP with wind power: An adaptive robust optimization-based analysis," *IEEE Transactions on Sustainable Energy*, vol. 6, no. 2, pp. 583–594, 2015, doi: 10.1109/TSTE.2015.2396971.

[61] H. Holttinen, J. J. Miettinen, and S. Sillanpää, "Wind power forecasting accuracy and uncertainty in Finland," VTT Technical Research Centre of Finland, Espoo, Finland, 2013.

[62] B.-M. Hodge et al., "Wind power forecasting error distributions: An international comparison," National Renewable Energy Laboratory, Golden, CO, 2012. NREL/CP-5500-56130. Presented at the 11th Annual International Workshop on Large-Scale Integration of Wind Power into Power Systems as well as on Transmission Networks for Offshore Wind Power Plants Conference.

[63] R. T. Marler and J. S. Arora, "The weighted sum method for multi-objective optimization: New insights," *Structural and Multidisciplinary Optimization*, vol. 41, no. 6, pp. 853–862, 2010, doi: 10.1007/s00158-009-0460-7.

[64] L. Wu and M. Shahidehpour, "Accelerating the benders decomposition for network-constrained unit commitment problems," *Energy Systems*, vol. 1, no. 3, pp. 339–376, 2010, doi: 10.1007/s12667-010-0015-4.

[65] Q. P. Zheng, J. Wang, P. M. Pardalos, and Y. Guan, "A decomposition approach to the two-stage stochastic unit commitment problem," *Annals of Operations Research*, vol. 210, no. 1, pp. 387–410, 2013, doi: 10.1007/s10479-012-1092-7.

[66] R. T. Marler and J. S. Arora, "Survey of multi-objective optimization methods for engineering," *Structural and Multidisciplinary Optimization*, vol. 26, no. 6, pp. 369–395, 2004, doi: 10.1007/s00158-003-0368-6.

[67] I. Giagkiozis and P. J. Fleming, "Methods for multi-objective optimization: An analysis," *Information Sciences*, vol. 293, pp. 338–350, 2015, doi: 10.1016/j.ins.2014.08.071.

[68] M. Zelany, "A concept of compromise solutions and the method of the displaced ideal," *Computers & Operations Research*, vol. 1, no. 3, pp. 479–496, 1974, doi: 10.1016/0305-0548(74)90064-1.

[69] K. Miettinen, "No-preference methods," in *Nonlinear Multiobjective Optimization*, International Series in Operations Research & Management Science, vol. 12, Springer, Boston, MA, 1998, doi: 10.1007/978-1-4615-5563-6_3.

[70] C Monteiro, R Bessa, V Miranda, A Botterud, J Wang, and G Conzelmann, "Wind power forecasting: State-of-the-art 2009," Argonne National Laboratory, Argonne, Illinois, 2009.

[71] P. Pinson and G. Kariniotakis, "Conditional prediction intervals of wind power generation," *IEEE Transactions on Power Systems*, vol. 25, no. 4, pp. 1845–1856, 2010, doi: 10.1109/TPWRS.2010.2045774.

[72] H. Madsen, P. Pinson, G. Kariniotakis, H. A. Nielsen, and T. S. Nielsen, "Standardizing the performance evaluation of short-term wind power prediction models," *Wind engineering*, vol. 29, no. 6, pp. 475–489, 2005, doi: 10.1260/030952405776234599.

[73] P. Pinson, "Estimation of the uncertainty in wind power forecasting," PhD thesis, École Nationale Supérieure des Mines de Paris, France, 2006.

[74] F. Magnago, J. Alemany, and J. Lin, "Impact of demand response resources on unit commitment and dispatch in a day-ahead electricity market," *International Journal of Electrical Power & Energy Systems*, vol. 68, pp. 142–149, 2015, doi: 10.1016/j.ijepes.2014.12.035.

[75] L. Zhao and B. Zeng, "An exact algorithm for two-stage robust optimization with mixed integer recourse problems," University of South Florida, Tampa, Florida, 2012. [Online]. Available: http://www.optimization-online.org/DB_HTML/2012/01/3310.html. [Accessed: Jul. 27, 2020].

[76] D. Bertsimas, I. Dunning, and M. Lubin, "Reformulation versus cutting-planes for robust optimization," *Computational Management Science*, vol. 13, no. 2, pp. 195–217, 2016, doi: 10.1007/s10287-015-0236-z.

[77] C. Ordoudis, P. Pinson, J. M. Morales, and M. Zugno, "An updated version of the IEEE RTS 24-bus system for electricity market and power system operation studies," Technical University of Denmark, Lyngby, Denmark, 2016.

[78] W. A. Bukhsh, C. Zhang, and P. Pinson, "Wind scenarios," *Data for Stochastic Multiperiod Optimal Power Flow Problem*, 2015. [Online]. Available: https://sites.google.com/site/datasmopf/wind-scenarios. [Accessed: Jun. 15, 2019].

[79] Y. Du, Y. Li, C. Duan, H. B. Gooi, and L. Jiang, "Adjustable uncertainty set constrained unit commitment with operation risk reduced through demand response," *IEEE Transactions on Industrial Informatics*, vol. 17, no. 2, pp. 1154–1165, 2021, doi: 10.1109/TII.2020.2979215.